HIGHER ORDER SLIDING MODE BASED PARAMETER ESTIMATION AND CONTROL OF A PRESSURIZED WATER REACTOR

by

Safdar Hussain
PE113005

A thesis submitted to the
Electronic Engineering Department
in partial fulfillment of the requirements for the degree of
DOCTOR OF PHILOSOPHY IN ELECTRONIC ENGINEERING

Faculty of Engineering
Mohammad Ali Jinnah University
Islamabad

April 2014

Dedicated to my parents

ACKNOWLEDGMENT

First of all, thanks to Almighty Allah Who granted me the courage, determination and environment to start my research. All respects to Holy Prophet Muhammad (P.B.U.H), who is the last messenger, whose life is a perfect model for the whole humanity.

I am very thankful to my supervisor Dr. Aamer Iqbal Bhatti for all the support, guidance and discussions in finding research direction and research work. I am also thankful to Dr.Abdus Samee, Dr. Syed Hameed Qaiser, Dr. Fazal ur Rehman and all members of Control and Signal Processing Research ($CASPR$) group for their support and suggestions.

Special thanks are due to my parent organization CHASHMA NUCLEAR POWER PLANT for facilitating my studies with study leave and to HEC for funding my postgraduate studies at Mohammad Ali Jinnah University Islamabad.

ABSTRACT

In this thesis a novel model validation, parameter estimation and controller design for a 998 MW pressurized water reactor is presented. First of all, the non-linear model of the pressurized water reactor is validated with experimental data. The change in reactivity which is calculated from control rod position, is given to the nonlinear model. Two measurable outputs of the reactor are compared with the output of the model. The parameters of the model are calculated from design documents and available literature. After that, important parameters of a pressurized water reactor like precursor density, change in reactivity and average fuel temperature are estimated. The precursors are important parameters which make the control of nuclear reactor possible. There is no physical sensor to measure precursor density directly. A second order sliding mode observer is designed to estimate precursor density. The change in reactivity is an input to the reactor. If reactivity is positive then the reactor power increases and if it is negative the reactor power decreases. In case of zero reactivity the reactor power is in steady state. The change in reactivity cannot be measured directly so an observer is required to estimate it. Average fuel temperature of reactor is also an important parameter directly related to safety of reactor. In the existing technology there is no device to measure fuel temperature. Therefore, its estimation is also required. A uniform robust exact differentiator observer is designed to estimate the change in reactivity and average fuel temperature. After parameter estimation robust controller is designed for controlling thermal power and reactor core outlet temperature. The pressurized water reactor controller takes the turbine power as reference. For controlling the output power of the reactor a robust controller is required which can cope with non-linearities and parameter variations due to fuel burn up and change in power level. Therefore, a second order sliding mode controller is designed in two different ways. In the first method super twisting algorithm is used which needs only the measurement of reactor power. While in the second method real twisting algorithm is used which needs the measurement of power and coolant temperature. Transient and steady state response of a pressurized water reactor in the presence of disturbance and model uncertainties is evaluated.

Keywords: PWR (Pressurized Water Reactor), Reactivity, Precursor density, USOSMO(Uniform Second Order Sliding Mode Observer), URED (Uniform Robust Exact Differentiator)

LIST OF PUBLICATIONS

Journal Publications

1. Journal Publication 1

   Safdar Hussain, A. I. Bhatti, A. Samee, and S. H. Qaiser, "'Estimation of precursor density of a power reactor using uniform second order sliding mode observer,"' Annals of Nuclear Energy, vol. 54, pp. 233-239, 2013, ISSN=0306-4549, IF=0.8

2. Journal Publication 2

   Safdar Hussain, A. I. Bhatti, A. Samee, and S. H. Qaiser,"'Estimation of reactivity and average fuel temperature of a pressurized water reactor using second order sliding mode differentiator observer"',IEEE Transaction on Nuclear Sciences. vol. 60, no. 4, pp. 3025-3032, August 2013, ISSN=0018-9499, IF=1.21

3. Journal Publication 3

   Safdar Hussain, A. I. Bhatti, A. Samee, and S. H. Qaiser,"'Second-Order Sliding Mode Based Controller Design for a Pressurized Water Reactor"', reviewer's comments received in IEEE Transaction on Nuclear Sciences.

TABLE OF CONTENTS

Chapter 5

Chapter 6

LIST OF FIGURES

LIST OF TABLES

LIST OF ACRONYMS

n_r	normalized neutron density
c_{ri}	normalized i^{th} group precursor density
ρ	$(k-1)/k$,reactivity$(\Delta k/k)$
k k_{eff},	effective neutron multiplication factor
λ_i	decay constant for ith group delayed neutron precursor (s^{-1})
Λ	effective prompt neutron life time
β_i	i^{th} group delayed neutron fraction
β	average delayed neutron fraction
T_f	average reactor fuel temperature (^{0}C)
T_e	reactor inlet temperature (^{0}C)
T_l	reactor outlet temperature (^{0}C)
T_c	average reactor coolant temperature (^{0}C)
f_f	fraction of reactor power deposited in fuel
P_{a0}	initial equilibrium Power (MW)
μ_f	heat capacity of fuel (MWs/ ^{0}C)
μ_c	heat capacity of reactor coolant (MWs/ ^{0}C)
Ω	heat transfer coefficient between coolant and fuel (MW/ ^{0}C)
M	Mass flow rate multiplied by heat capacity of coolant (MW/ ^{0}C)
Z_r	control rod speed in steps/sec
G_r	Control rod worth (Δk/k/step)
α_c	coolant temperature reactivity coefficient(Δk/k/ ^{0}C)
α_f	fuel temperature reactivity coefficient (Δk/k/ ^{0}C)

Chapter 1

INTRODUCTION

Nuclear power is safe for environment. In this Chapter importance of nuclear power and brief history of nuclear reactors is given in Section 1.1. The source of nuclear energy i.e. the fission reaction is introduced in section 1.2. Brief literature review to formulate estimation and control problem is given in Section 1.4. The estimation and control problems are described in Section 1.5. The use of sliding mode is motivated in Section 1.6. Thesis contribution and structure is given in Sections 1.7 and 1.8 respectively. Chapter Summary is given in Section 1.9

1.1 Brief History of Nuclear Reactors

Nuclear power is becoming important because conventional sources of energy are depleting . About 3% of total world energy is generated by nuclear power plants [10]. Among other uses, nuclear reactors are used for electricity generation, submarine propulsion and isotope production. In nuclear reactor fission reaction is controlled by some neutron poisoning source that the produced thermal energy is utilized in efficient way. The thermal energy produced in controlled fission is used to produce steam. From this steam, turbine is operated. The turbine shaft is coupled to electrical generator and electricity is generated. Nuclear reactors have different types like Light Water Reactors, Heavy Water Reactors, Gas Cooled Reactors and Liquid Metal Cooled Fast Breeder Reactors. The reactors which are mostly used for electricity generation are light water reactors and heavy water reactors. Light water reactors have further two types: Pressurized Water Reactor (PWR) and Boiling Water Reactor (BWR).

The development of nuclear reactors for the production of power began after the World War II. The construction of first experimental breeder reactor ($EBR-I$) was started in 1949. In 1951 it was made critical and started producing $45KW$ of electricity. It was a sodium cooled fast breeder reactor and shown in Fig. 1.1.

FIGURE 1.1: First Electricity Generating Reactor, EBR-I

The first Experimental Boiling Water Reactor was made critical in 1957. Its capacity was 5 Mega Watt Electric (MWe) and 20 Mega Watt Thermal (MWt). The first PWR which was made critical in 1957 was designed by Westinghouse company. Its capacity was 68 Mega Watt Electric (MWe) and 231 Mega Watt Thermal (MWt).

1.2 Fission Process and Nuclear Energy

The splitting of heavy nucleus of an atom into two or more nuclei accompanied by a large amount of energy is called fission. The fuel in the reactor absorbs neutron and fission process occurs and results in splitting of fissionable material that make the fuel. U235 is used as reactor fuel because

- It absorbs neutron and becomes highly unstable atom of U236.
- Probability of fission for U236 is very high
- In fission of U236 heat energy is released which can be used to produce high pressure steam and ultimately the electricity.
- Fission of U236 also released two or three neutrons which can be used to cause another fission and sustain nuclear chain reaction.

1.3 Pressurized Water Reactor(PWR)

In pressurized water reactor heat energy is generated in the reactor core by controlled fission chain reaction. About 2.5 neutrons and an energy of 210 Mev is produced is fission of one Uranium atom. The production of neutrons in the core is governed by the equations called the point kinetic model. This model shows that the neutron population depends upon the production of prompt neutrons and delayed neutrons. Prompt neutrons are direct consequence of fission reaction while delayed neutrons are emitted by unstable fission fragments. Delayed neutrons are important due to which the reactor period is increased and reactor control is possible.

The ordinary water is circulated through the core at high pressure. The circulation of reactor coolant is forced by reactor coolant pumps. The heat energy from this high temperature and pressure coolant is transferred to secondary side water in steam generator. Steam is produced in steam generator by secondary side water. The steam generated in this way is used to run turbine generator set and electricity is produced. The electricity is then provided to national grid.

1.4 Literature Review

1.5 Estimation and Control Problems

Parameter estimation and control of nuclear is active area of research. Different techniques have been used in the past for the estimation of different parameters of a nuclear reactor . Some examples are [11],[12], [13], Qing Li and Bernard, J.A. [14], Cadini, F. and Zio, E. [15], Fazekas et al. [16]. Peng Wang estimated the reactivity in a nuclear reactor. Xenon concentration was also estimated. The reactivity was estimated by using point kinetic model of reactor while Chernick' model was used for estimation of Xenon concentration. Qaiser et al. [12], [13] estmated the precursor concentration and reactivity of a nuclear research reactor. This experiment was done in steady state of power and super twisting based algorithm was used.

Nuclear reactors consist of a number of different subsystems and some of which are most complicated. In PWR the systems directly related to reactor building are called primary systems and those related to turbine building are named as secondary systems. The focus of this research is parameter estimation and control of reactor core parameters. There are a large number of parameters which are available from measurement. But some of these parameters are not measurable because of inadequate sensors and thus need to be estimated. Precursor density, average fuel temperature and change in reactivity are few parameters which cannot be measured directly. There is no physical sensor in existing technology which can be mounted inside the reactor. In this research a novel uniform second order sliding mode differentiator and observer is designed for estimating reactor core parameters. The output power of the reactor is directly proportional to the neutron density. The density depends upon the rate of fission reaction. If the fission reaction is not controlled then it can cause major accident like Three Miles Island and Chernobyl. Therefor a robust controller is required to regulate the output power of the reactor in the presence of uncertainties and variation of parameters. The sliding mode technique is used to regulate the output power of reactor. In next paragraph the sliding mode is motivated.

1.6 Why Sliding Mode

The sliding mode technique has been used recently in a variety of applications due to its simple structure, capability to control nonlinear system and robustness e.g. [5],[6], [9], [7]. Davila et al. [5] proposed a super twisting based velocity observer using the measurement of position. The observer can also be used for parameter estimation. The drawback of this algorithm is its requirement for initial conditions for the system. Cruz Zavala et al. [6] modified super twisting based velocity observer which is independent of initial conditions. The observer requires the knowledge of the measurement of position and it can also be used for parameter estimation. Levant [9] devised sliding mode based robust exact differentiator. The differentiator gives the derivative of input signal and it is also robust. Cruz Zavala et al. [7] formulated a modified super twisting based uniform differentiator which is also exact and robust.

The sliding mode technique has two good features which attract the control community. One of them is robustness against parameter variations, disturbance rejection and model reduction. The second feature is easy implementation of controller. The drawback of standard sliding mode is that it has chattering effect which can damage actuators. Researchers have used different techniques to reduce chattering effect. One of the technique is higher order sliding mode technique which reduces the chattering effect. Similarly the sliding mode observers and differentiators have the properties of fast convergence, robustness to parameter variations, modeling uncertainties and measurement noise. Therefore sliding mode observer and differentiator are used for parameter estimation in this research work. Sliding mode control is a technique for controlling nonlinear systems to overcome the problems of performance and robustness. Therefor sliding mode technique is very promising for parameter estimation and control of a pressurized water reactor.

1.7 Thesis Contribution

The contributions of the research are

1. **Model validation of a pressurized water reactor.** The nonlinear model of a pressrurized water reactor has been validated. The model has four states like neutron density, precursor density, fuel temperature and coolant temperature. Two measurements of out put of reactor have been used for model validation. One is neutron density and other is coolant temperature. The input to the model is reactivity which has been calculated from measured control rod position. The neutron density and coolant temperature obtained by model are compared with the respective measurements and found close to each other.

2. **Estimation of the precursor density of a pressurized water reactor.**

   The unstable fission fragments are called precursor. These become stable after emitting neutron and other particles. The neutrons emitted by precursor are

called delayed neutron. The control of the nuclear reactor is possible due to the presence of delayed neutrons. Therefore, precursor play important role in control of the nuclear reactor. The density of precursor in the reactor cannot be measured directly. Therefore, an observer is designed to estimate id from available measurements of neutron density and coolant temperature.

3. **Estimation of the change in reactivity of a PWR.**
   The change in reactivity is input to the reactor. Its value can be positive, negative or zero. In case of positive reactivity, reactor power increases. In case of negative reactivity reactor power decreases. While, in case of zero reactivity reactor power remains in steady state. The change in reactivity causes due to control rod movement, change in boron concentration, change in fuel temperature and change in coolant temperature. There is no physical sensor to measure change in reactivity and it requires to be estimated from available measurements. In this research an observer is designed to estimate overall change in reactivity.

4. **Estimation of the average fuel temperature of a PWR.**
   The fuel of a PWR is made up of lightly enriched Uranium dioxide. The fuel cladding is made of Zirc Alloy. The knowledge of average fuel temperature of reactor is important for safe operation of reactor. The fuel temperature cannot be measured because there are limitation to mount sensor inside fuel assembly. Therefore, an observer is also designed to estimate average fuel temperature of the reactor.

5. **Design of a second order sliding mode controller for controlling the output power of reactor.** The PWR follows the mechanical power of turbine. For controlling the output power of reactor a robust controller is required which can work on nonlinear system and cope with parameter variations due to power level and fuel burn up. Therefore a second order sliding mode controller is designed in two different ways. In first method super twisting algorithm is used which needs only the measurement of reactor power. While in second method real twisting controller is used which needs the measurement of power and coolant temperature.

1.8 Thesis Structure

This thesis consists of six chapters.

- **Chapter 1**

  In this chapter motivation, thesis contribution and thesis structure is given.

- **Chapter 2**

  This chapter is an introduction to pressurized water reactor. Here the main primary equipments, primary side systems, Emergency systems and primary side control systems of a PWR are discussed. The model description and validation for a 998 MW thermal reactor is presented.

- **Chapter 3**

  This chapter provides the discussions about the basic theory of sliding mode technique. First of all literature on sliding mode technique is given. The details of higher order sliding mode controllers, observers and differentiators are discussed with simulations in different sections. Super twisting, smooth super twisting, real twisting and smooth real twisting algorithms are described. Finally two variants of second order sliding mode observer and two differentiators are presented.

- **Chapter 4**

  In this chapter we have estimated three important parameters of a pressurized water reactor. Uniform second order sliding mode observer is designed for reactor model and precursor density is estimated. Then a uniform robust exact differentiator observer is designed for reactor neutronic and coolant temperature model. Change in reactivity and average fuel temperature are estimated using this observer.

- **Chapter 5**

  In this chapter smooth second order sliding mode control is used for tracking and disturbance rejection in output power of a pressurized water reactor. Two

different schemes are used. In first method smooth super twisting algorithm is used to regulate output power of reactor. In second method real twisting algorithm is used to regulate the reactor average coolant temperature and power. Simulation results of both the controllers are satisfactory in the presence of disturbance as proved by the simulation results.

- **Chapter 6**
  Conclusion of work done in the thesis and future work is highlighted.

1.9 Summary

In this chapter brief history of nuclear reactor was given. Then importance of research work, reason to use sliding mode, thesis contribution and thesis structure was discussed. In the next chapter overview of Pressurize Water Reactor along with model description and validation will be discussed.

Chapter 2

PRESSURIZED WATER REACTOR OVERVIEW

This chapter is an introduction to pressurized water reactor. Here the detail of main primary equipments is given in Section 2.1. Primary side systems and primary side control systems of a PWR are discussed in Section 2.2. The model description is given in Section 2.3. Model validation for a 998 MW thermal reactor is presented in Section 2.4. Summary of the Chapter is given in Section 2.5.

2.1 Pressurized Water Reactor Primary Side Equipment

Pressurized water reactor has primary and secondary side.The primary loop of pressurized water reactor is given in Fig. 2.1

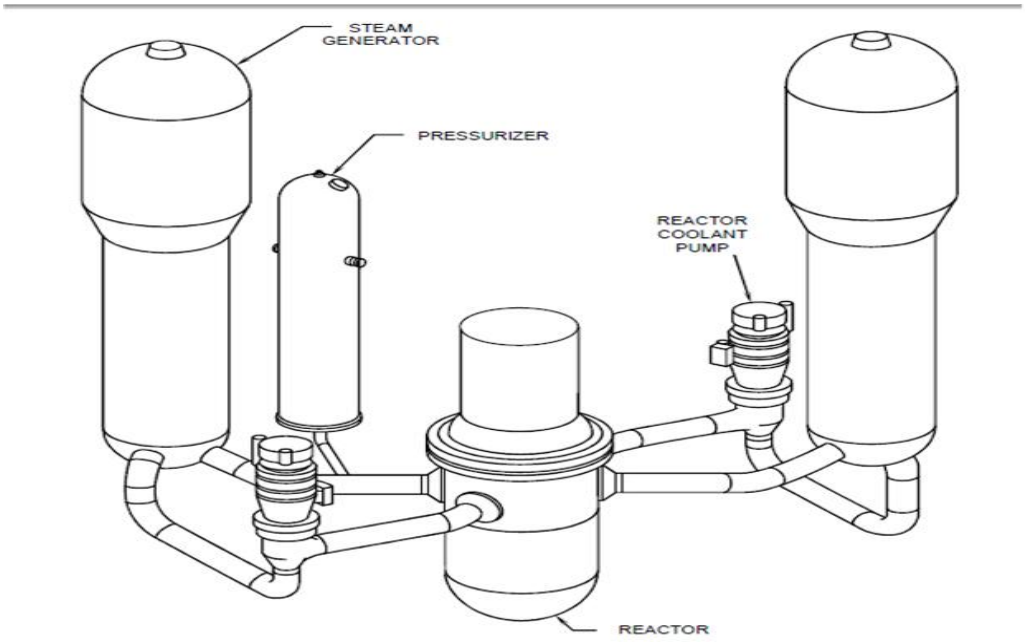

FIGURE 2.1: Pressurized Water Reactor Primary Loop

Primary side equipment are

1. Reactor pressure vessel.
2. Pressurizer
3. Reactor coolant pumps
4. Steam Generators.

The detail of each equipment is given.

2.1.1 Reactor Pressure Vessel

The function of reactor vessel is to enclose and support the reactor core components like fuel rods and control rods. Moreover it directs the reactor coolant from reactor piping's through the reactor core and back to reactor coolant system piping. The reactor vessel consist of heavy wall cylindrical tank. It has rounded bottom. Its rounded top is removable. The top is fitted to vessel all the time of operation except during refueling and special maintenance.

The reactor pressure vessel has upper core sport structure and lower core sport structure. In the reactor core there are lightly enriched uranium fuel assemblies, control rods cluster assemblies, special poison rods and neutron source rods. The lower core support structure encloses the core. The fuel assemblies are held in their proper location by upper core sport structure. The coolant is forced to flow upward through the core where the heat from fuel is removed. The coolant exits the vessel through the outlet nozzles.

2.1.1.1 Reactor Fuel

The fuel has fissile material to support fission reaction. The fission reaction produces thermal energy from which primary coolant is heated. PWR fuel is slightly enriched uranium in the form of uranium dioxide, UO_2. The fuel of a PWR is slightly enriched between $2 - 3.5\%$ of U_{235}. The fuel pellets of UO_2 are stacked to form fuel rods, which are kept inside Zirconium alloy cladding. A fuel assembly has a number of fuel rods ranging from vendor to vendor.

2.1.1.2 Control Rods

Control rod system is used to control nuclear fission process. This is done by inserting control rods into the core. Control rods are absorbers of neutrons. During the start up the control rod are slowly removed from the core. For shutdown purposes these are fully inserted in the core. Control rods are made of boron carbide mixture or silver-indium-cadmium. Several control rods are combined to make a control rod cluster assembly. To control the thermal power level of reactor control rod cluster assemblies are moved down or up.

2.1.2 Reactor coolant pumps (RCP)

In each primary coolant loop at least one RCP is installed. RCP is a mechanical device and it is driven electrically. The RCP takes the coolant from steam generator and injects it to the reactor at high flow rate. The heat from the fuel is transferred to the coolant by this flow.

2.1.3 Pressurizer

The pressurizer is installed at one of the cold leg of reactor. It is a cylindrical tank with rounded bottom and top. It serves two purposes, high pressure of 15.2 MPa is established and maintained by it, so that there is no chance of boiling of primary coolant. If primary coolant is boiled then there are bubble formation in the core and fuel will be damaged. Secondly pressurizer acts as surge volume for primary coolant, it serves as source of water for primary coolant if the temperature is decreased. It receives the water from the primary coolant if temperature increases. The top of pressurizer contains pressure relief valves and spray nozzles to reduce pressure. There is a bank of electrical heaters at bottom of pressurizer. When heaters are energized the pressure will increase.

2.1.4 Steam Generators

Steam generator transfer heat from the primary coolant to secondary system. Steam generator has thousand of U Shaped metal tubes. The coolant enters the steam generator

through inlet channel and directed upward in to the tubes. The heat of primary coolant is transferred to secondary system water through these tubes. The coolant exits the tube through outlet channel ad goes to the suction of RCP.

2.2 Pressurized Water Reactor Primary System

2.2.1 Reactor Coolant System

The primary side of pressurized waters reactor consists of two, three, or four coolant loops and a reactor. Each loop contains RCP, steam generator, stainless steel piping and instrumentation. The main objective of reactor coolant system is to take heat from core and transfer it to secondary coolant in steam generator. Pressurized water reactor has also a pressurizer connected to one of its coolant loop. Pressurizer keeps the pressure of primary coolant high enough to avoid boiling in the core. The schematic diagram of Reactor Coolant System is given in Fig. 2.2
The SRC has following functions.

1. It acts as coolant
2. It acts as moderator
3. It acts as reflector.

Detail of these functions is given below.

1. **SRC as reactor coolant.**
   One function of SRC is the transportation of heated coolant from the reactor core through steam generator and back to the reactor core for reheating. This action prevents fuel from becoming too hot, otherwise, which could lead to the fuel damage.
2. **SRC as moderator**
   The coolant also acts as neutron moderator. The process of slowing down of

neutrons to thermal energy level is called moderation. The probability of fission of Uranium atom increased if neutrons are moving slower.

3. **SRC as reflector**

   The reactor coolant also serves as neutron reflector. It causes to bounce back any high energy neutrons that try to escape.

2.2.2 Residual Heat Removal System (RHR)

It is also known as the decay heat removal system. During plant shut down or emergency core condition, this system removes heat from the primary coolant system.
RHR system transfers thermal energy from the reactor coolant system to the Component Cooling Water (CCW) system during shutdown. The component cooling water system transfers heat from RHR system to the environment.
RHR injects emergency cooling water into the primary coolant during plant emergencies. This is also called low pressure safety injection. The schematic diagram of RHR system is given in Fig. 2.2

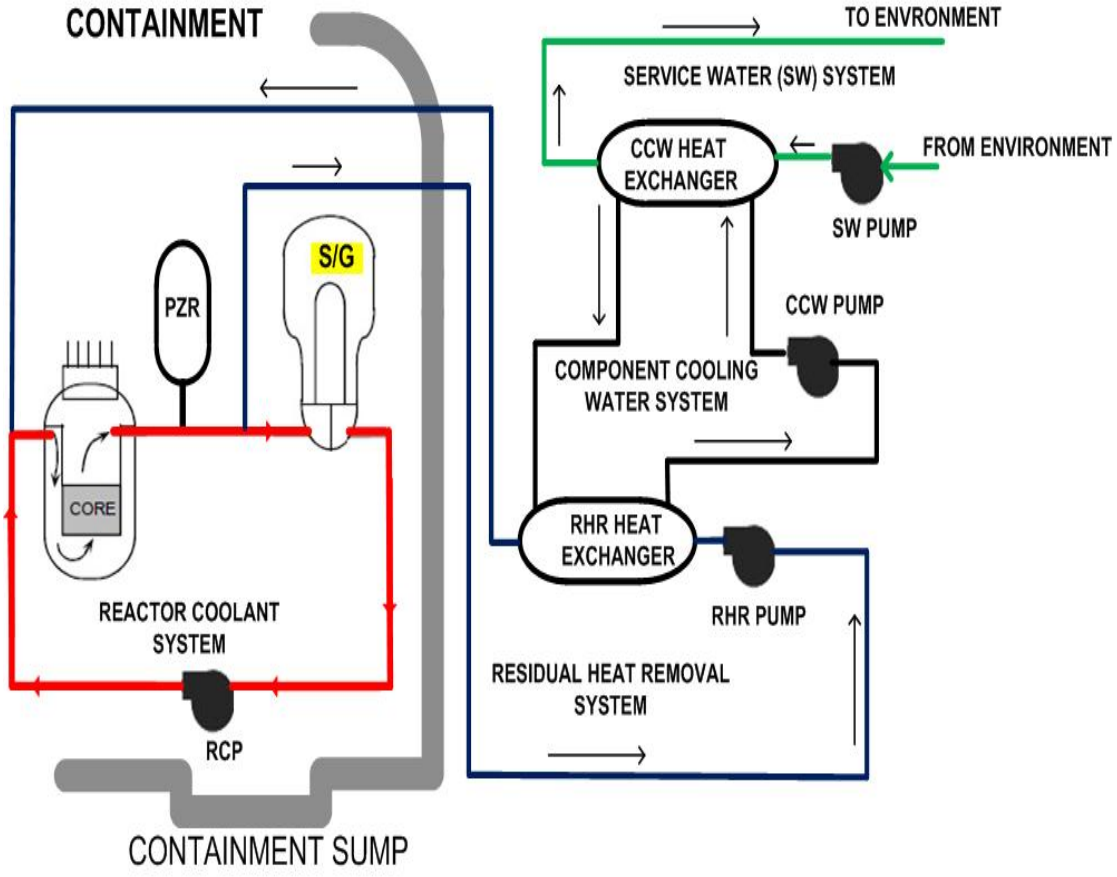

FIGURE 2.2: Reactor Coolant System, Residual Heat Removal System

2.2.3 Chemical and Volume Control System

The main equipment of SCV is volume control tank, charging pump, pure water transfer pump, boric acid transfer pump, pure water tank and boric acid storage tank. Boric acid is neutron poison. The variation of its concentration in SRC can be used to change the reactor power level. To increase power pure water is pumped in SRC so that boric acid concentration is decreased. If power level of reactor is required to be decreased then concentrated boric acid is injected in SRC.

The function of this system is

- Cleaning of primary coolant and addition of chemical material to control corrosion.

- Maintaining the inventory of primary coolant at desired level. It adds water in primary coolant to increase volume and drains water to decrease its volume.
- Changing of boric acid concentration in the primary coolant. It adds concentrated boric acid in primary coolant if decrease in power level is required. It adds diluted water in primary coolant if increase in power level is required.
- This system is a part of emergency core cooling.

The schematic diagram of Chemical and Volume Control System is given in Fig. 2.3

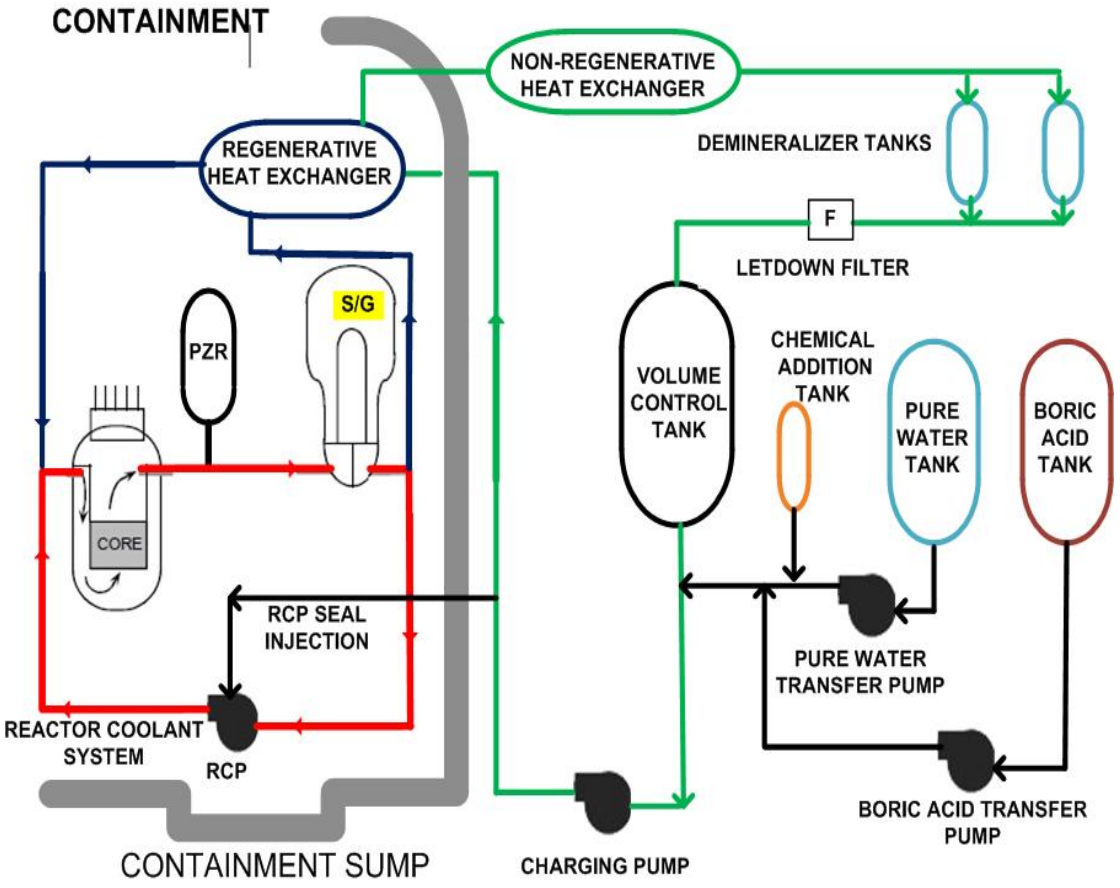

FIGURE 2.3: Chemical and Volume Control System

2.2.4 Primary Side Control Systems

Pressurized Water Reactor supplies electrical energy to national grid on demand. To achieve this goal reactor core must produce heat energy in proportion to grid demand. The steam generator must produce moisture free steam for running turbine. This is done by coordinated action of several control systems. Major control systems at primary side are

- Rod Control System
- Reactor Protection System
- Pressurizer Control System
- Steam Generator Level Control System

2.2.4.1 Rod Control System

The Westinghouse designed reactor thermal power follows the turbine load. The power control system (rod control system) takes the reference from turbine mechanical power and adjusts the thermal power of the reactor accordingly. This system can be operated in manual or automatic mode. In case of abnormal plant operation the reactor protection system de-energizes the power supply of control rods and reactor is shutdown.

2.2.4.2 Reactor Protection System

It is an important system which is related to the safety of the plant. It alerts the reactor operator for appropriate action in case of any abnormal condition. It also actuates Engineered Safeguards and reactor trip signals in case of safety limits reaching. The reactor will shutdown when safety limits are exceeded. This helps

- To prevent fuel from damage.
- To prevent core damage.
- To protect primary coolant pressure boundary.

2.2.4.3 Pressurizer Control System

This system maintains the pressure of primary coolant within the design limits. The controller energizes the heater when pressure is decreased and actuates spray valves if pressure is increased. This control system also maintains the inventory of primary coolant by automatically adjusting the Chemical and Volume Control System (CVCS) charging and letdown flow rates.

2.2.4.4 Steam Generator Level Control System

This system maintains the water level in the steam generator by regulating the flow of feed water into the steam generator. This system monitors the steam generator water level, steam flow in main steam line and feed water flow and regulate feed water control valve to ensure steam generator level at desired level. In next Section the PWR model description and validation is given.

2.3 PWR Model Description

This work has already been published as the author own publication [8]. The nomenclature related to this section is given in beginning of the thesis and parameter values are given in Appendix-A.

2.3.1 Existing Modeling Techniques

Edwards et al.[17] developed the five state model of a nuclear reactor. The states were neutron density, precursor density, fuel temperature, coolant temperature and control rod speed. In this work the effects of Xenon were ignored. Gabor et al. [18] presented a procedure for modelling and identification of VVER type pressurized water reactor.The developed nonlinear state space model was suitable for control oriented model analysis and experiments for controller design. Qaiser et al. [19] validated the model of a nuclear research reactor. The measurement of power was used and model parameters were calculated from design documents of a nuclear research reactor. A second order sliding mode controller was also designed to control the output power of reactor. Lathouwer

et al. [20] presented the coupling of thermal hydraulics, neutronics and fluidization in a theoretical model of reactor. The model was linearized and it was perturbed around equilibrium points. The stability of the system was checked by root locus methods.

2.3.2 Neutronic Model

Neutronic Model of a PWR describes the behavior of neutron population and precursor density. This model is function of space as well as time. But we have considered its temporal behavior in space limped parameter model is assumed. With these assumptions the model is called point kinetic model. The point kinetic model in normalized form is [17] as follows

$$\frac{dn_r}{dt} = \frac{\delta\rho - \beta}{\Lambda} n_r(t) + \frac{1}{\Lambda} \sum_{i=1}^{6} \beta_i c_{ri} \tag{2.1}$$

$$\frac{dc_{ri}}{dt} = \lambda_i n_r(t) - \lambda_i c_{ri}(t) \qquad i = 1, 2.....6 \tag{2.2}$$

Where n_r is normalized neutron density, $\delta\rho$ is change in reactivity, β is delayed neutron fraction, Λ is prompt neutron life time, λ_i is decay constant of i^{th} group precursor, c_{ri} is i^{th} group normalized precursor density.

The equation *(2.1)* describes that the rate of change in neutron population depends upon rate of change due to prompt neutrons as well as rate of change due to delayed neutrons. The rate of production of precursor minus its decay rate is described as rate of change in precursor density *(2.2)*. Precursors are divided into six groups on the basis of their decay constants.

2.3.3 Thermal Hydraulic Model

In Pressurized water reactor the heat energy is produced in the fuel due to controlled fission chain reaction. This heat $P_c(t)$is transferred to coolant according to the following equation

$$P_c(t) = \Omega(T_f - T_c) \tag{2.3}$$

Where Ω is heat transfer coefficient between fuel and coolant, T_f and T_c are fuel and coolant temperatures respectively. The heat energy $P_e(t)$ gained by reactor coolant is used to produce steam in steam generator shown in Fig. 2.4. This amount of heat is given as

$$P_e(t) = M(T_l - T_e) \tag{2.4}$$

Where M is heat capacity of coolant multiplied by mass flow rate, T_e and T_l are temperature of coolant entering and leaving the core respectively. The pressurized water reactor power P_a is expressed as

$$P_a = P_{a0} n_r \tag{2.5}$$

where n_r is normalized neutron density and P_{a0} is initial equilibrium power of the reactor. The equations for fuel and coolant which depend on time are [17]

$$f_f P_{a0} n_r(t) = \mu_f \frac{dT_f}{dt} + P_c(t) \tag{2.6}$$

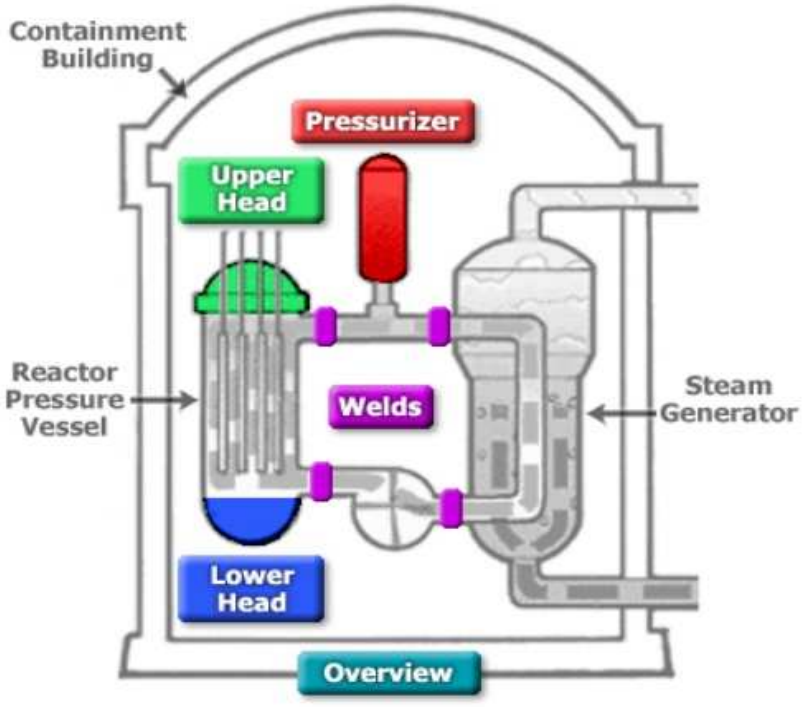

FIGURE 2.4: Pressurized Water Reactor Primary Loop [8]

$$(1 - f_f)P_{a0}n_r(t) + P_c(t) = \mu c\frac{dT_l}{dt} + P_e(t) \tag{2.7}$$

By rearranging terms in *(2.6)*,*(2.7)* we get

$$\frac{dT_f}{dt} = \frac{1}{\mu_f}\left[f_f P_{a0} n_r(t) - \Omega(T_f - T_c)\right] \tag{2.8}$$

$$\frac{dT_l}{dt} = \frac{1}{\mu c}[(1 - f_f)P_{a0}n_r(t) + \Omega(T_f - T_c) - M(T_l - T_e)] \tag{2.9}$$

2.3.4 Reactivity Model

The rate of change in reactivity due to control rod movement is

$$\frac{d\rho_r}{dt} = G_r Z_r \tag{2.10}$$

where ρ_r is change in reactivity due to control rods, control rod speed is Z_r and control rod worth is G_r.

The change in reactivity due to change in fuel temperature, change in coolant temperature and control rod movement is

$$\delta\rho = \alpha_f(T_f - T_{f0}) + \alpha_c(T_c - T_{c0}) + \rho_r \tag{2.11}$$

T_{f0} and T_{c0} are equilibrium temperatures of fuel and coolant. These are obtained by equating the equations *(2.9)* and *(2.8)* to zero. These equilibrium temperatures are given as [17]

$$\begin{aligned} T_{c0} &= \frac{P_{a0} n_r}{2M} + T_e \\ T_{f0} &= \frac{f_f P_{a0} n_r}{\Omega} + T_{co} \end{aligned} \tag{2.12}$$

The temperatures T_{f0} and T_{c0} depend upon power level or equivalently neutron density and equations *(2.12)* can be used in transients.

2.3.5 Complete Nonlinear Model

The model of a nuclear reactor is time varying and nonlinear. The parameters of the model are also function of power level and fuel burn up. It has ten states. One state is neutron density, six are related to precursor density, other states are fuel temperature, coolant temperature and change in reactivity. The complete nonlinear model is given as

[17]

$$\begin{aligned}
\frac{dn_r}{dt} &= \frac{\delta\rho(t)-\beta}{\Lambda}n_r(t)+\frac{1}{\Lambda}\sum_{i=1}^{6}\beta_i c_{ri} \\
\frac{dc_{ri}}{dt} &= \lambda_i n_r(t)-\lambda_i c_{ri}(t), \qquad i=1,2.....6 \\
\frac{dT_f}{dt} &= \frac{1}{\mu f}[f_f P_{a0} n_r(t)-\Omega(T_f-T_c)] \\
\frac{dT_l}{dt} &= \frac{1}{\mu c}[(1-f_f)P_{a0}nr(t)+\Omega(T_f-T_c)-M(T_l-T_e)]
\end{aligned} \tag{2.13}$$

The system states are:$[n_r, c_{ri}, T_f, T_l]^T$ The system input is : $[\delta\rho]$ Outputs are :$[n_r, T_l]$ The parameters of the model are calculated from design documents and available literature. These are given in Appendix-A. In next section model validation of a $998MWPWR$ is given.

2.4 PWR Model Validation

There are four control rod banks namely T_1, T_2, T_3 and T_4 for controlling the power of reactor under consideration. Anyone or combination of these banks is used to change the power of reactor from 0% to 100% and vice versa. In the experiment of present work power was changed between 65% 100% for which first three banks were outside the reactor and T_4 was used for control purpose. The change in reactivity was obtained by multiplying the control rod worth with control rod position. The boron concentration was constant and effects of fuel burnup and Xenon poison were consdered to be negligible. The nonlinear model of a pressurized water reactor *(2.13)* is validated with experimental data. The change in reactivity which is calculated from control rod position is given to the nonlinear model. Two measurable outputs of the reactor are compared with the outputs of model. One output is normalized neutron density and the second is temperature of coolant leaving the core.

2.4.1 Results and Discussions

For model validation steady state and transient conditions are considered. The power level is maintained at 95% for two hours following a decrease in power from 95% to 64% in about two hours. Then power level is maintained at 64% for three hours and restored to 96% in three hours. The measured and modeled neutron density are shown in Fig. 2.5 and error between them is given in Fig. 2.6. The error is minimum in steady state and has a small value in transient conditions. There is a measurement noise seen in the measured neutron density. The measured and modeled coolant temperature leaving the core are shown in Fig. 2.7 and error between them is given in Fig. 2.8. The error is minimum in steady state and has a small value in transient conditions. There is a measurement noise seen in the measured coolant temperature.

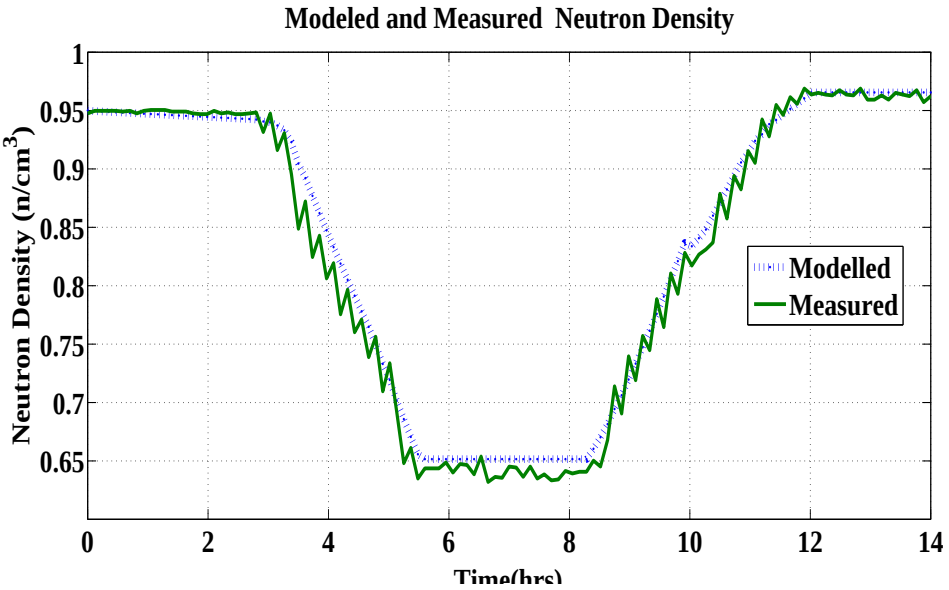

FIGURE 2.5: Comparison of Measured and Modeled Neutron Density

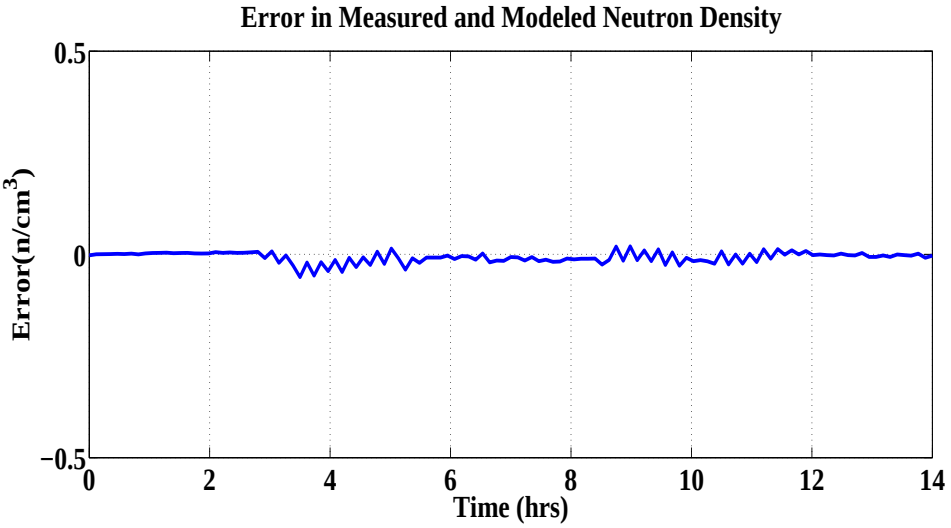

FIGURE 2.6: Error in Measured and Modeled Neutron Density

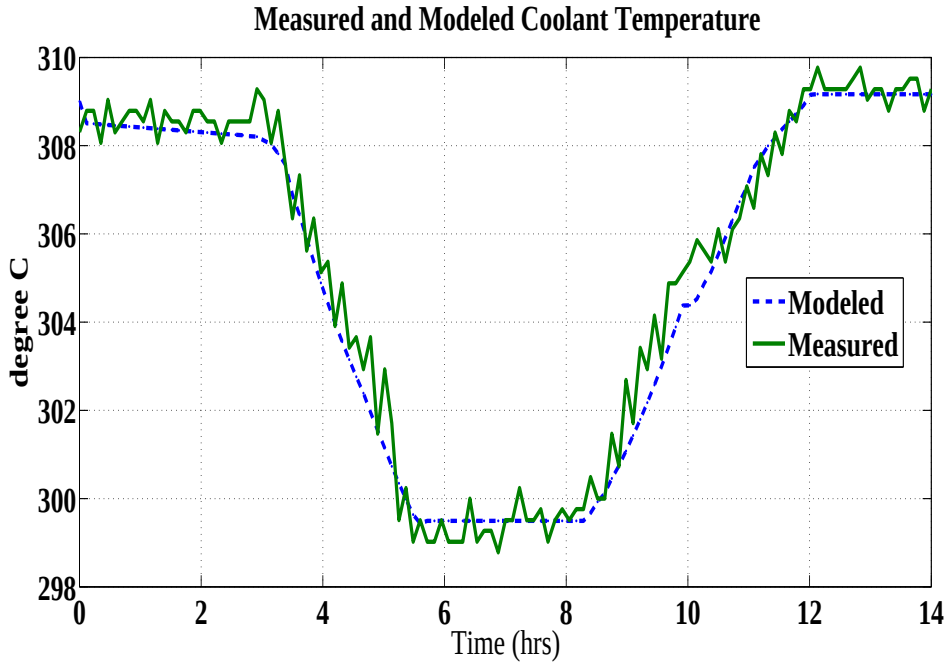

FIGURE 2.7: Comparison of Measured and Modeled Coolant Temperature

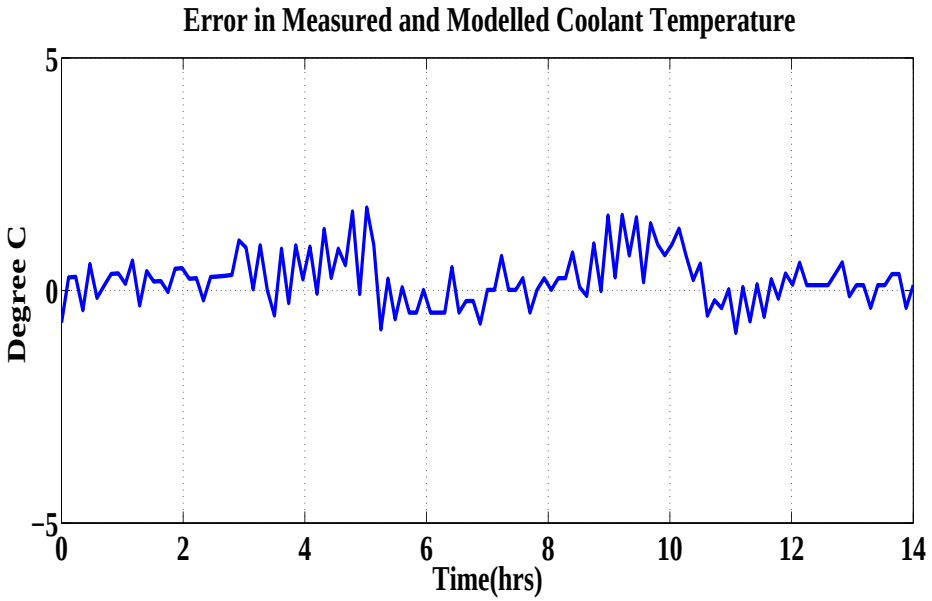

FIGURE 2.8: Error in Measured and Modeled Coolant Temperature

The results show that the modeled and measured values of parameters (neutron density and coolant temperature) are close to each other. The minor difference is due to measurement noise and unmodeled plant dynamics. One reason of difference in values in transients condition is that we have assumed the temperature reactivity coefficient as constant, but, these are also function of power level.

2.5 Summary

In this chapter brief overview of pressurized water reactor was given. Details of primary side coolant systems and primary side control systems were given along with the block diagrams. Then the nonlinear model of reactor was described and validated. Experimental results of model validation were presented and discussed. In the next chapter the basic theory of sliding mode will be given. Different algorithms of sliding mode controllers, observers and differentiators will be discussed with simulation examples.

Chapter 3

SLIDING MODE TECHNIQUE

This chapter provides the discussion about the basic theory of sliding mode technique. First of all literature on sliding mode technique is given. The details of higher order sliding mode controllers, observers and differentiators are discussed with simulations in different sections. Super twisting, smooth super twisting, real twisting and smooth real twisting algorithms are described. Then two variants of second order sliding mode observer and two differentiators are presented.

3.1 Literature Review

Sliding mode control is a technique which belongs to the class of variable structure systems [21], [22] and can be used for linear and non linear systems. Sliding mode is used in industrial applications due to robustness, invariance to parameter variations and unmodeled dynamics [23]. The main problem in sliding mode control is high frequency switching control. Levant [9], Bartolini[24] and Orlov [25] mitigate the chattering by using higher order sliding modes. Rizzoni et al. [26], Emel'yanov [27], Saif et al [28], Spurgeon [29], Alwi and Edwards [30], Sankaranarayanan et al [31],Behnam Ganji et al. [32], Li-Ying Hao and Guang-Hong Yang [33],Rafael Iriarte et al. [34], Xiaoguang Zhang et al. [35], Pupadubsin R et al [36], Jezernik et al. [37] and Beltran et al. [38] are some example of sliding mode control in different industrial applications.

Sliding mode technique is used in combination with fuzzy logic in most of the applications. For example Ho et al.[39], Yeong et al. [40], Zhankui Song and Kaibiao Sun [41],Saoudi et al. [42] and Ruey et al. [43]. Xinghuo Yu [44] presented a survey of sliding mode with soft computing. Application of combining sliding mode with neural networks and fuzzy logic are discussed separately. Xiaoguang et al. [35] used sliding mode controller for speed control of a permanent magnet synchronous motor. First sliding mode control is used for tracking of speed, then an observer is used to estimate uncertainties

and disturbances. Pupadubsin et al. [36] designed a sliding mode controller for position control of a variable reluctance motor. The proposed controller is suitable for high accuracy application. Jezernik et al. [37] developed FPGA based sliding mode controller to reduce the ripples in torque in a permanent magnet synchronous motor. In this work, for torque and speed control sliding mode based FPGA logic has been developed. Beltran et al. [38] designed a sliding mode controller for a generator of a wind turbine. The proposed controller works efficiently without mechanical stress to turbine, robust to unmodeled dynamics of generator and turbine and external disturbances from grid.

Sliding mode technique is also used for observer design other than the controller design. Sliding mode observers has the property of fast convergence, robustness to model and parameter uncertainties and easy implementation. Sliding mode observers have been used extensively for state and parameter estimation in literature. Chen et al. [45], Iqbal et al.[46],Ahmed and Bhatti [47], Butt et al. [48],Imine et al. [49], Xing et al. [50], Liu et al. [51] and Veluvolu et al [52] used sliding mode observers for different parameter estimation problems.

Chen et al. [45] designed a disturbance observer for controlling a class of uncertain nonlinear systems. By selecting the appropriate gains of observer the disturbance can be exactly estimated and is easily rejected by the controller. The stability of closed loop system is proved. Ahmed and Bhatti [47]used a second order sliding mode observer to estimate the parameters of a gasoline engine. The estimated parameters are combustion efficiency, throttle discharge coefficient, volumetric efficiency and frictional torque. For parameter estimation two state model of an automotive engine is used. Then the estimated parameters were used for fault diagnosis. Iqbal et al. [46] developed a parameter estimation scheme for non linear system. A sliding mode differentiator is used for this technique. Two different schemes were used to show the efficacy of design. First parameters of a non linear system were estimated. In the second scheme the unknown parameters of an automotive engine were estimated from the measurement of available data. Butt et al. [48] used sliding mode observer for on-line parameter estimation of a gasoline engine. In this work body discharge coefficient is estimated using sliding mode observer. The stability of the observer is proved by Lyaponov method and its validity by

experimental results. Imine et al. [49] devised a sliding mode control for lane guidance of a vehicle. A sliding mode observer is devised for vehicle dynamics estimation, then the estimated parameters were used for controller design.

Differentiation of signals is also a topic of research. Different techniques have been used in the past for differentiating signals. Chitour, Y. [53], Ball, A.A. and Khalil, H.K. [54],Efimov, D.V and Fridman, L [55], Wang X and Lin H [56], Hongyinping Feng and Shengjia Li [57], Tian et al. [58], Bao-Zhu Guo and Zhi-Liang Zhao [59] are few to name. The researchers has also used the sliding mode technique for differentiation of signals. The sliding mode differentiators also pertain to the properties of variable structure system like robustness to model uncertainties, parameter variation and fast convergence to actual derivative. Different version of sliding mode differentiators are available in literature as can be seen in the work of Levant [9], Levant [60], [61], Kobayashi, Seiichi and Furuta, Katsuhisa [62], Cruz Zaval et al [7] and Angulo et al [63]. Levant [9], [1] presented a sliding mode differentiator of ordinary order. The differentiator is robust against model and parameter uncertainties and gives the derivative of signal in finite time. In simulation results the derivative is compared with linear derivative and its results are more accurate. Efimov, D.V and Fridman, L [55] devised a finite time hybrid robust differentiator. In this work a type of super twisting differentiator is used which has a global differentiation ability with hybrid algorithm. The differentiator is independent of signal amplitude and measurement noise. Cruz Zavala et al. [7] designed a modified super twisting algorithm base differentiator which is independent of initial conditions. Higher order terms are used in super twisting algorithm which make it uniformly convergent. The differentiator is robust and converges in finite time. The condition for this differentiator is that the second derivative of signal should be upper bounded by its Lipschitz constant. Angulo et al [63] suggested a sliding mode differentiator of arbitrary order. It converges in finite time in the absence of noise and is also independent of initial conditions. The condition for this differentiator is that the signal to be differentiated $m-1$ times should have m^{th} derivative bounded by a Lipschitz constant. To gain better insight of sliding mode technique let us consider following example.

Example 3.1. *Let us take the model of a simple pendulum without friction as*

$$\begin{aligned} \dot{x}_1 &= x_2 \\ \dot{x}_2 &= asin(x_1) + u_c \end{aligned} \tag{3.1}$$

Where x_1 represents the velocity, x_2 represents the acceleration of pendulum and $a = mgl$. m is mass of pendulum, l is length of pendulum and g is gravitational accelration. Selecting the sliding surface as

$$s = cx_1 + x_2 \tag{3.2}$$

with control law

$$u_c = -k_d sign(s) - cx_2 \tag{3.3}$$

By choosing $k_d = c = 1$ and $a = 0.2$ the phase portrait of x_1 and x_2 with initial condition $[0.8, 0]$ is given in Fig. 3.1. The control effort required for the system is given in Fig. 3.2

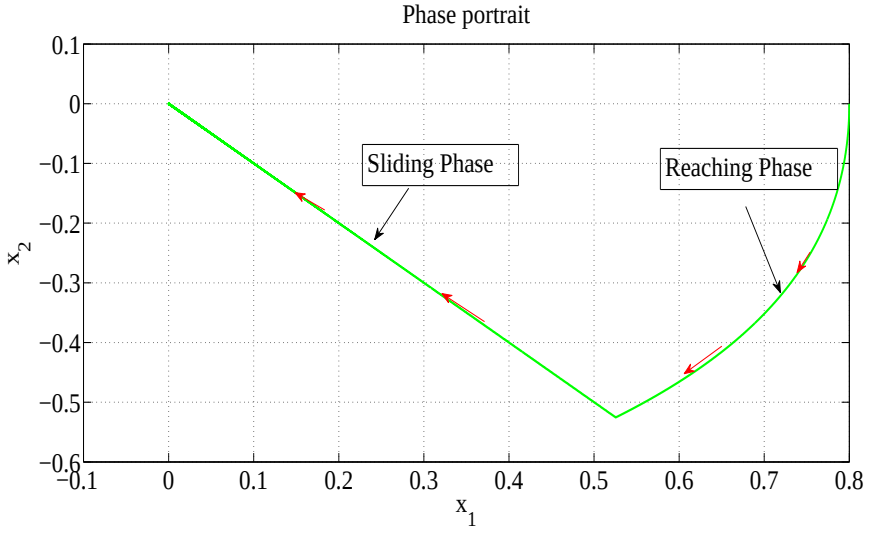

FIGURE 3.1: Phase portrait of simple pendulum

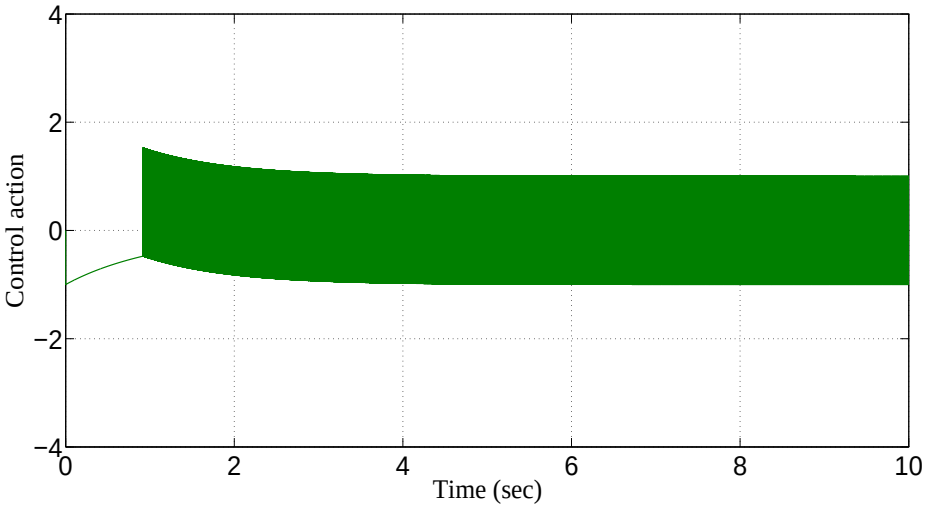

FIGURE 3.2: Control effort for pendulum

The sliding surface is self chosen dynamics which are stable. During sliding the system order is reduced and system nonlinearity is completely rejected. The cancellation of nonlinearity can be seen in Fig. 3.3 with $a = .2$ and $a = 0$ in sliding phase. The nonlinearity has contribution in reaching phase only. In sliding phase both the trajectories are similar. The controller is robust because it is insensitive to controller and plant mismatches.

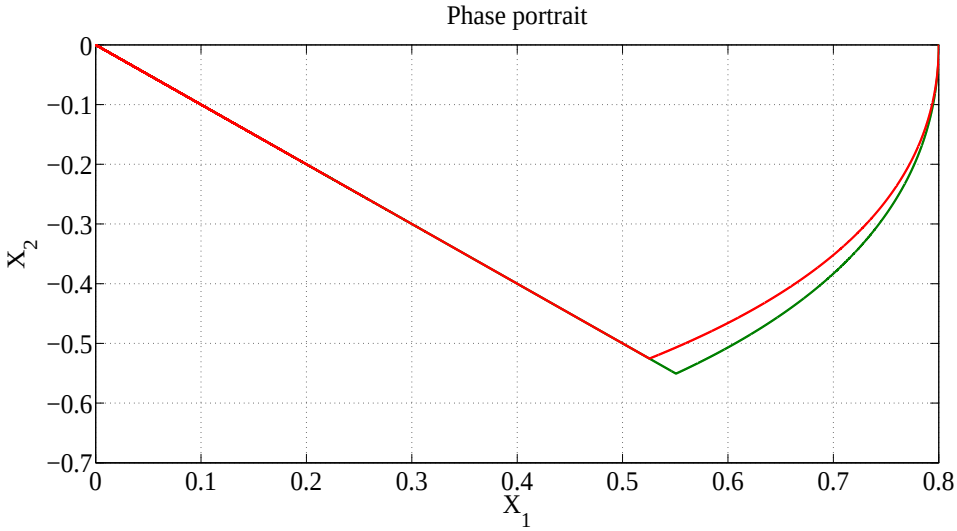

FIGURE 3.3: Phase portrait for simple pendulum with a=0,a=0.20

3.2 Higher order sliding mode

Sliding mode control is a technique for controlling nonlinear systems to overcome the problems of performance and robustness. For sliding mode a manifold σ is designed then a high frequency control switching brings the state of the systems to that manifold. This is called the reachability condition. When the system reaches the constrained manifold $\sigma = 0$, it is called ideal sliding. But the system remains in the neighborhood of constrained manifold and it is called real sliding [64]. When sliding mode is achieved the system order is reduced and it becomes insensitive to parameter variations along with the disturbances. If we have to keep the smooth function $\sigma = 0$, then the number of continuous total derivatives of σ in the neighborhood of sliding mode is called sliding order. Therefore, in r-th order sliding mode, with $s = \sigma$ we have

$$s = \dot{s} = \ddot{s} = ...s^{r-1} = 0 \tag{3.4}$$

The standard sliding mode is a variable structure system based and it has some limitations. Firstly, the relative degree of the system should be one. Secondly high frequency switching causes chattering effect which can damage the plant or its actuators. Different techniques have been used to cater the problem of chattering . One is the approximation of sign function with saturation function. Equivalent control [65] is used to reduce discontinuous control part but this can reduce the robustness property of sliding mode. Higher order sliding mode can be used to overcome the problems of standard sliding mode without loosing the robustness. The main problem in implementation of this technique is the increased information demand on the availability of higher derivatives of sliding manifold. For example for second order sliding mode s and $\dot{s}$ should be available. Second order sliding mode trajectory is given in Fig. 3.4.

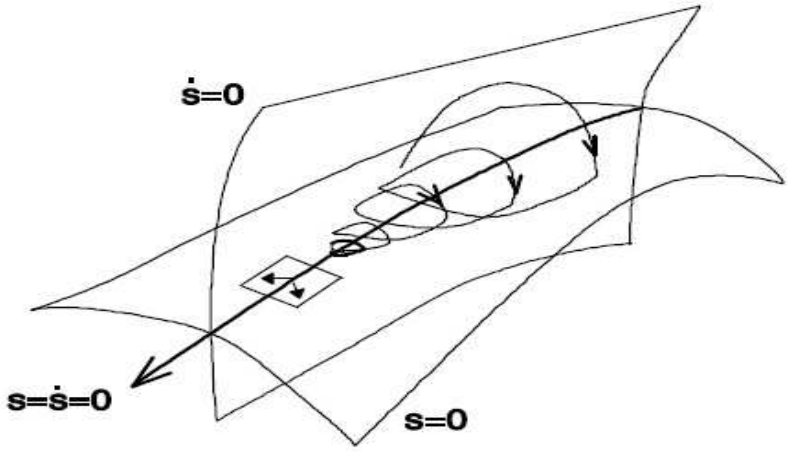

FIGURE 3.4: Trajectory of second order sliding mode [9]

3.2.1 Super Twisting Algorithm [1]

As mentioned earlier, for second order sliding mode the information of σ and $\dot{\sigma}$ is required. The super twisting algorithm requires only the information of σ, although it is second order sliding mode based. In this algorithm the derivative of σ is not required to achieve $\sigma = \dot{\sigma} = 0$. The phase trajectory of super twisting with $\sigma = s$ is given in Fig. 3.5. As shown in figure the trajectories are twisting around the origin on 2-sliding plane. The main advantage of super twisting is that it is second order sliding mode based and does not require the derivative of sliding surface. The drawback of super twisting algorithm is that it cannot be applied to systems having relative degree two.

The modified super twisting algorithm proposed by [1] is

$$u = -\lambda|\sigma|^{\frac{1}{2}} sign(\sigma) + w \qquad (3.5a)$$

$$\dot{w} = -W sign(\sigma) \qquad (3.5b)$$

Where λ and W are positive gains to be designed. This control law establishes an exponentially stable 2-sliding mode. This algorithm shows that the information of σ is sufficient for its implementation. The information of higher derivatives of the σ is not required. Due to its robustness property this algorithm is used for robust exact differentiation.

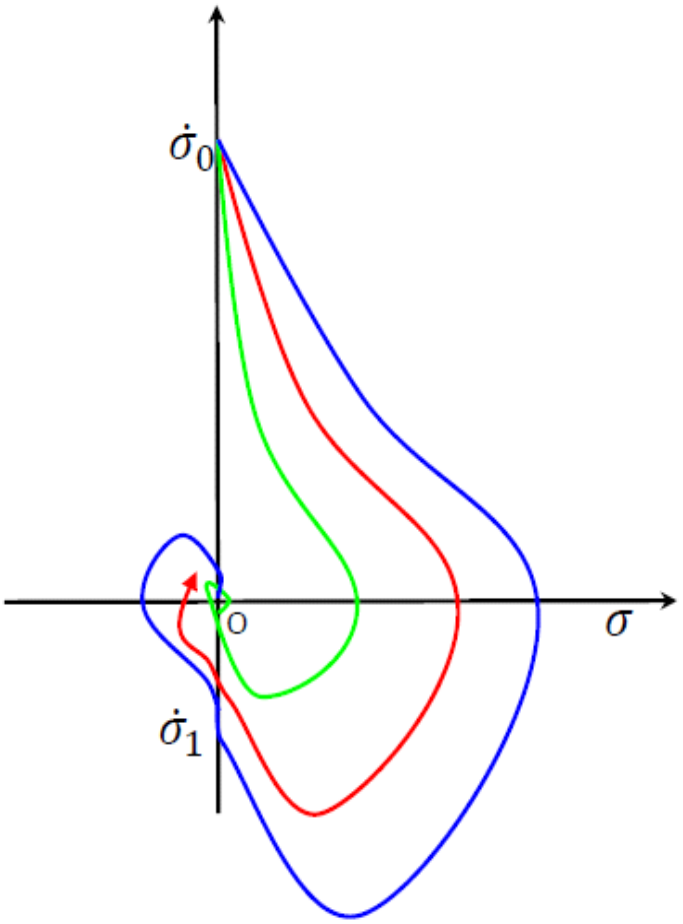

FIGURE 3.5: Phase portrait for super twisting algorithm.

3.2.2 Smooth Super Twisting Algorithm, [2]

Consider the following SISO dynamics

$$\dot{s} = f(t) + u, s \in \Re \tag{3.6}$$

For the sliding mode, the sliding surface is defined by condition $s, \dot{s} = 0$. $f(t)$ is uncertain function which is sufficiently smooth and bounded. $u \in \Re$ is smooth control input. s dynamics in the equation are chosen as

$$\begin{aligned} u &= -k(s)^{\frac{m-1}{m}} sign(s) + w \\ \dot{w} &= -p(s)^{\frac{m-2}{m}} sign(s) \end{aligned} \tag{3.7}$$

Theorem 3.1. *[2] Let $k, p > 0$ and $m \geq 2$ the settling time of the system (3.7) is a continuous function of initial conditions with origin as the equilibrium point and it is finite time stable.*

Proof. Proof of Theorem 3.1 is given in [2]. □

3.2.3 Smooth Super Twisting Algorithm with Disturbance Observer

The dynamics in *(3.6)* is sensitive to term $f(t)$. An observer is required to estimate this term. Let $u(t)$ be Lebesgue measurable and $f(t)$ be differentiable $m-1$ times. Then s is continuous function absolutely defined $\forall t \geq 0$. Now the smooth second order sliding mode control *(3.7)* in the presence of disturbance is given as

$$\begin{aligned} u &= -\chi_1 - \zeta_1 |s|^{\frac{q-1}{q}} + w \\ \dot{w} &= -\zeta_2 |s|^{\frac{q-2}{q}} sign(s) \end{aligned} \tag{3.8}$$

Where χ_1 is the estimate of $f(t)$ obtained by disturbance observer given in Appendix-B. The smooth super twisting algorithm has the properties of simple super twisting in addition to smoothness in control effort.

3.2.4 Real Twisting Algorithm, [3]

This type of controller eliminates the chattering effect while maintaining the robustness properties of standard sliding mode. It requires the measurement of s and $\dot{s}$ for its implementation. This control effort converges the state trajectories in finite time, and it can be be used for relative degree one or relative degree two systems. For relative degree one system the real twisting algorithm is given as [3]

$$\dot{\xi}_1 = \begin{cases} -\xi & \text{if } |\xi| > 1 \\ -\alpha_n sign(s) & \text{if } s\dot{s} \leq 0; |\xi| \leq 1 \\ -\alpha_N sign(s) & \text{if } s\dot{s} > 0; |\xi| \leq 1 \end{cases} \tag{3.9}$$

The main drawback of this algorithm is that the measurement of $\dot{s}$ may not be available at all times. The real twisting algorithm for relative degree two systems is given as

$$\dot{\xi}_1 = \begin{cases} -k_m sign(s) & \text{if } |\xi| > 1 \\ -k_M sign(s) & \text{if } |\xi| \leq 1 \end{cases} \tag{3.10}$$

The convergence of real twisting algorithm is shown in Fig. 3.6. [3]

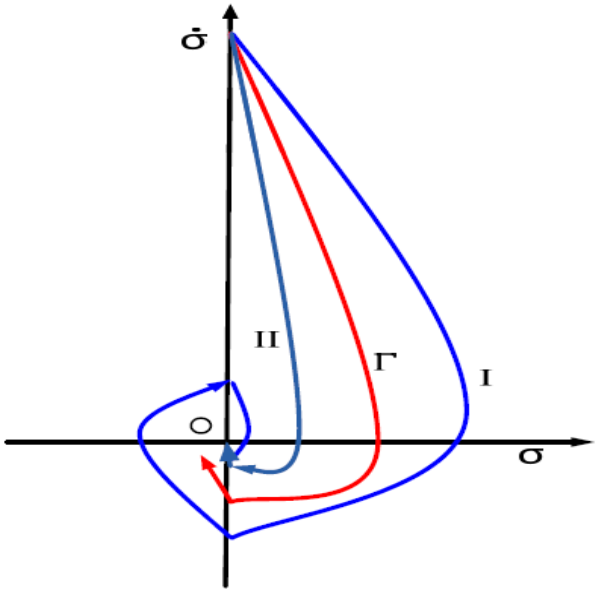

FIGURE 3.6: Phase portrait for real twisting algorithm

The real twisting algorithm can used for relative degree one and. Its main drawback is that it also requires the knowledge of the derivative sliding surface.

3.2.5 Smooth Real Twisting Algorithm,[4]

Consider a SISO system having relative degree two

$$\ddot{\omega} = f(\omega, \dot{\omega}, t) + u \tag{3.11}$$

In *(3.11)* $\omega \in \Re$ and $f(\omega, \dot{\omega}, t)$ is bounded drift term. The control effort $u \in \Re$ is required to be smooth. If the drift term is estimated properly and canceled out then the nominal system can be represented as double integrator.

$$\ddot{\omega} = u \tag{3.12}$$

Then the smooth control law [4] is given as

$$u = -k_1|\omega_0|^{\frac{r-2}{r}} sign(\omega_0) - k_2|\omega_1|^{\frac{r-2}{r}} sign(\omega_1) \quad (3.13)$$

with $\omega_0 = \omega$ and $\omega_1 = \dot{\omega}$, $k_1, k_2 > 0$ and $r \geq 2$.
The closed loop system is

$$\begin{aligned} \dot{\omega}_0 &= \omega_1 \\ \dot{\omega}_1 &= -k_1|\omega_0|^{\frac{r-2}{r}} sign(\omega_0) - k_2|\omega_1|^{\frac{r-2}{r}} sign(\omega_1) \end{aligned} \quad (3.14)$$

Theorem 3.2. *[4] The system (3.14) is globally uniformly finite time stable and generates smooth 2-sliding mode at the origin only.*

Proof. Proof of Theorem 3.2 is given in [4]. □

3.2.6 Smooth real Twisting Algorithm with Disturbance Observer, [4]

The control law given in *(3.13)* is smooth and closed loop system *(3.14)* may be sensitive to drift term $f(\omega, \omega_1, t)$. Therefore an estimate of drift term is required to ensure the robustness of closed loop system. Let us assume that ω, ω_1 are available and u is Lebesgue measurable. The drift term $f(\omega, \omega_1, t)$ is unknown but $(n-1)$ times differentiable and bounded. Now the control law for system *(3.11)* with the disturbance is given as

$$u = -\hat{f} - k_1|\omega_0|^{\frac{r-2}{r}} sign(\omega_0) - k_2|\hat{\omega}_1|^{\frac{r-2}{r}} sign(\hat{\omega}_1) \quad (3.15)$$

with $r = m + 1$, $m \geq 2$ and the drift term $\hat{f}$ is obtained with the help of robust disturbance observer given in Appendix-C. The closed loop system is

$$\begin{aligned} \dot{\omega}_0 &= \omega_1 \\ \dot{\omega}_1 &= f(\omega_0, \omega_1, t) - \hat{f} - k_1 |\omega_0|^{\frac{r-2}{r}} sign(\omega_0) \\ &- k_2 |\hat{\omega}_1|^{\frac{r-2}{r}} sign(\hat{\omega}_1) \end{aligned} \tag{3.16}$$

Theorem 3.3. *[4] Suppose the drift term in (3.11) is upper bonded by Lipschitz constant and it is $n-1$ times differentiable then the system (3.11), (4) and (3.15) are finite time stable.*

Proof. Proof of Theorem 3.3 is given in [4] □

3.3 Sliding Mode Observers

3.3.1 Second Order Sliding Mode Observer [5]

Let us consider a system as

$$\begin{aligned} \dot{\zeta}_1 &= \zeta_2 \\ \dot{\zeta}_2 &= g(\zeta_1, \zeta_2, t, u) + \xi(\zeta, t, u) \\ y &= \zeta_1 \end{aligned} \tag{3.17}$$

where

$[\zeta_1, \zeta_2]^T$: is state vector

y: is output of the system

$\zeta(\zeta, t, u)$: represents uncertainty

$g(\zeta_1, \zeta_2, t, u)$: nonlinear dynamics of the system model which are known

$$\begin{aligned} \dot{\hat{\zeta}}_1 &= \hat{\zeta}_2 + z_1 \\ \dot{\hat{\zeta}}_2 &= g(t, \zeta_1, \hat{\zeta}_2, u) + z_2 \\ \hat{y} &= \hat{\zeta}_1 \end{aligned} \tag{3.18}$$

where
$[\hat{\zeta}_1, \hat{\zeta}_2]^T$ is state estimation vector
z_1 and z_2 are output injection terms. These are expressed as [5].

$$\begin{aligned} z_1 &= \lambda |s_1|^{1/2} sign(s_1) \\ z_2 &= \alpha sign(s_1) \end{aligned} \tag{3.19}$$

Where $s_1 = \zeta_1 - \hat{\zeta}_1$ be the sliding surface Taking $s_2 = \zeta_2 - \hat{\zeta}_2$ the error equations are obtained as

$$\begin{aligned} \dot{s}_1 &= s_2 - \lambda |s_1|^{1/2} sign(s_1) \\ \dot{s}_2 &= G(\zeta_1, \hat{\zeta}_2, \zeta_2, t) - \alpha sign(s_1) \end{aligned} \tag{3.20}$$

Where
$G(\zeta_1, , \hat{\zeta}_2, \zeta_2, t) = g(\zeta_1, \zeta_2, t, u) + \xi(t, \zeta_1, \hat{\zeta}_2, u) - g(\zeta_1, \hat{\zeta}_2, t, u)$ Assume that the system

is bounded and following inequality holds for any possible ζ_2, ζ_1, t ,constant g^+ and $|\hat{\zeta}_2| \leq 2sup|\zeta_2|$.

$$|G(\zeta_1, \hat{\zeta}_2, t), \zeta_2| < g^+ \tag{3.21}$$

Then the existence is ensured. Let λ and β satisfy the inequalities

$$\begin{aligned} \beta &> g^+ \\ \lambda &> \sqrt{\frac{2}{\beta - g^+}} \frac{(\beta + g^+)(1+m)}{(1-m)} \end{aligned} \tag{3.22}$$

Theorem 3.4. *[5] Suppose the condition (3.21) holds for the system (3.17) and the parameters of the observer (3.18),(3.19) are selected according to (3.22). Then , the estimated states of the observer (3.18),(3.19) converge to the states of the system (3.17) in finite time.*

Proof. Proof of Theorem 3.4 is given in [5]. □

Example 3.2. *Consider a model of simple pendulum with external perturbation and Coulomb friction given below*

$$\ddot{\phi} = -\frac{g}{L} sin\phi - \frac{V_s}{J}\dot{\phi} + \frac{1}{J}\tau + v \tag{3.23}$$

The values are taken as $g = 9.815$, $M = 1.1$, $L = 0.9$ $J = 0.891$ *and* $V_s = 0.18$. $|v| \leq 1$ *is a perturbation term. In simulation it was taken as* $v = 0.5sin2t + 0.5cos5t$ *Let the controller for (3.23) be*

$$\tau = -30sign(\phi - \phi_r) - 15sign(\dot{\phi} - \dot{\phi}_r) \tag{3.24}$$

where $\phi_r = sint$ and $\dot{\phi}_r = cost$ are the reference signals to be tracked by control effort. The model (3.23) can be expressed in state space form as

$$\begin{aligned} \dot{\zeta}_1 &= \zeta_2 \\ \dot{\zeta}_2 &= -\frac{g}{L}sin\zeta_1 - \frac{V_s}{J}\zeta_2 + \frac{1}{J}\tau + v \end{aligned} \tag{3.25}$$

The velovity observer has the form

$$\begin{aligned} \dot{\hat{\zeta}}_1 &= \hat{\zeta}_2 + 1.5(g^+)^{\frac{1}{2}}sign(\zeta_1 - \hat{\zeta}_1) \\ \dot{\hat{\zeta}}_2 &= \frac{1}{J_m}\tau - \frac{g}{L_m}sin\zeta_1 - \frac{V_s}{J}\hat{\zeta}_2 + 1.1g^+sign(\zeta_1 - \hat{\zeta}_1) \end{aligned} \tag{3.26}$$

The nominal values of the parameters are as $g = 9.815$, $L_m = 1$,$M_m = 1$,$V_s = 0.2$ and $J_m = M_m L_m^2 = 1$. The observer parameters are $g^+ = 6$, $\lambda = 4$ and $\beta = 6.6$. The estimated velocity converges to real velocity in finite time as shown in Fig. 3.7 with $\zeta_1 = x_1$. Estimation error for $\zeta_2 = x_2$ is given in Fig. 3.8. The portrait of errors is shown in Fig. 3.9

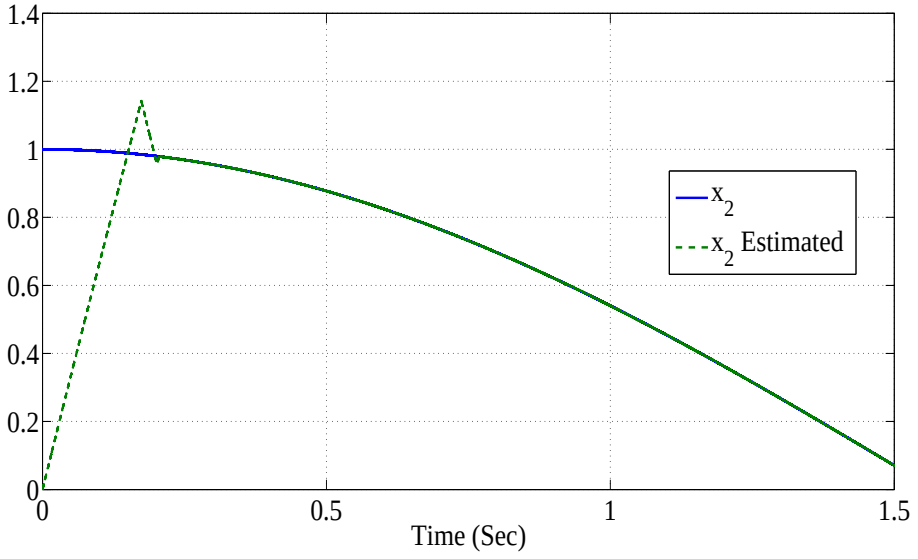

FIGURE 3.7: Real and Estimated Velocity

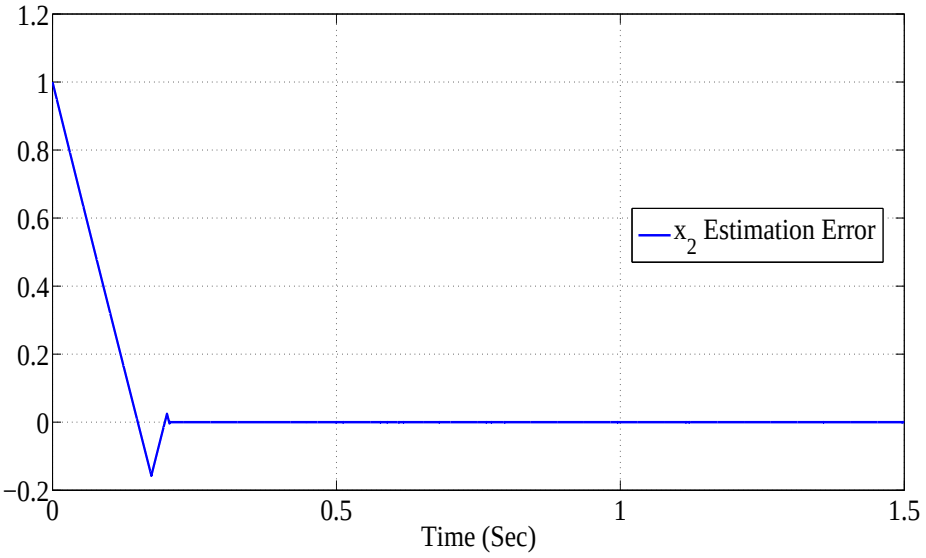

FIGURE 3.8: Estimation Error

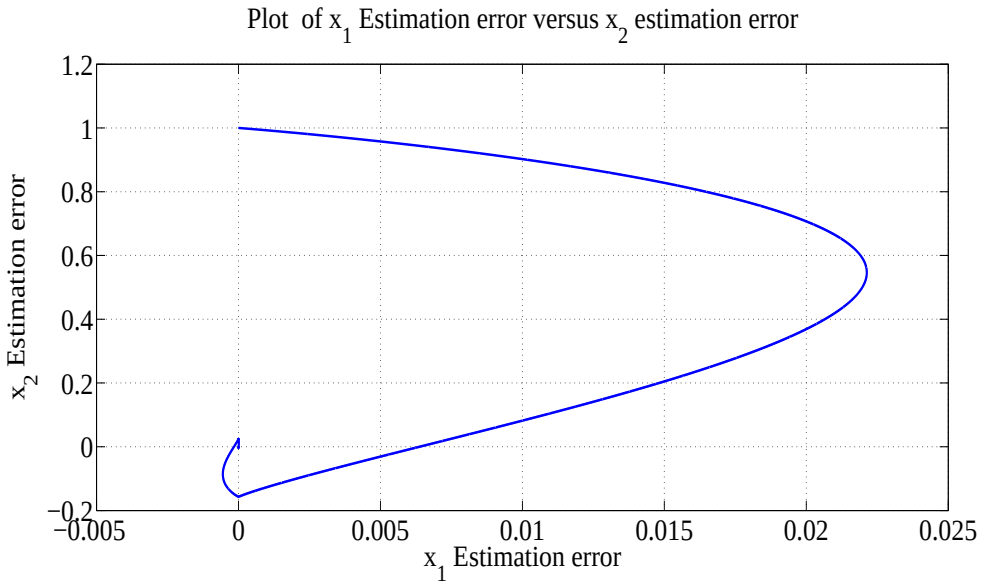

FIGURE 3.9: Phase Portrait

3.3.2 Uniform Second Order Sliding Mode Observer,[6]

Based on the system dynamics *(3.17)*the uniform second order sliding mode observer is given by

$$\dot{\hat{\zeta}}_1 = +p_1\phi_1(s_1) + \hat{\zeta}_2 \quad (3.27)$$

$$\dot{\hat{\zeta}}_2 = +p_2\phi_2(s_1) + g(\zeta_1, \hat{\zeta}_2, t, u) \quad (3.28)$$

$$\hat{y} = \hat{\zeta}_1 \quad (3.29)$$

where

$[\hat{\zeta}_1, \hat{\zeta}_2]^T$ is state estimation vector

and estimation errors are

$s_1 = \zeta_1 - \hat{\zeta}_1$

$s_2 = \zeta_2 - \hat{\zeta}_2$

p_1, p_2 are observer gains which are positive and satisfy conditions to be mentioned later.

$\phi_1(s_1)$ and $\phi_2(s_2)$ are output injection terms which are defined as [6]

$$\begin{aligned} \phi_1(s_1) &= \mu_2|s_1|^{3/2}sign(s_1) + \mu_1|s_1|^{1/2}sign(s_1) \\ \phi_2(s_1) &= \frac{3}{2}\mu_2^2|s_1|^2 sign(s_1) + 2\mu_1\mu_2 s_1 + \mu_1^2 sign(s_1) \end{aligned} \quad (3.30)$$

$\mu_1 \geq 0$ and $\mu_2 \geq 0$ are scalars. The error dynamics of the observer are given as [6]

$$\dot{s}_1 = s_2 - p_1\phi_1(s_1) \quad (3.31)$$

$$\dot{s}_2 = +G(t, \zeta_1, \zeta_2, \hat{\zeta}_2) - p_2\phi_2(s_1) \quad (3.32)$$

$G(\zeta_2, \zeta_1, \hat{\zeta}_2, t) = +\xi(\hat{\zeta}_2, \zeta_1, t, u) + g(\zeta_2, \zeta_1, t, u) - g(\hat{\zeta}_2, \zeta_1, t, u)$

The equation *(3.32)* has a solution in Filippov sense.[66]

Now consider the following definitions.

Theorem 3.5. *[6] Let us assume that* $|G(t, \zeta_2, \zeta_1, \hat{\zeta}_2,)| \leq \chi$ *with* χ *is a constant which is already known. Under the following two conditions the system (3.32) is uniformly exact convergent .*

i) p_1 *and* p_2 *are chosen in such a manner that following two inequalities are satisfied.* $2p_2^2 > p_1^2$ *and* $p_1^2(p_2 - \frac{1}{4}p_1^2) > \chi^2$

ii) $p_2 > \chi$ *and* $p_1^2 > 2p_2$ *or*

Proof. Proof of Theorem 3.5 is given in [6]. □

3.4 Sliding Mode Differentiator

3.4.1 Robust Exact Differentiator [3]

Sliding mode technique has the inherent property of robustness to modeling, parameter uncertainties and disturbance. Therefore the researchers have also used the sliding mode other than the observer and controller design i.e. for derivative estimation. Let $g(t)$ be a Lebesgue measurable signal on $[0, \infty)$ and consisting of a base signal $g_0(t)$ and noise $v(t)$ Base signal $g_0(t)$ has a derivative with Lipschitz constant $L > 0$. The task is to estimate higher derivatives of $g(t)$ from the measurement of $g(t)$. Let us introduce another system with $\dot{z}_0 = v$,$s(t, z_0) = z_0 - g(t)$. The objective is to make $s, \dot{s}$ vanish in finite time by the measurement of $g(t)$ and control. This mean we have to establish 2-sliding mode.

Here the robust exact r^{th} order differentiator proposed by Levant [9],[1] is given as

$$\begin{aligned}
\dot{\chi}_0 &= \zeta_0 \\
\zeta_0 &= \lambda_0|\chi_0 - g(t)|^{r/(r+1)} sign(\chi_0 - g(t)) + \chi_1 \\
\dot{\chi_1} &= \zeta_1, \zeta_1 = \lambda_1|\chi_1 - \zeta_0|^{(r-1)/(r)} sign(\chi_1 - \zeta_0) + \chi_2 \\
&. \\
&. \\
&. \\
\dot{\chi}_{r-1} &= \zeta_{r-1}, \\
\zeta_{r-1} &= \lambda_{r-1}|\chi_{r-1} - \zeta_{r-2}|^{1/2} sign(\chi_{r-1} - \zeta_{r-2}) + \chi_r \\
\dot{\chi}_r &= \lambda_r sign(\chi_r - \zeta_{r-1}) \qquad (3.33) \\
& \qquad (3.34)
\end{aligned}$$

Theorem 3.6. *: [1] If the parameters λ_i are properly chosen, the following equalities hold in finite time in the absence of input noises.*
$\chi_0 = g_0(t); \chi_i = \zeta_{i-1} = g_0^{(i)}(t), i = 1, ..., r$
Moreover the solution of the dynamic systems is finite time stable.

Proof. Proof of Theorem 3.6 is given in [1] □

Example 3.3. *Let $g(t)$ as given below, be the signal to be differentiated*

$$g(t) = 5t + sint + 0.01cos10t \qquad (3.35)$$

The derivative of (3.35) is $dg/dt = 5 + cost - 0.1sin10t$. Now we obtain the derivative of (3.35) by linear differentiator $s/(0.1s+1)^2$ and given in Fig. 3.10. While the derivative obtained by Levant's differentiator is shown in Fig. 3.11. There is a steady state error in linear differentiator while the Levant's differentiator is exact.

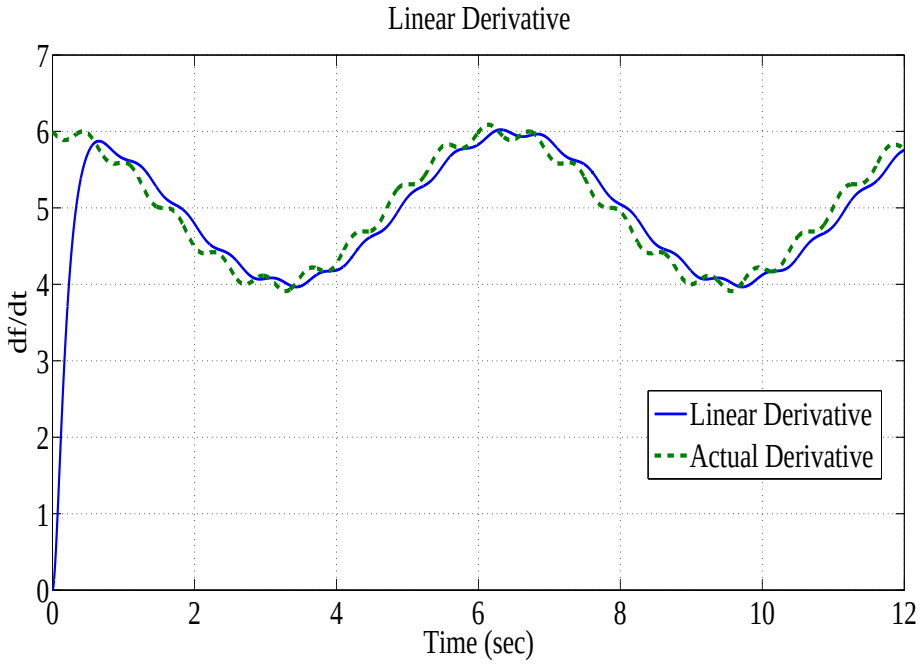

FIGURE 3.10: Linear differentiator results of signal *(3.35)*

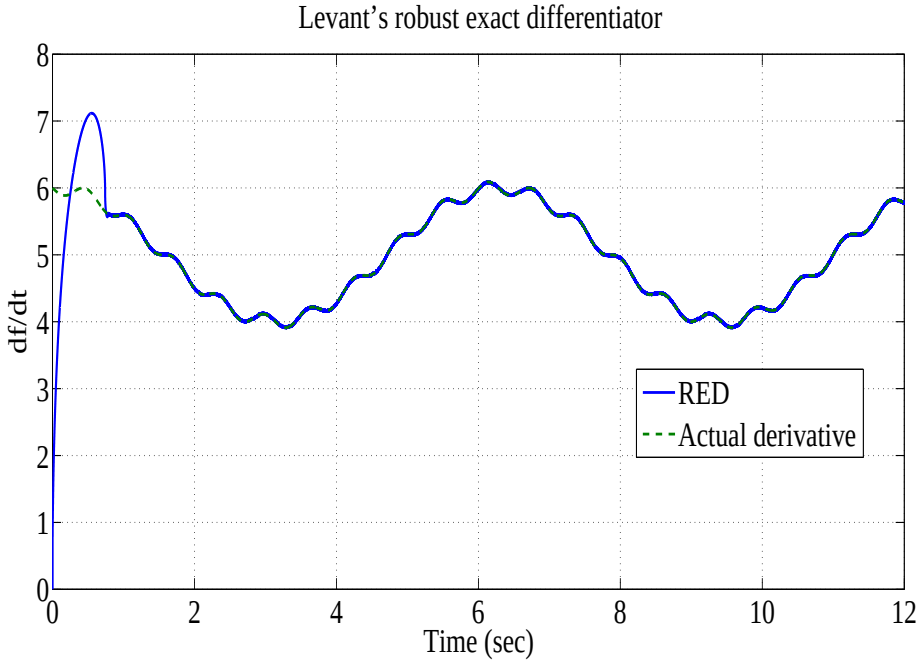

FIGURE 3.11: Levant's differentiator results of signal *(3.35)*

3.4.2 Uniform Robust Exact Differentiator, [7]

The differentiator presented in [7] is second order sliding mode based and provides the derivative of input signal in finite time independent of initial conditions. The structure of differentiator is given below.

Let us assume that the differentiator input $g(t)$ is a Lebesgue-measurable function defined on $[0, \infty)$, $g(t)$ is decomposed into two parts. i.e $f(t) = g_0(t) + v(t)$. The first term $g_0(t)$ is twice differentiable base signal and its derivative has a Lipschitz constant $L > 0$ while the second term is bounded noise signal. The differentiator estimates the derivative of $g(t)$ in the absence of noise in a finite time[7] . Let $\varsigma_0 = g_0(t)$ and $\varsigma_1 = \dot{g}_0(t)$ the state space representation of the base signal is given as

$$\begin{aligned} \dot{\varsigma}_0 &= \varsigma_1 \\ \dot{\varsigma}_1 &= \ddot{g}_0(t) \end{aligned} \tag{3.36}$$

Based on the uniform robust exact differentiator [7] the structure of the estimator is given as

$$\begin{aligned} \dot{z}_0 &= -k_1\phi_1(e_0) + z_1 \\ \dot{z}_1 &= -k_2\phi_2(e_0) \end{aligned} \tag{3.37}$$

Here $e_0 = z_0 - \varsigma_0$

k_1, k_2 are gains which are greater than zero to be designed later. While $\phi_1(e_0)$ and $\phi_2(e_0)$ are injection terms given by [7]

$$\begin{aligned}\phi_1(e_0) &= |e_0|^{\frac{1}{2}} sign(e_0) + \mu |e_0|^{\frac{3}{2}} sign(e_0) \\ \phi_2(e_0) &= \frac{1}{2} sign(e_0) + 2\mu e_0 + \frac{3}{2}\mu |e_0|^2 sign(e_0) \end{aligned} \tag{3.38}$$

μ is a scalar and its value may be equal to or greater than zero. When $\mu = 0$ the robust exact differentiator of [67] is achieved . With $\mu > 0$ the higher order terms $|e_0|^{\frac{3}{2}} sign(e_0)$ and $|e_0|^2 sign(e_0)$ are responsible for uniform convergence of the differentiator. z_0 and z_1 are the estimates of $g_0(t)$ and $\dot{g_0}(t)$ respectively. The estimation error between the differentiator output and base signal derivative is $e_1 = z_1 - \varsigma_1$. Now the estimation error dynamics are given as

$$\dot{e}_0 = -k_1 \phi_1(e_0) + e_1 \tag{3.39}$$

$$\dot{e}_1 = -k_2 \phi_2(e_0) - \ddot{g}_0(t) \tag{3.40}$$

Solution of error dynamics equation exists in Filipov's sense.[66]

When the second derivative of the input signal is bounded with $|\ddot{g}_0(t)| \leq L$, where $L > 0$ a known positive constant and $\mu > 0$ the differentiator *(3.37)* is uniformly exact convergent if the gains k_1, k_2 are in the set given in [7].

Example 3.4. *We compare the Levant's robust differentiator with URED.* $g_0(t) = 5t + sint$ *is base signal to be differentiated and* $v(t) = 0.01cos10t$ *is noise term. The overall*

signal becomes

$$g(t) \quad = \quad 5t + sint + 0.01cos10t \tag{3.41}$$

The derivative of (3.41) is $dg/dt = 5 + cost - 0.1sin10t$. *The simulation results of Levant's differentiator and URED with* $L = 2.5, k_1 = 2\sqrt{3}, k_2 = 6$ *are shown in Fig. 3.12 for initial condition (0,0)and in Fig. 3.13 for initial condition (10,0). In both the cases the URED has better results.*

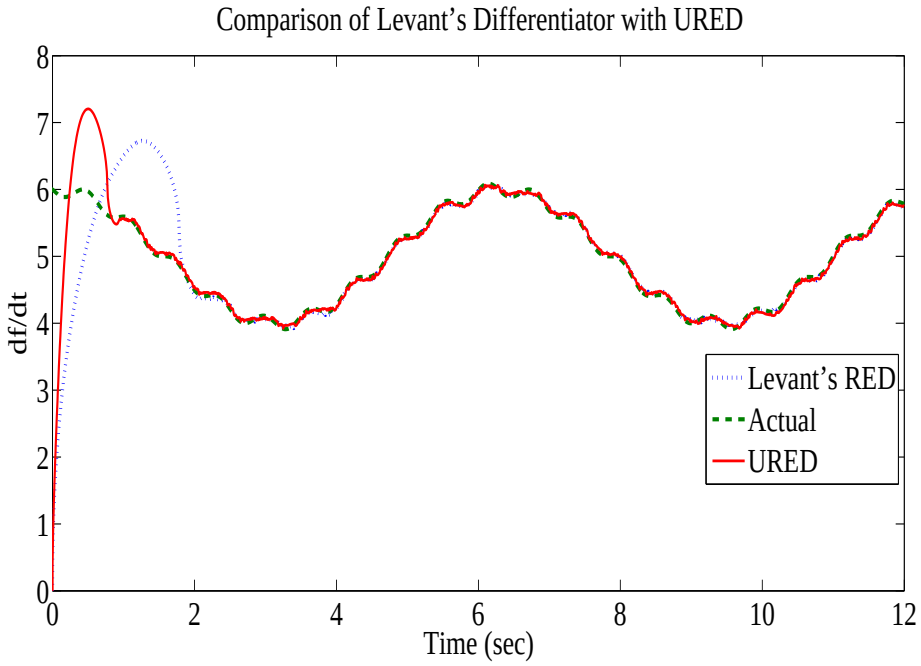

FIGURE 3.12: Differentiation of *(3.41)*, with initial condition (0,0)

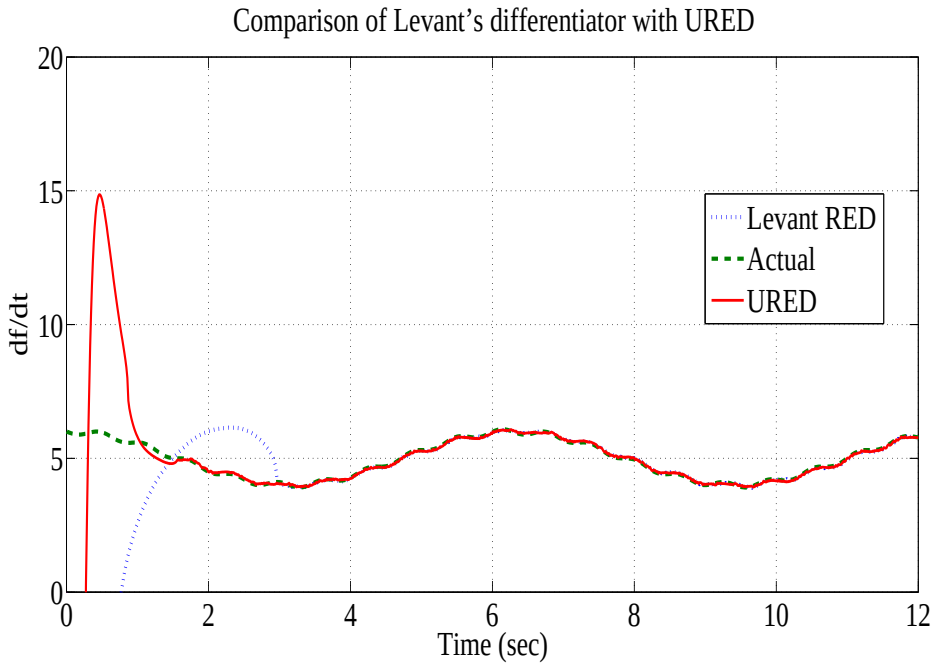

FIGURE 3.13: Differentiation of *(3.41)*, with initial condition (10,0)

3.5 Summary

In this chapter the basic theory of sliding mode based controllers, observers and differentiators had been presented. Super twisting, smooth super twisting, real twisting and smooth real twisting algorithms were discussed. Then second order sliding mode observer and uniform second order sliding mod observers were presented. Robust exact differentiator and uniform robust exact differentiators were discussed with simulation examples. In next chapter three important parameters of a pressurized water reactor will be estimated using sliding mode technique.

Chapter 4

ESTIMATION OF PARAMETERS OF A PRESSURIZED WATER REACTOR

In this chapter three important parameters of a pressurized water reactor are estimated. First parameter i.e. precursor density is estimated using uniform second order sliding mode observer. The remaining two parameters are estimated using uniform robust exact differentiator. Literature review on parameter estimation is given in Section 4.1 Importance of estimated parameters is given in Section 4.2. Pertinent model properties are discussed in Section 4.3. Then the parameters are estimated and their results are discussed in Section 4.4 and 4.5. The summary of work done in this chapter is given in Section 4.6.

4.1 Literature Review

The control, safety and operation of a nuclear reactor mainly depends upon the available measurements of different parameters. There are redundant sensors for measurement of parameters. But most of the parameters cannot be measured directly because of the unavailability of adequate sensors. Different techniques have been used in the past for the estimation of different parameters. Some examples are Qing Li and Bernard, J.A. [14], Cadini, F. and Zio, E. [15], Fazekas et al. [16] , Nagaya et al. [68], Kiss et al. [69], Nahid Sadeghi [70] Gy. Hegyi [71], Monteyne et al [72], Yasunobu Nagaya and Takamasa Mori [73], Mohammad Rahgoshay and Omid Noori-Kalkhoran [74], Vrban et al. [75]. Yasunobu Nagaya and Takamasa Mori [73] devised a method for estimation of effective delayed neutron fraction of different fissile materials. Monte Carlo calculations are used for this purpose. The β_{eff} of fissile materials having different shapes and geometries are estimated. The results are in close agreement with the results obtained by deterministic methods. Rahgoshay et al [74] calculated the temperature reactivity coefficients of coolant and fuel. The control rod worth was also calculated for a nuclear

reactor. To perform the neutronic calculations the reactor core was simulated by computer codes. The value of control rod worth calculated was compared with experimental results and temperature reactivity coefficients were compared with results of simulation model. Vrban et al. [75] calculated the temperature coefficients for the first fuel loading of Mochocvce unit 3 and unit 4. Previously deterministic and stochastic approaches were used separately to get independent results. The reactivity coefficients were estimated for the use in the planned first start up of both reactors. The calculations were performed using MCNP5 1.6 code. For verification of results the experimental data of Mochovce unit 2 was used.

Reactivity and precursor concentration of a nuclear reactor have also been estimated using different techniques in literature. Wang et al. [11],H. Kazeminejad [76],Perez-Cruz, J.H. and Poznyak, A. [77], Diaz et al [78],[79], Bhatt et al[80], Dos et al. [81], Hessam Malmir and Naser Vosoughi [82], Antolin et al. [83], Lobat Tayebi and Daryoosh Vashaee [84]. Peng Wang et al. [11] used first order sliding mode observer to estimate the reactivity in a nuclear reactor. Reactor point kinetic model with nominal parameter values were used for this technique. A sinusoidal input is considered for this scheme and reactivity is estimated. Perez-Cruz, J.H. and Poznyak, A. [77] used neural observer to estimate the internal reactivity and precursor concentration in a research reactor. The parameters are estimated from the available input and neutron power. This observer has also the correction terms which are sliding mode based and Luenberger based. The neural observer is trained by obtaining the data from third order reactor model. Once the observer is trained then it can estimate the parameters from available data with out model. Diaz et al [78] proposed solution of precursor concentration to calculate the reactivity. This method does not require the history of nuclear power and any other transformation. It gives the results with high accuracy depending upon the step size. This method has been validated with different step sizes and different type of powers. Bhatt et al. [80] proposed a method for estimation of shutdown reactivity of a nuclear reactor. Two different techniques for reactivity estimation of reactivity are compared. One technique is Kalman Filtering based and the other is inverse point kinetic. The Kalman Filtering technique proved to be better than the inverse point kinetic technique in terms of robustness, accuracy and noise supression. Qaiser et al. [12], [13] designed a

second order sliding mode observer for estimating the precursor concentration and reactivity of a research reactor. The validated model of Pakistan research reactor was used for parameter estimation. The second derivative of neutron density was estimated from the measurement of neutron density using super twisting algorithm. The experimental results were verified by comparing with theoretically calculated values.

Fuel of nuclear reactor is an important component. Its temperature cannot be measured by available sensors. Its health mainly depends upon temperature. Estimation of fuel temperature and detection of fuel failure system is also found in literature. Terada et al. [85], [86], [87] and Katagiri et al. [88] developed a fuel failure detection system for a nuclear reactor. Vaidya et al. [89] estimated fuel temperature of research reactor in the period of de fuelling. During de fueling the decay heat from fuel is removed by air flow to keep the temperature of fuel in acceptable range. The temperature of fuel for different level of decay is estimated by Phoenix code. The lumped parameter thermal hydraulic model is also use for estimation scheme.

4.2 Importance of Parameters

The short description and importance of precursor density, change in reactivity and average fuel temperature are given below.

4.2.1 Precursor Density

When fission of U_{235} occurs then two fission fragments along with an average about of 2.5 neutrons are emitted. These neutrons are called prompt neutrons as shown in Fig 4.1. Some fission products are unstable and carry a series of decay process. These unstable nuclei are called precursors. These are important because they produce delayed neutrons. Control of a nuclear power reactor is possible due to the presence of delayed neutrons. Following example is considered to analyze the the role of precursor density in reactor control.

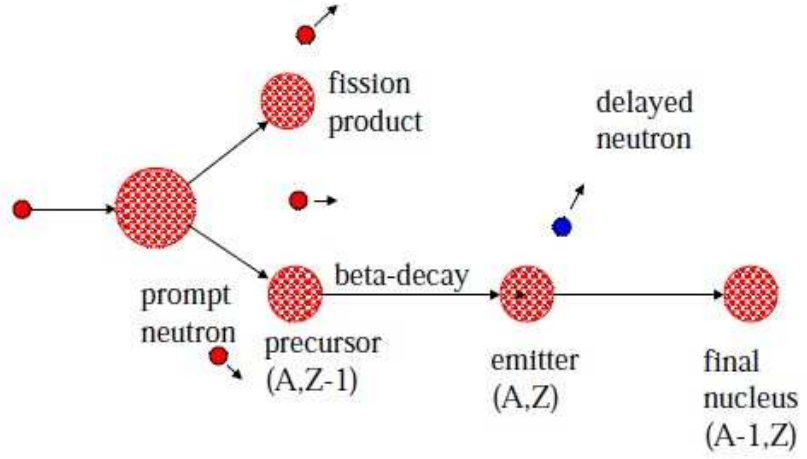

FIGURE 4.1: Production of delayed neutrons

Example 4.1. *The relationship for growth of neutron population in a nuclear fission reaction is given as*

$$n(t) \approx n(0) \exp\left(\frac{t}{T}\right) \tag{4.1}$$

where T is reactor period given by

$T = \frac{l}{k_\infty - 1}$

First we assume that the delayed neutrons do not exist. When $(k_\infty = 1)$ changes to $(k_\infty = 1.001)$ and for U_{235}, in the presence of delayed neutrons $l = 0.06$ sec. the generation will become equal to three times in $t = 60$ sec , which is a controllable quantity.

Now we assume that the delayed neutrons do not exist. When $(k_\infty = 1)$ changes to $(k_\infty = 1.001)$ and for U_{235}, $l = 24e^{-6}$ sec. the generation will become equal to $6.39e^{17}$ times in $t = 1$ sec , which is not a controllable quantity.

The above example shows that the delayed neutrons play important role in control of a nuclear reactor. These delayed neutrons are produced by precursors which cannot be measured directly. Therefore, there is a need to estimate them from the available measurement of other parameters.

4.2.2 Reactivity

Reactivity ρ is defined as

$\rho = (k-1)/k$

where

k= neutron multiplication factor

Approximately 2.5 neutrons are generated in fission of one U_{235} atom. Some of the neutrons are moderated to thermal level and contribute in next fission while other neutrons are leaked out from the core. The neutrons which are still in excess are absorbed by the neutron absorbing material deliberately. For this purpose control rods or soluble neutron poison like boric acid is used. Control rods are made of Cadmium alloy. Boric acid is mixed in coolant in water cooled reactors in order to achieve desired reactivity. If there is a need of positive reactivity then the primary coolant is diluted. Some other parameters also effect the core reactivity like change in coolant temperature, change in fuel temperature and some fission products like Xenon and Samarium which act as neutron poison. Pressurized water reactor has two types of control rods. One type is called "'black rods"' which are used for shutdown purpose. These are not used for control purposes. These rods completely absorb the neutrons and fission chain reaction is stopped. The other type of control rods is called gray rods. These are used for control purposes. These are partially inserted in the core to achieve desired power level. Reactivity is expressed in pcm where 1 $pcm = 10^{-5}\Delta k/k$

4.2.3 Fuel Temperature

Fuel temperature is directly related to the safety of nuclear reactor. It is an important parameter which cannot be measured directly so an observer is required to estimate

it. This parameter depends upon the shape of reactor, but in this work lumped fuel model is considered and average fuel temperature is estimated. The fuel temperature has negative reactivity coefficient so when fuel temperature increases the reactivity decreases. Therefore operation of a pressurized water reactor is inherently safe. But for safety reasons it is necessary to monitor fuel temperature otherwise the clad will rupture and primary coolant will be contaminated.

4.3 Pertinent Model Properties

Let us consider the following nonlinear dynamical system

$$\begin{aligned} \dot{x} &= f(x, p, t, u) \\ y &= h(x, p, t, u) \end{aligned} \tag{4.2}$$

$x \in \Re^n$ are the states of the system

$p \in \Re^p$ are the parameters of the system

$u \in \Re^q$ are the inputs to the system

$y \in \Re^l$ are the states of the system

Following definitions are useful for understanding the coming sections before the estimation scheme.

4.3.1 Observability

In differential geometry, if the following observability matrix is full rank then the nonlinear system *(4.2)* is said to be observable.

$$J_O = \left[\frac{\partial}{\partial x_{j_1}} L_f h_i \right] \tag{4.3}$$

Where i=1,2,3....n and j_1=1,2,3....n

State observer can be designed on the basis of input and available output if the system obeys the observability criteria *(5.4)*.

4.3.2 Identifiability

If the following identifiability matrix does not loose rank then then the system *(4.2)* is called identifiable with respect to parameter p,[46]

$$J_I = \left[\frac{\partial}{\partial p_{j_2}} L_f h_i\right] \tag{4.4}$$

Where i=1,2,3....n and $j_2 = 1, 2, 3....n$

Under identifiability analysis we inspect that the parameters of interest are identifiable or not.

4.4 Estimation of precursor density

In this section uniform second order sliding mode observer is designed for the reactor model and precursor density is estimated. Before the estimation the second order system is developed comprising of known and unknown parts utilizing the first equation of point kinetic model.

4.4.1 Development of system

The first equation of neutronic model of pressurized water reactor is simplified as

$$\dot{n}_r = \frac{\delta\rho - \beta}{\Lambda} n_r + \frac{\beta}{\Lambda} C_r$$

$$\dot{n}_r = \frac{\delta\rho}{\Lambda} n_r - \frac{\beta}{\Lambda} n_r + \frac{\beta}{\Lambda} C_r \tag{4.5}$$

(4.6)

The second derivative of neutron density is given as

$$\ddot{n}_r = \frac{\dot{\delta\rho}}{\Lambda} n_r + \frac{\delta\rho}{\Lambda}\dot{n}_r - \frac{\beta}{\Lambda}\dot{n}_r + \frac{\beta}{\Lambda}(\dot{C}_r) \tag{4.7}$$

The reactivity $\delta\rho$ depends upon the control rod speed, change in fuel temperature and change in coolant temperature. Mathematically reactivity and its derivative can be represented as

$$\begin{aligned} \delta\rho &= \delta\rho_r + \alpha_f(T_f - T_{fo}) + \alpha_c(T_c - T_{co}) = \psi_1 \\ \dot{\delta\rho} &= \delta\dot{\rho}_r + \alpha_f(\dot{T}_f) + \alpha_c(\dot{T}_c) = \psi_2 \end{aligned} \tag{4.8}$$

Then the equation *(4.7)* becomes

$$\ddot{n}_r = \frac{\psi_2}{\Lambda} n_r + \frac{\psi_1}{\Lambda}\dot{n}_r - \frac{\beta}{\Lambda}\dot{n}_r + \frac{\beta}{\Lambda}(\lambda n_r - \lambda C r) \tag{4.9}$$

Where

$$\begin{aligned} \psi_1 &= \rho(t) = \delta\rho_r + \alpha_f(T_f - T_{fo}) + \alpha_c(T_c - T_{co}) \\ \psi_2 &= \alpha_f(\dot{T}_f) + \alpha_c(\dot{T}_c) + \dot{\delta}\rho_r \end{aligned} \tag{4.10}$$

writing *(4.9)* in state space and taking

$$\begin{aligned} x_1 &= n_r(t) \\ \dot{x}_1 &= x_2 = \dot{n}_r \\ \ddot{x}_1 &= \dot{x_2} = \ddot{n}_r \\ \dot{x}_2 &= \frac{\psi_2}{\Lambda}x_1 + \frac{\psi_1}{\Lambda}x_2 - \frac{\beta}{\Lambda}x_2 + \frac{\beta}{\Lambda}\lambda x_1 - \frac{\beta}{\Lambda}\lambda C_r \end{aligned} \tag{4.11}$$

The equation *(4.11)* can be written as

$$\begin{aligned} \dot{x}_1 &= x_2 = f_1(x,t,u) \\ \dot{x}_2 &= \frac{\psi_2}{\Lambda}x_1 + \frac{\psi_1}{\Lambda}x_2 - \frac{\beta}{\Lambda}x_2 + \frac{\beta}{\Lambda}\lambda x_1 - \frac{\beta}{\Lambda}\lambda \hat{C}_r = f_2(x,t,u) \end{aligned} \tag{4.12}$$

4.4.2 observability analysis

The observability Jacobian for system *(4.12)* is given as

$$JO_1 = \begin{bmatrix} \frac{\psi_1-\beta}{\Lambda} & 0 \\ \frac{\psi_2}{\Lambda} + \frac{\beta}{\Lambda}\lambda & \frac{\psi_1}{\Lambda} - \frac{\beta}{\Lambda} \end{bmatrix} \tag{4.13}$$

where $0 \leq \psi_1 \leq |\gamma_1|$ and $0 \leq \psi_2 \leq |\gamma_2|$ and $|\gamma_1|, |\gamma_2|$ are slightly greater than zero. x_1 is greater than zero. The observability Jacobian is non singular which confirms the observability of system *(4.12)*

4.4.3 Structure of observer

The structure of the observer for the system *(4.12)* is given as

$$\begin{aligned} \dot{\hat{x}}_1 &= \hat{x}_2 + k_1\phi_1(\tilde{x}_1) \\ \dot{\hat{x}}_2 &= \frac{\psi_2}{\Lambda}x_1 + \frac{\psi_1}{\Lambda}\hat{x}_2 - \frac{\beta}{\Lambda}\hat{x}_2 + \frac{\beta}{\Lambda}x_1 + k_2\phi_2(\tilde{x}_1) \end{aligned} \tag{4.14}$$

Where

x_1 is output available from measurement, $\hat{x}_2$ is estimate of $\dot{x_1}$ and other parameters are known.

Using the structure of system model *(4.12)* and observer *(4.14)*, the error dynamics are

$$\dot{\tilde{x}}_1 = \tilde{x}_2 - k_1\phi_1(\tilde{x}_1) \tag{4.15}$$

$$\dot{\tilde{x}}_2 = -\frac{\beta}{\Lambda}\lambda\hat{C}r - k_2\phi_2(\tilde{x}_1) \tag{4.16}$$

4.4.4 Precursor density

For sliding mode $\tilde{x}_1 = s$ is taken as sliding surface and when system reaches the sliding mode the sliding surface $\tilde{x}_1$ approaches zero and $\dot{\tilde{x}}_2$ goes to zero then the error equation *(4.16)* becomes $k_2\phi_2(\tilde{x}_1) = -\frac{\beta}{\Lambda}\lambda\hat{C}r$, solving the above equation for $\hat{C}_r$ we have

$$\hat{C}r = -k_2\phi_2(\tilde{x}_1)\frac{\Lambda}{\beta}/\lambda \tag{4.17}$$

TABLE 4.1: Observer gain

Parameter	Value	Parameter	Value
μ_1	1.5	μ_2	1.5
k_1	20	k_2	50

4.4.5 Experimental results

The nonlinear model of a pressurized water reactor has been validated in Section 2.4. This validated model has been used for estimation of precursor density. System model is developed in standard form of uniform sliding mode observer in Section 4.4.1. Then the observer is designed for the formulated model. The estimated value of precursor density is obtained from *(4.17)*. Observer gains used for observer are shown in Table 4.1. With these observer gains convergence is achieved in finite time. Estimated and Modeled precursor density are given in Fig. 4.2 and Fig. 4.3 respectively. The comparison of estimated and modeled precursor density is given in Fig. 4.4 and error between them is given in Fig. 4.5. Estimated and modeled precursor density are same in steady state but differ in varying load conditions slightly. This difference is due to the value of decay constant in modeled precursor density which is assumed to be constant. The estimated results show that this value is a function of decrease or increase in power level.

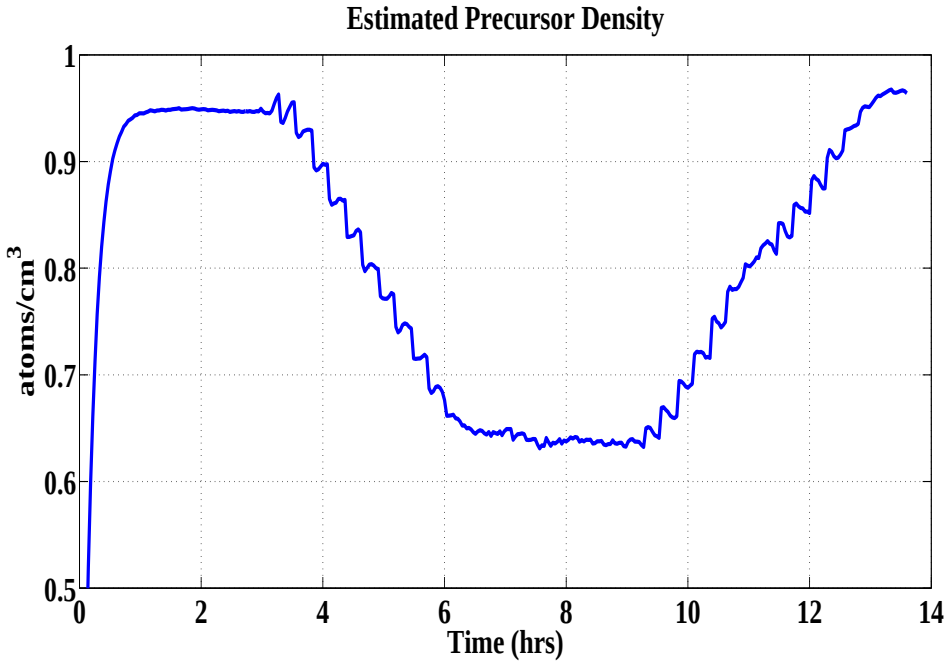

FIGURE 4.2: Estimated Precursor Density from experiment

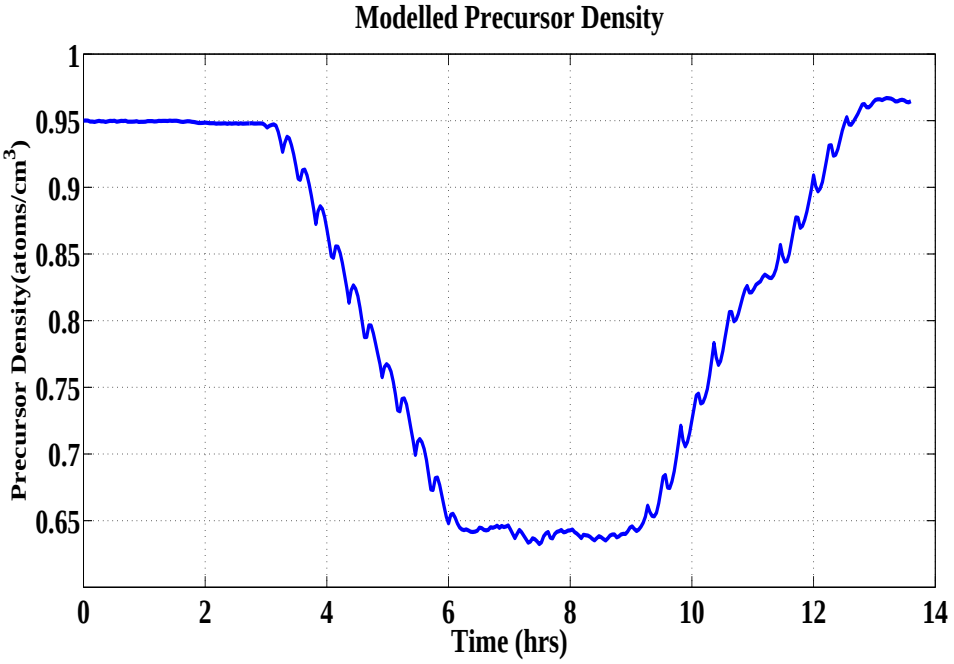

FIGURE 4.3: Modeled Precursor Density

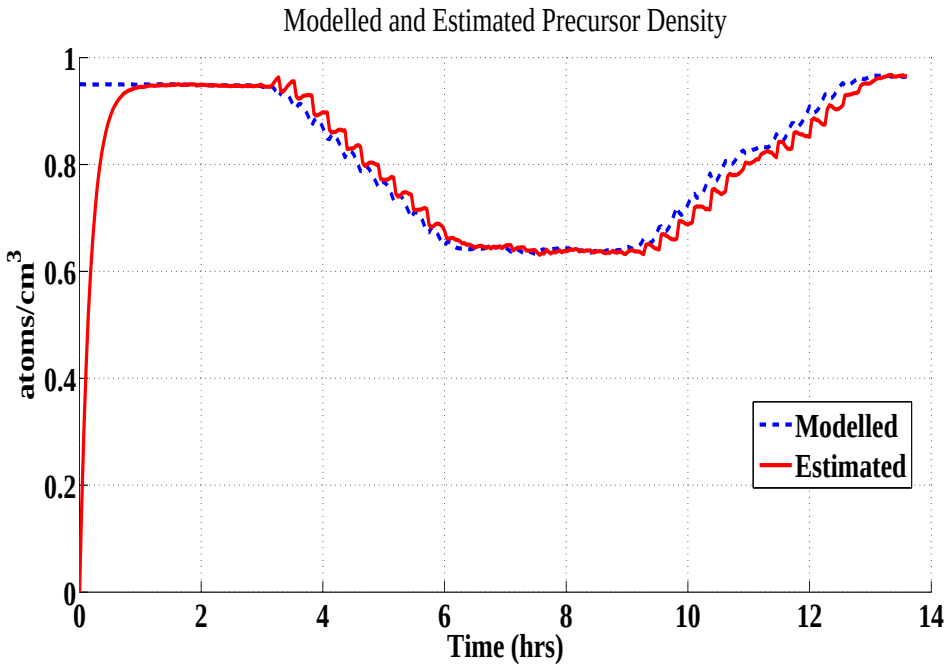

FIGURE 4.4: Comparison of Estimated and Modelled Precursor Density

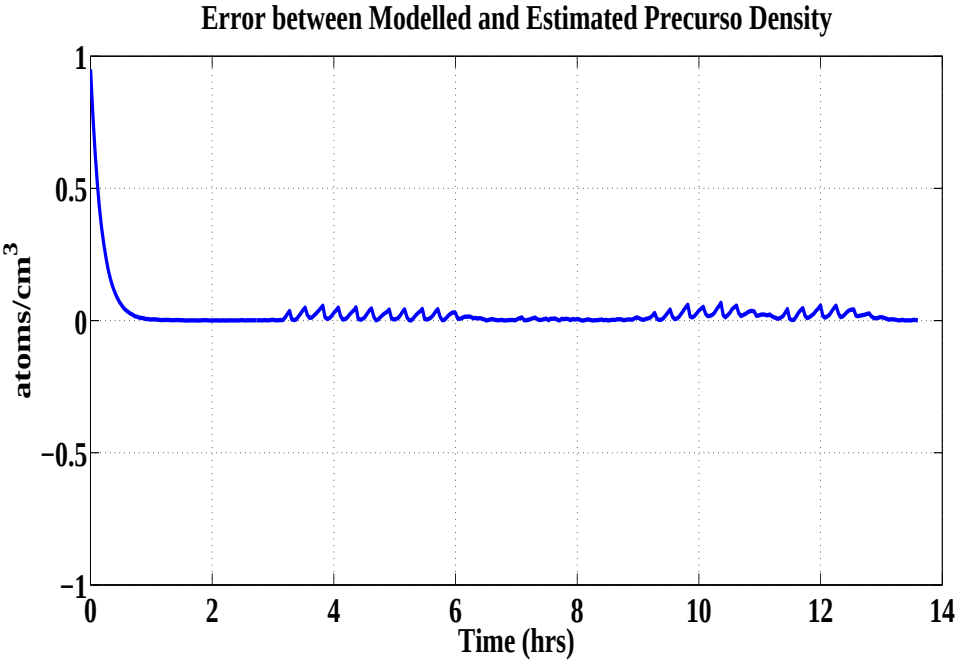

FIGURE 4.5: Error between Estimated and Modelled Precursor Density

4.5 Estimation of change in reactivity and average fuel temperature

The equations of neutron density *(2.1)* with the single delayed neutron group and reactor coolant temperature leaving the core *(2.9)* can written in state space as

$$\dot{x}_1 = \frac{\delta\rho}{\Lambda}x_1 - \frac{\beta}{\Lambda}x_1 + \frac{\beta}{\Lambda}C_r \tag{4.18}$$

$$\dot{x}_2 = \frac{1}{\mu_c}\left[(1-f_f)P_{a0}x_1 + \Omega T_f - \psi_3 x_2 + \psi_4 T_e\right] \tag{4.19}$$

where

$$\psi_3 = \frac{2M+\Omega}{2}$$

$$\psi_4 = \frac{2M-\Omega}{2}$$

Here x_1 denotes the neutron density and x_2 denotes the coolant temperature at outlet of the reactor core. These are two outputs of reactor and measurements are available.

4.5.1 Observability Analysis

For observability analysis $f(x,p,t,u)$ and $h(x,p,t,u)$ are as

$$f(x,p,t,u) = \begin{bmatrix} \frac{\delta\rho}{\Lambda}x_1 - \frac{\beta}{\Lambda}x_1 + \frac{\beta}{\Lambda}C_r \\ \\ \frac{1}{\mu_c}\left[(1-f_f)P_{a0}x_1 + \Omega T_f - \psi_3 x_2 + \psi_4 T_e\right] \end{bmatrix} = \begin{bmatrix} f_3\left(x,p,t,u\right) \\ f_4\left(x,p,t,u\right) \end{bmatrix} \tag{4.20}$$

$$h(x,p,t,u) = \begin{bmatrix} y_1 \\ y_2 \end{bmatrix} = \begin{bmatrix} x_1 \\ x_2 \end{bmatrix} \tag{4.21}$$

The observability matrix J_O2 for the system dynamics *(4.20)* and *(4.21)* becomes

$$J_O2 = \begin{bmatrix} \frac{\delta\rho-\beta}{\Lambda} & 0 \\ \\ \frac{1}{\mu_c}(1-f_f)P_{a0} & -\psi_3 \end{bmatrix} \tag{4.22}$$

The determinant of observability matrix *(4.22)* is given as

$$\begin{aligned} |J_O2| &= -\frac{\delta\rho-\beta}{\Lambda}\psi_3 \\ &\neq 0 \end{aligned}$$

The difference $\delta\rho - \beta$ is non zero , parameter Λ is a constant value and ψ_3 is also nonzero so that the observability matrix does not loose its rank which confirms system observability.

4.5.2 Identifiability Analysis

Here identifiability condition of change in reactivity $\delta\rho$ and average fuel temperature T_f is checked for system *(4.20)* and *(4.21)*.

$$p = \begin{bmatrix} p_1 \\ p_2 \end{bmatrix} = \begin{bmatrix} \delta\rho \\ T_f \end{bmatrix} \tag{4.23}$$

For the dynamics of *(4.20)* and *(4.21)* the identifiability Jacobian comes out to be

$$J_I = \begin{bmatrix} \frac{x_1}{\Lambda} & 0 \\ \\ 0 & \frac{\Omega}{\mu_c} \end{bmatrix} \tag{4.24}$$

The determinant of identifiability matrix *(4.24)* is given as

$$\begin{aligned} |J_I| &= -\frac{x_1}{\Lambda}\frac{\Omega}{\mu_c} \\ &\neq 0 \end{aligned} \tag{4.25}$$

The parameters x_1 is measurement of neutron density which is greater than zero, Λ and Ω are constants greater than zero so that the identifiability matrix does not loose its rank which confirms the system identifiability.

4.5.3 Estimation of Change in Reactivity

Uniform robust exact differentiator observer is designed for estimation of change in reactivity of a pressurized water reactor. The derivative of neutron density is estimated using URED *(3.37)* from the measurement of neutron density. The differentiator *(3.37)* for neutron density is given as

$$\begin{aligned} \dot{z}_0 &= -k_1\phi_1(e_0) + z_1 \\ \dot{z}_1 &= -k_2\phi_2(e_0) \end{aligned} \tag{4.26}$$

where k_1 and k_2 are observer gains to be designed. e_0 is the sliding surface and it is the difference between estimate of neutron density, x_1 ant its measurement. e_1 is difference between estimate of derivative of neutron density, x_1 and its actual derivative. These two are given as

$$\begin{aligned} e_0 &= z_0 - x_1 \\ e_1 &= z_1 - \dot{x}_1 \end{aligned} \tag{4.27}$$

The error dynamics for *(4.26)* are [7]

$$\begin{aligned}\dot{e}_0 &= -k_1\phi_1(e_0) + z_1 - \dot{x}_1 \\ \dot{e}_1 &= -k_2\phi_2(e_0) - \ddot{x}_1\end{aligned}$$

The second derivative of neutron density $|\ddot{x}_1|$ is bounded by its Lipschitz constant. When the sliding mode is established, the differentiator gives the estimate of x_1 as z_o and derivative of x_1 as z_1. This means that the differentiator estimates the derivative of x_1 in a finite time independent of initial conditions. Substituting $\dot{x}_1$ in *(4.18)* with z_1

$$\frac{\delta\rho}{\Lambda}x_1 - \frac{\beta}{\Lambda}x_1 + \frac{\beta}{\Lambda}C_r = z_1 \tag{4.28}$$

Solving *(4.28)* for $\hat{\delta\rho}$ we get

$$\hat{\delta\rho} = \frac{\Lambda}{x_1}z_1 - \frac{\beta}{x_1}C_r + \beta \tag{4.29}$$

Here prompt neutron life time Λ , delayed neutron fraction β are known reactor parameters, precursor density C_r is known from model *(2.2)* with single delayed neutron group , neuton density x_1 is available measurement, k_1 is design constant ,z_0 and z_1 are defined based on *(4.26)* for the measurement of neutron density. The estimated change in reactivity is overall change in reactivity due to control rods, temperature feedback due to fuel and coolant. The estimated value is zero at constant power level. This value decreases with decreasing power level and increases with increases in power level. The comparison of filtered version of estimated change in reactivity *(4.29)* and calculated change in reactivity *(2.11)* is given in Fig. 4.6. The error between estimated and calculated change in reactivity is given in Fig. 4.7. The sliding surface e_0 is given in Fig. 4.8 which shows the convergence of observer.

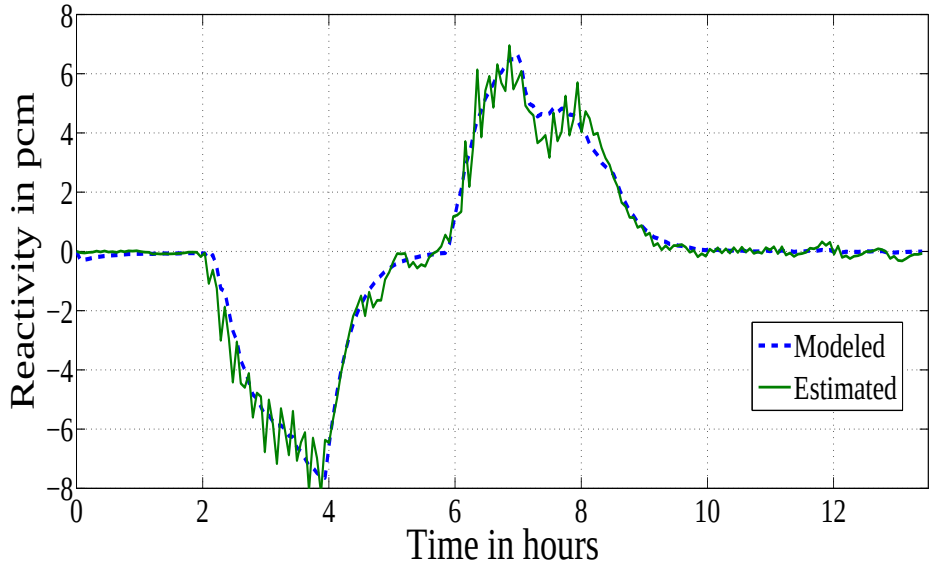

FIGURE 4.6: Comparison of Estimated from experiment and Modeled change in Reactivity

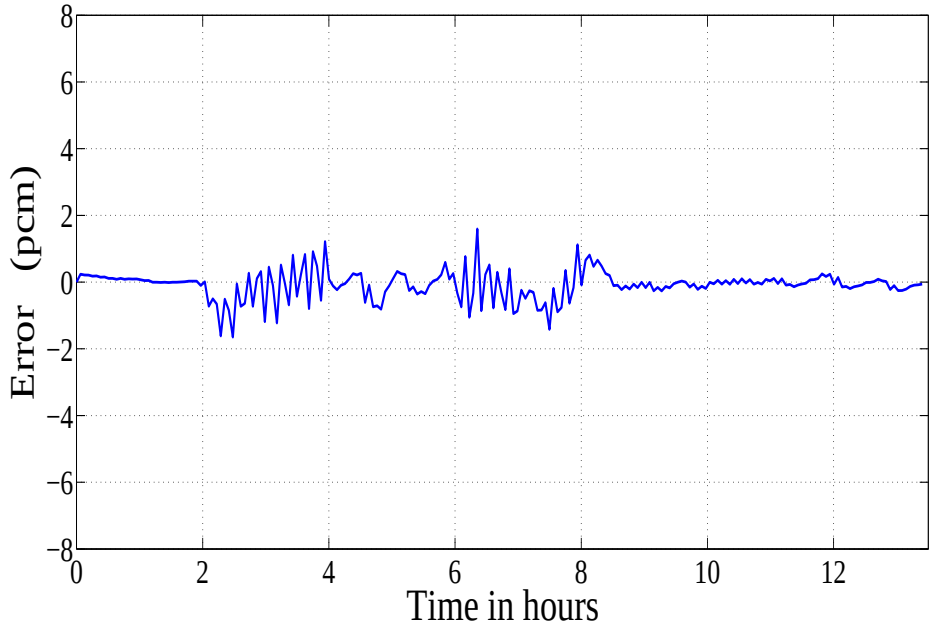

FIGURE 4.7: Error in Estimated and Modeled change in Reactivity

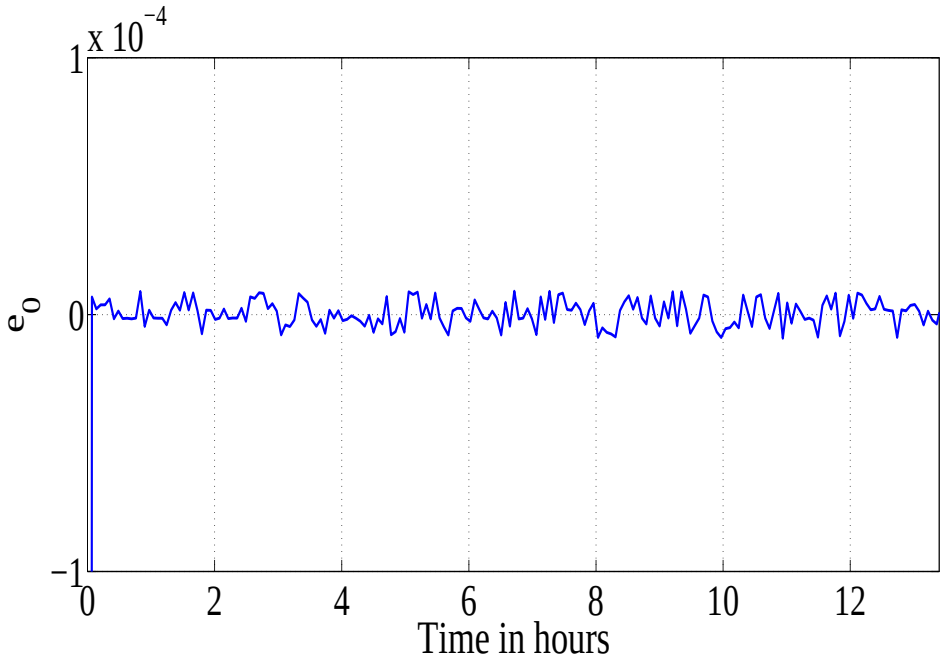

FIGURE 4.8: e_0, (Error between Measured and Estimated Neutron Density)

4.5.4 Estimation of Average Fuel Temperature

Uniform robust exact differentiator observer is designed for estimating the average fuel temperature of a pressurized water reactor. The first derivative of coolant leaving the reactor core is estimated by using the measurement of coolant temperature. Then the state equation *(4.19)* is used to calculate average fuel temperature of reactor. The design procedure is given below

In *(4.19)*, $x_1 = n_r$ is the neutron density and $x_2 = T_l$ is reactor coolant temperature at outlet of core. Then URED for this system becomes

$$\begin{aligned} \dot{z}_3 &= -k_3\phi_3(e_3) + z_4 \\ \dot{z}_4 &= -k_4\phi_4(e_3) \end{aligned} \tag{4.30}$$

Where

$$\begin{aligned}\phi_3(e_3) &= |e_3|^{\frac{1}{2}}\, sign(e_3) + \mu\, |e_3|^{\frac{3}{2}}\, sign(e_3)\\ \phi_4(e_3) &= \frac{1}{2} sign(e_3) + 2\mu e_3 + \frac{3}{2}\mu\, |e_3|^2\, sign(e_3)\end{aligned}$$

where e_3 is the sliding surface defined as the difference between estimate of x_2 ant its measurement and e_4 is difference between estimate of derivative of x_2 and its actual derivative. These are given as

$$\begin{aligned}e_3 &= z_3 - x_2\\ e_4 &= z_4 - \dot{x}_2\end{aligned}$$

The error dynamics for *(4.30)* are

$$\begin{aligned}\dot{e}_3 &= -k_3\phi_3(e_3) + z_4 - \dot{x}_2\\ \dot{e}_4 &= -k_4\phi_4(e_3) - \ddot{x}_2\end{aligned}$$

When sliding phase is reached z_3 gives the estimate of the measurement of coolant temperature and z_4 gives the the estimated first derivative of coolant temperature x_2. Now equating *(4.19)* to z_4 we have

$$z_4 = \frac{1}{\mu c}\left[(1-f_f)P_{a0}x_1 + \Omega T_f - \psi_1 x_2 + \psi_2 T_e\right] \qquad (4.31)$$

Solving *(4.31)* for $\hat{T}_f$ we get

$$\hat{T}_f = \frac{1}{\Omega}\left[\mu_c z_4 - (1 - f_f)\, P_{a0} x_1 + \psi_1 x_2 - \psi_2 T_e\right] \tag{4.32}$$

The equation *(4.32)* gives the estimate of average fuel temperature. $\Omega, \mu_c, (1 - f_f), P_{a0}, \psi_1$and ψ_2 are constant parameters and measurements of neutron density and temperature of coolant leaving the reactor are available. The differentiator $z_4$gives the estimate of the estimate of the derivative of the measurement of coolant temperature and z_3 gives the estimate of the measurement of coolant temperature. The comparison of filtered version of estimated average fuel temperature *(4.32)* modeled average fuel temperature *(2.8)* is given in Fig. 4.9. The error between them is given in Fig. 4.10. The sliding surface e_3 which is difference in measured and estimated coolant temperature is given in Fig. 4.11. Observer gains are given in Table 4.2

TABLE 4.2: Observer gain

Parameter	Value	Parameter	Value
k_1	0.1	k_2	1
k_3	9	k_4	25
μ	1	-	-

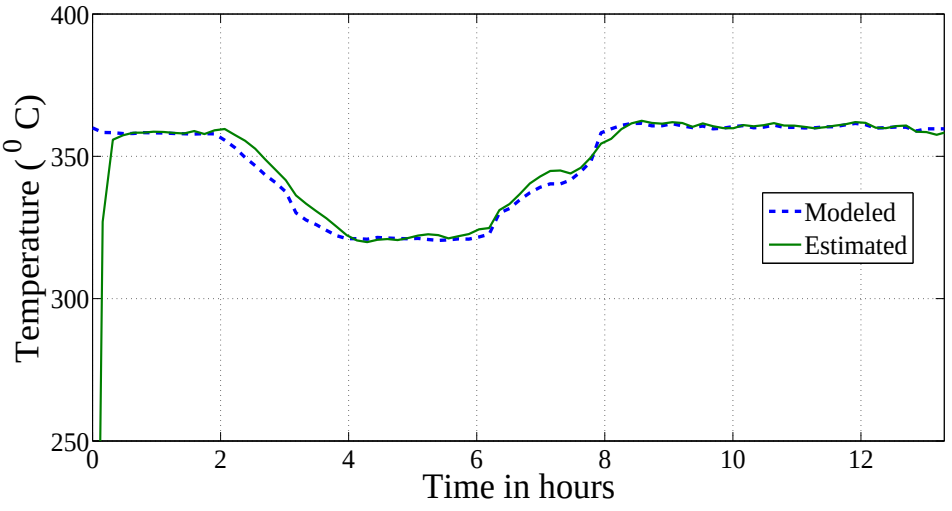

FIGURE 4.9: Comparison of Estimated from experiment and Modeled Average Fuel Temperature

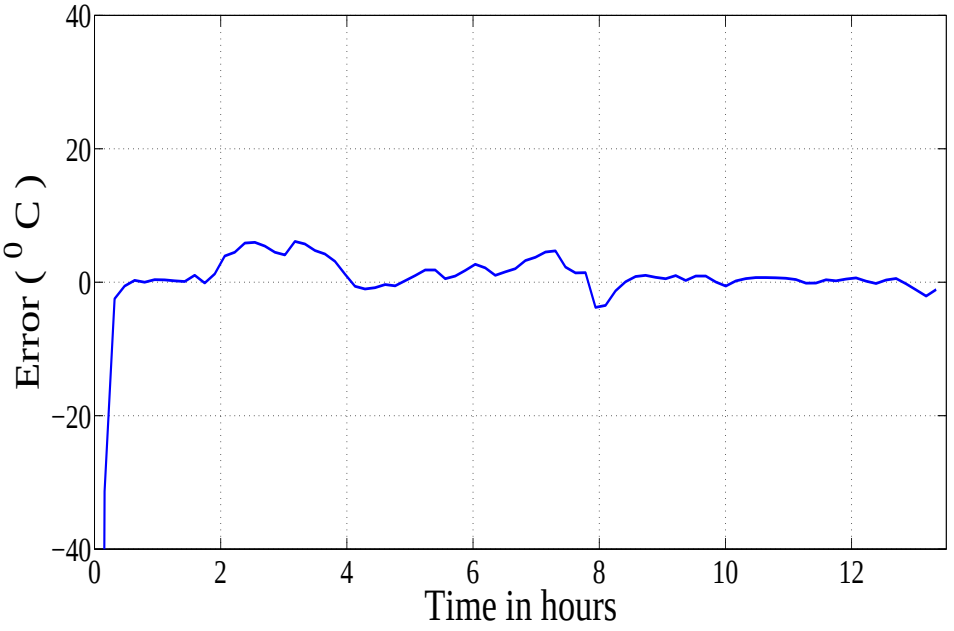

FIGURE 4.10: Error in Estimated and Modeled Average Fuel Temperature

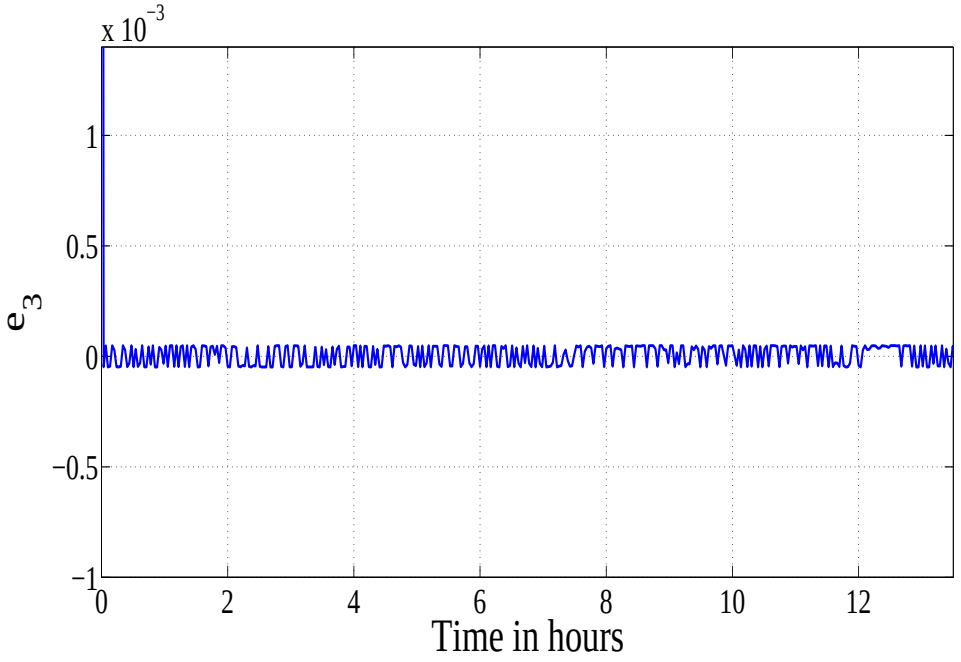

FIGURE 4.11: e_3, (Error between Measured and Estimated Coolant Temperature)

4.6 Summary

In this chapter we have estimated three important parameters of a pressurized water reactor. Uniform second order sliding mode observer was designed for reactor model and precursor density was estimated. Then a uniform robust exact differentiator observer was designed for reactor neutronic and coolant temperature model. Change in reactivity and average fuel temperature were estimated using this observer. In the next chapter sliding mode based controller will be designed to control the power of a pressurized water reactor.

Chapter 5

CONTROL OF NUCLEAR POWER BY SECOND ORDER SLIDING MODE

The control of a nuclear power plant is a difficult job as the dynamics of nuclear power plant are time varying and nonlinear. One method to design controller is to linearize the plant model about the equilibrium point and then design controller [17]. But the behavior of controller will be satisfactory only near the equilibrium point. Therefore a controller is required which can satisfactorily work for the non linear model. In this chapter two different strategies have been used for controlling the output power of nuclear reactor. First super twisting algorithm is used with output power feedback. Then real twisting algorithm is used to control the average coolant temperature and power.

5.1 Literature Review

Different methods are found in literature to regulate the output power of a nuclear reactor. Dong Zhe [90], [91], Torabi et al. [92], Hashemian, H.M. [93], Dasgupta et al. [94], RojasRamrez et al. [95], Gang Li and Fuyu Zhao [96] and Munje et al. [97] are few to mention. Non linear state feedback dissipation power level control is proposed in [91]. This technique ensures asymptotic closed loop stability and state observation. Hamiltonian function is used for closed loop stability. The power level control law is highly satisfactory with high observer gain and proper feedback gain. H.Eliasi [98] presented a model predictive control of PWR which is also robust. This controller can be used for load following operation by considering robust constraints on input and output. In this work five state model of PWR is used. These five states are neutron density, precursor density, Iodine concentration, Xenon concentration and control rod speed. The drawback of this method is not taking into account the model of fuel and coolant temperatures which can also effect the robustness and performance of the controller. Graphical modeling of a nuclear power plant was done based on the reactor average

coolant temperature [99]. Initial condition was set to 100% of full power then load was decreased to 20% of full power. Simulations were done using traditional control and fuzzy control and better results were obtained using fuzzy control. The quantitative feedback theory method is used for robust power level control of a pressurized water reactor [91]. Uncertain nonlinear dynamic system has been considered for the reactor. Robust stability of controller is analyzed and robust tracking is achieved. The proposed controller has a satisfactory performance over a wide range of operating conditions. Sliding mode technique has also been used to control the output power of a nuclear reactor. Zhengyu et al. [100], Qaiser et al. [19] and Munje et al. [101] are few examples. Zhengyu et al. [100] designed a recursive sliding mode controller for an advanced boiling water reactor to control reactor water level, reactor pressure and turbine power. The controller works in recursive way and easily rejects disturbances. For implementation of controller the model is transformed to canonical form and designed controller has also better performance than the conventional PID controller. Qaiser et al. [19] validated the linear and nonlinear model of a research reactor and designed a second order sliding mode controoler to control output power of reactor. The designed controller has good performance and robustness properties.

5.2 Controllability

The nonlinear model of a PWR consists of nine states. Seven states describe the neutronic behavior of the reactor and remaining two are related to thermal hydraulic behavior of the reactor. The states of neutronic model are normalized neutron density and remaining six are normalized precursor density. While the states of thermal hydraulic model are fuel temperature and coolant temperature. The dynamical model of PWR is

[17]

$$
\begin{aligned}
\frac{dn_r}{dt} &= \frac{\rho-\beta}{\Lambda}n_r + \frac{1}{\Lambda}\sum_{i=1}^{6}\beta_i c_{ri} \\
\frac{dc_{ri}}{dt} &= \lambda_i n_r - \lambda_i c_{ri}, \quad i = 1, 2.....6 \\
\frac{dT_f}{dt} &= \frac{1}{\mu_f}[f_f P_{a0} n_r - \Omega T_f + \frac{\Omega}{2}T_l + \frac{\Omega}{2}T_e] \\
\frac{dT_l}{dt} &= \frac{1}{\mu_c}(1-f_f)P_{a0}n_r + \frac{\Omega T_f}{\mu_c} - \frac{2M+\Omega}{2\mu_c}T_l \\
&\quad + \frac{2M-\Omega}{2\mu_c}T_e
\end{aligned}
\tag{5.1}
$$

$$
\rho = \delta\rho_r + \alpha_c(T_c - T_{c0}) + \alpha_f(T_f - T_{f0}) \tag{5.2}
$$

The system states are: $[n_r, c_r, T_f, T_l]^T$

Input is $[\delta\rho_r]$

Outputs are $[n_r, T_l]$

Initial equilibrium temperatures of coolant and fuel are given as [8]

$$
\begin{aligned}
T_{c0} &= \frac{P_{a0}n_r}{2M} + T_e \\
T_{f0} &= \frac{f_f P_{a0} n_r}{\Omega} + T_{c0}
\end{aligned}
$$

This model has been validated using the parameter values in Appendix-A and experimental data of an actual plant in [102]. Two measurable quantities normalized power and coolant temperature are compared with the corresponding modeled *(5.1)* values. A transient situation is selected in which power level remains constant at 95% for two hours. The power decreases to 65% in next two hours. This level is maintained for two hours then it is brought to origonal level. Now the validated model can be used for

controller design for steady state and transient situations.

5.2.1 Controllability Analysis

Before designing controller we check that the system is controllable or not. For this we find the controllability Jacobian of *(5.1)* using Lie algebra. This Jacobian must be full rank. The nonlinear system is written as

$$\dot{x} = f(x) + g(x)u \tag{5.3}$$

f and g being smooth vector fields.

Definition:- Let f and g be two vector fields on $\Re^n$. The Lie bracket of f and g is a third vector field defined by [103]

$[f, g] = \nabla g f - \nabla f g$

The Lie bracket is commonly written as $ad_f g$. Repeated Lie brackets are defined as

$ad_f^0 g = g$

$ad_f^i g = [f, ad_f^{i-1} g] \;\; i = 1, 2, 3....$

The controllability Jacobian for a fourth order system *(5.3)* is given as

$$J_C = \begin{bmatrix} g & ad_f g & ad_f^2 g & ad_f^3 g \end{bmatrix} \tag{5.4}$$

For the model *(5.1)* $f(x)$ and $g(x)$ are given as

$$f(x) = \begin{bmatrix} \frac{-\beta}{\Lambda} x_1 + \frac{\beta}{\Lambda} x_2 \\ \lambda x_1 - \lambda x_2 \\ \frac{1}{\mu_f}[f_f P_{a0} x_1 - \Omega x_3 + \frac{\Omega}{2} x_4 + \frac{\Omega}{2} T e] \\ \frac{1}{\mu_c}[1 - f_f P_{a0} x_1 + \Omega x_3 - \frac{2M+\Omega}{2} x_4 + \frac{2M-\Omega}{2} T e] \end{bmatrix} \tag{5.5}$$

where $[x_1, x_2, x_3, x_4]^T = [n_r, c_r, T_f, T_l]^T$

$$g(x) = \begin{bmatrix} \frac{1}{\Lambda} x_1 & 0 & 0 & 0 \end{bmatrix}^T \tag{5.6}$$

The controllability matrix for system *(5.1)* is given as

$$J_C = \begin{bmatrix} A_1 & A_2 & A_3 & A_4 \end{bmatrix} \tag{5.7}$$

$A_1 = g$

$$ad_f^1 g = \begin{bmatrix} f & g \end{bmatrix} = \nabla g.f - \nabla f.g \tag{5.8}$$

f and g are given in *(5.5)* and *(5.6)*

$\nabla g.f =$

$$\begin{bmatrix} \frac{-\beta}{\Lambda^2}x_1 + \frac{\beta}{\Lambda^2}x_2 + \frac{\alpha_f}{\Lambda}(x_3 - T_{f0})x_1 + \frac{\alpha_f}{\Lambda}(x_4 - T_{c0})x_1 \\ 0 \\ 0 \\ 0 \end{bmatrix} \tag{5.9}$$

$$\nabla f.g = \begin{bmatrix} \frac{-\beta}{\Lambda^2}x_1 \\ \\ \frac{\lambda}{\Lambda}x_1 \\ \\ \frac{1}{\Lambda\mu_f}f_f P_{a0}x_1 \\ \\ \frac{1}{\Lambda\mu_c}(1 - f_f)P_{a0}x_1 \\ \\ \end{bmatrix} \tag{5.10}$$

$$= \begin{bmatrix} \frac{-\beta}{\Lambda^2} x_1 \\ \\ \frac{\lambda}{\Lambda} x_1 \\ \\ \frac{1}{\Lambda \mu_f} f_f P_{a0} x_1 \\ \\ \frac{1}{\Lambda \mu_c} (1 - f_f) P_{a0} x_1 \\ \\ \end{bmatrix} = A_2 \tag{5.11}$$

$$ad_f^2 g = \begin{bmatrix} f & ad_f^1 g \end{bmatrix} = \begin{bmatrix} f & A_2 \end{bmatrix} \tag{5.12}$$

$$\begin{aligned} &= \nabla A_2 . f - \nabla f . A_2 \\ &= A_3' - A_3'' = A_3 \end{aligned} \tag{5.13}$$

$$A_3' = \begin{bmatrix} \frac{\beta}{\Lambda^2} \lambda x_1 - \frac{\beta}{\Lambda^2} \lambda x_2 \\ \\ \frac{\lambda}{\Lambda} x_1 \\ \\ \frac{1}{\Lambda \mu_f} f_f P_{a0} x_1 \\ \\ \frac{1}{\Lambda \mu_c} (1 - f_f) P_{a0} x_1 \\ \\ \end{bmatrix} \tag{5.14}$$

$$A_3'' = \begin{bmatrix} \frac{-\beta^2}{\Lambda^3}\lambda x_2 - \frac{\beta}{\Lambda^2}\lambda x_1 \\ \\ \frac{\beta\lambda}{\Lambda^2}x_2 - \frac{\beta}{\Lambda}\lambda^2 x_1 \\ \\ \frac{\beta}{\mu_f\Lambda^2}x_2 f_f P_{a0} x_2 + \frac{\Omega\beta}{\mu_f^2\Lambda}x_2 C P_{a0} x_1 + \frac{\Omega}{\mu_f\mu_c\Lambda}C P_{a0} x_1 \\ \\ \frac{\beta}{\mu_c\Lambda^2}C P_{a0} x_2 - \frac{\Omega}{\mu_c\mu_f\Lambda}f_f P_{a0} x_1 - \frac{2M+\Omega}{\Lambda^2\mu_c^2}C P_{a0} x_1 \end{bmatrix} \tag{5.15}$$

$$A_4 = \nabla A_3 f - \nabla f A_3 \tag{5.16}$$

The determinant of controllability matrix $|J_c|$ given in *(5.7)* is nonzero and system *(5.1)* is controllable.

5.3 Smooth Super Twisting based Reactor Controller

When we consider the power as output and reactivity as input the reactor model has relative degree one for which smooth super twisting algorithm ca be applied. Let n_{rd} be the desired normalized power and $x_1 = n_{rd} - n_r$ be tracking error. The non linear system *(5.1)* can be represented as

$$\dot{x}_1 \quad = \quad f(n_r, c_r, T_l, T_f) + \frac{-\rho}{\Lambda}(n_r) \tag{5.17}$$

where

$$
\begin{aligned}
f(n_r, c_r, T_l, T_f) &= \frac{\beta}{\Lambda} n_r + \frac{-\beta}{\Lambda} c_r - \alpha_f (T_f - T_{f0}) \\
&\quad -\alpha_c (T_c - T_c 0) + \dot{n_{rd}}
\end{aligned} \tag{5.18}
$$

Based on disturbance observer given in Appendix-B, the observer used to estimate drift term $\hat{f}$ is given as

$$
\begin{aligned}
\dot{\hat{x}}_1 &= \hat{f} + bu \\
\hat{f} &= \lambda_2 L^{\frac{1}{2}} (\hat{x}_1 - x_1) sign(\hat{x}_1 - x_1) + x_2 \\
\dot{\hat{x}}_2 &= -\lambda_1 L sign(\hat{x}_2 - \hat{f})
\end{aligned} \tag{5.19}
$$

Then the control law is

$$
\begin{aligned}
u &= \frac{1}{b}(-\hat{f} - k_1 |x_1|^{\frac{1}{2}} sign x_1 + w) \\
\dot{w} &= -k_2 |x_1|^{\frac{1}{3}} sign(x_1)
\end{aligned} \tag{5.20}
$$

5.3.1 Tracking Results

The control law *(5.20)* provides good tracking performance. As per design requirements of a PWR a load change of 5% ramp/minute is used. The schematic diagram for implementation of controller is shown in Fig. 5.1. The reference and output power are given in Fig. 5.2. The output power tracks the refrence is steady state as well as in transient conditions. The control effort is given in Fig. 5.3. The control effort which is change in reactivity, required to track the reference is within the design limits. This can be easily obtained by control rod movement.

5.3.2 Design of SSTA based Reactor Controller

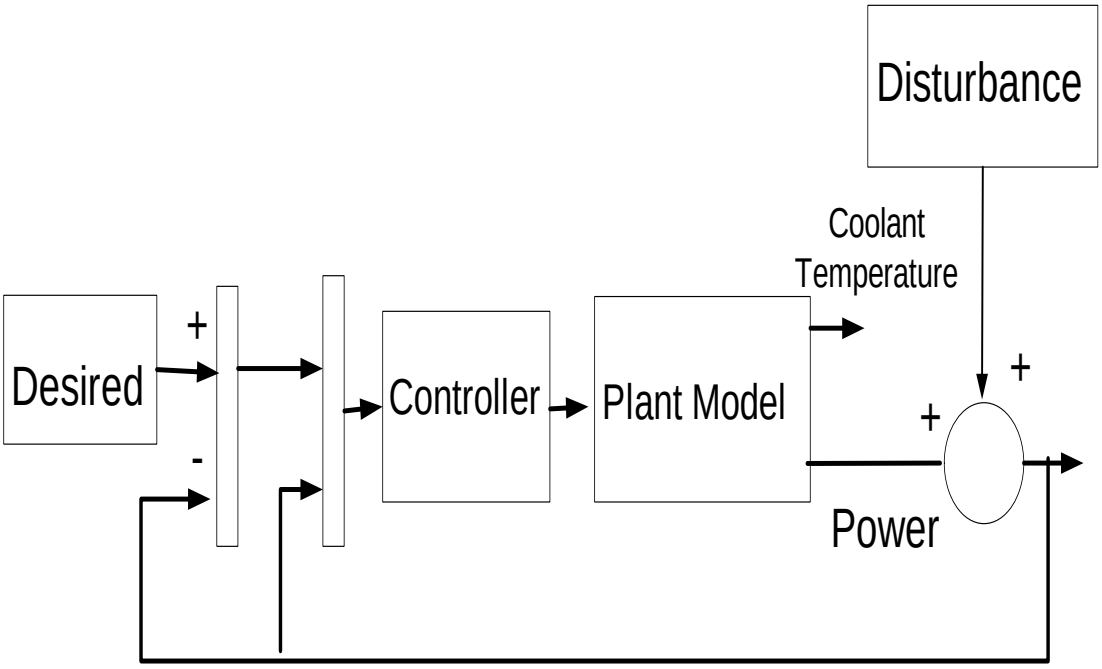

FIGURE 5.1: Controller Block diagram

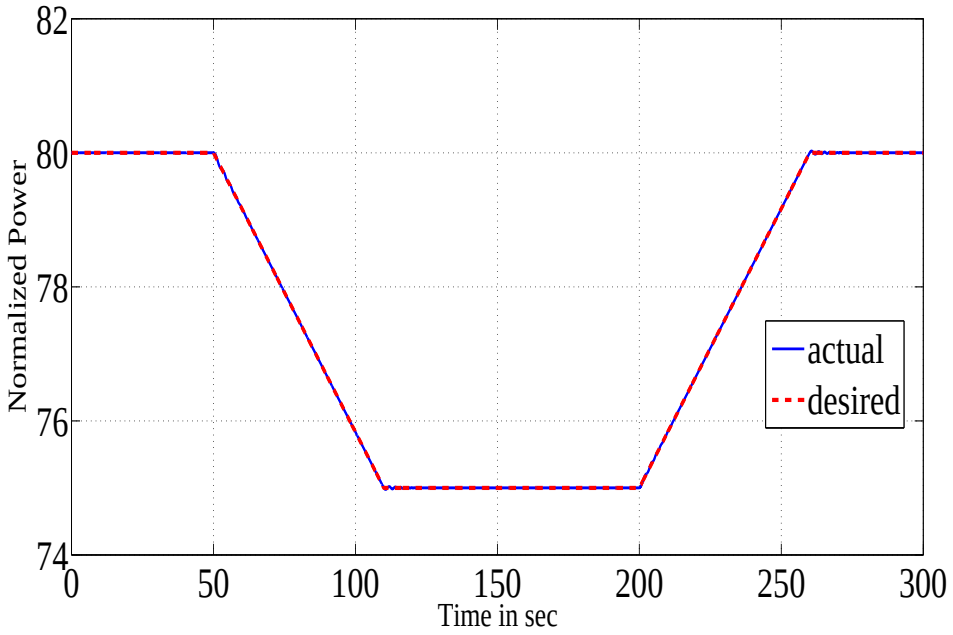

FIGURE 5.2: Comparison of reference and output power

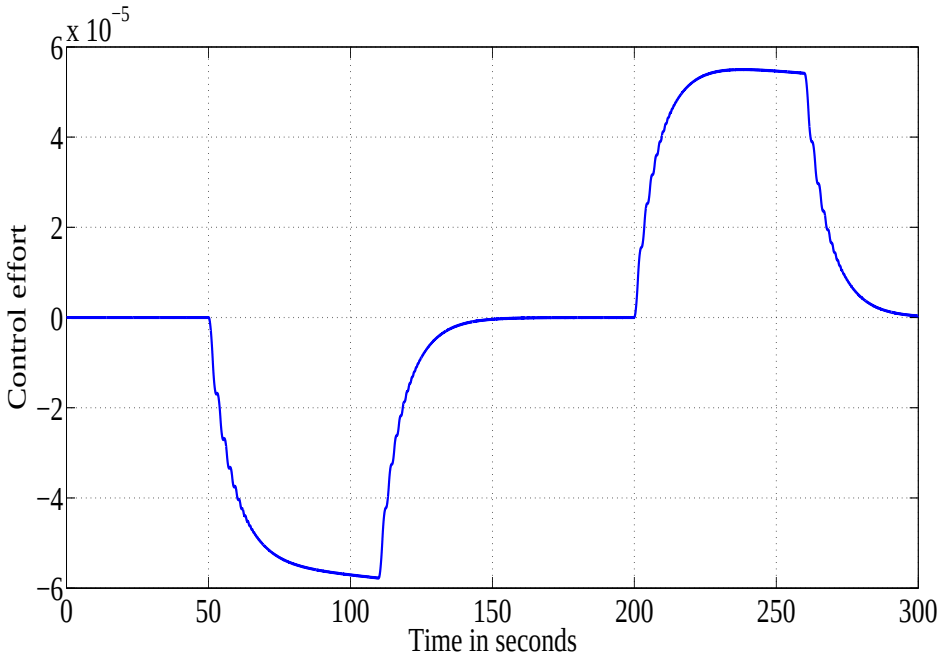

FIGURE 5.3: Control effort

5.3.3 Controller results with output disturbance

Output disturbance with 2% of full power is considered as given in Fig. 5.4. It may be due to fission product poisoning. It is easily rejected by the desihned controller. The control effort to reject the disturbance is given in Fig. 5.5. The control effort is change in reactivity and it is within allowable limits. The output power with disturbance is given in Fig. 5.6. This shows that the disturbance in output power is rejected within one second. The coolant temperature with disturbance is given in Fig. 5.7. The coolant temperature has slow response.

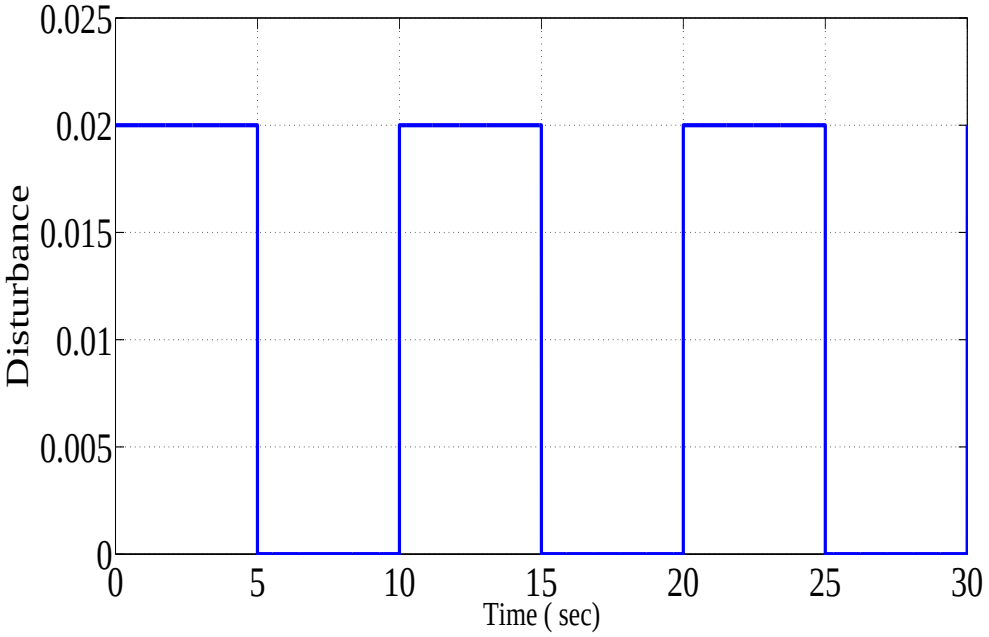

FIGURE 5.4: Output disturbance, may be due to neutron poisons

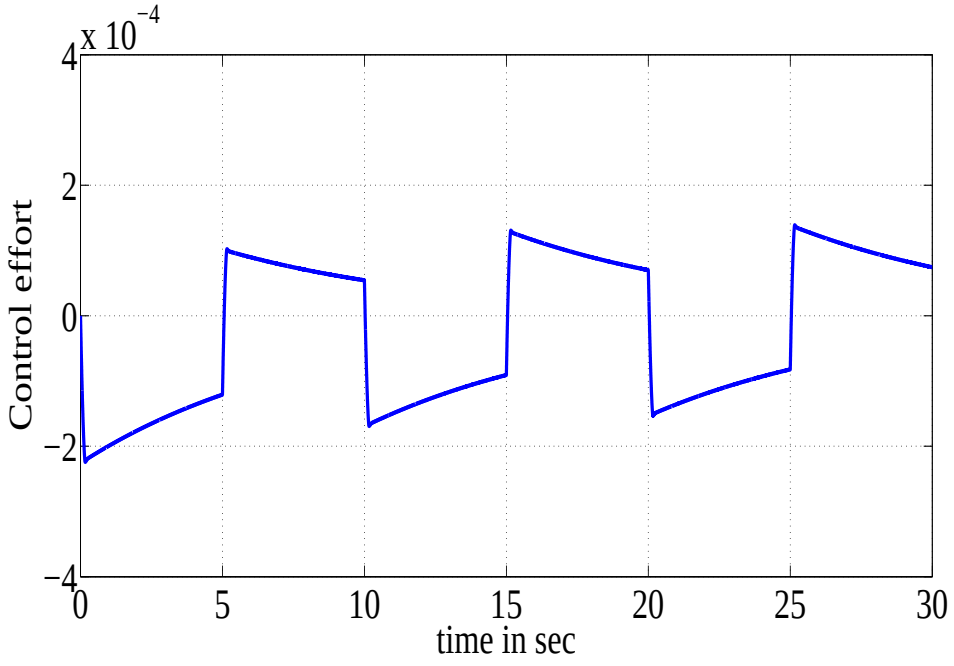

FIGURE 5.5: Control effort,(Change in reactivity)

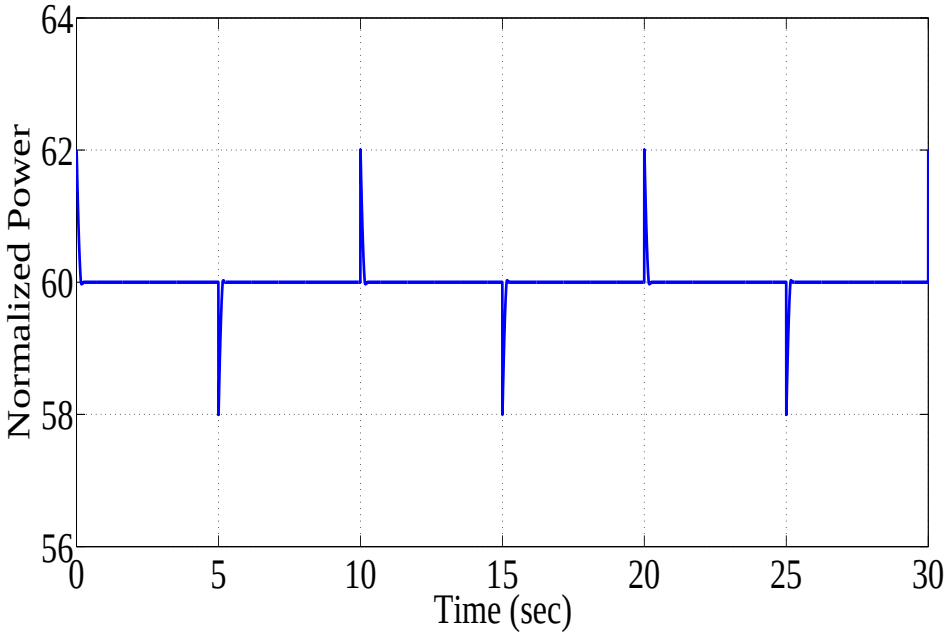

FIGURE 5.6: Reactor Power with output disturbance

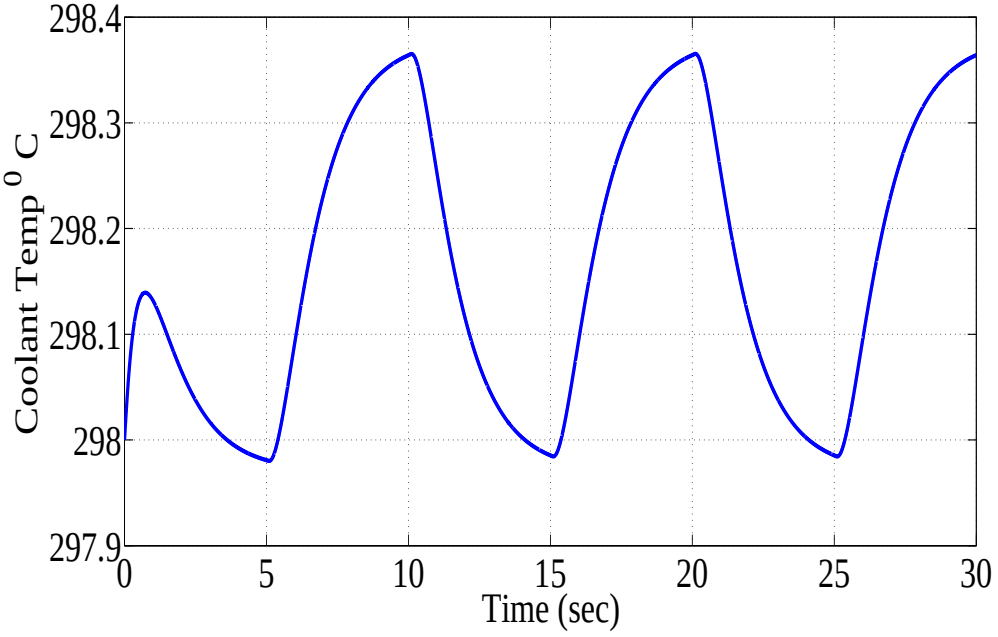

FIGURE 5.7: Coolant temperature

5.4 Design of Smooth Real Twisting based Reactor Controller

When we consider the coolant temperature as output and reactivity as input the reactor model has relative degree two. The second derivative of coolant temperature is given as

$$\ddot{T}_l = \frac{B_1}{\mu_c} + \frac{B_2}{\mu_c} - B_3\frac{\beta}{\Lambda}n_r + B_3\frac{\beta}{\Lambda}c_r + B_3\frac{\rho}{\Lambda} \tag{5.21}$$

B_1, B_2 and B_3 are given as.

$$B_1 = \frac{\Omega P_{a0} n_r}{\mu_c \mu_f} + \frac{\Omega T_l}{2\mu_c \mu_f} + \frac{\Omega T_e}{2\mu_c \mu_f} \tag{5.22}$$

$$B_2 = \frac{2M + \Omega}{2\mu_c}\dot{T}_l \tag{5.23}$$

$$B_3 = \frac{1}{\mu_c}[-25T_f + 70.5T_l - 45.5T_e] \tag{5.24}$$

Let T_{ref} be the reference coolant temperature, $x_1 = T_{ref} - T_c$ and $x_2 = \dot{x}_1$ then the dynamical system *(5.21)* can be represented as

$$\begin{aligned} \dot{x}_1 &= x_2 \\ \dot{x}_2 &= f(x_1, x_2, t) + bu \end{aligned} \tag{5.25}$$

where $f(x_1, x_2, t)$ and b are given as

$$f(x_1, x_2, t) = \ddot{T}_{ref} - \frac{B_1}{\mu_c} - \frac{B_2}{\mu_c} + B_3\frac{\beta}{\Lambda}n_r - B_3\frac{\beta}{\Lambda}c_r \tag{5.26}$$

$b = \frac{\Lambda}{B_3 n_r}$

A second order sliding surface $x_1 = x_2 = 0$ is selected for PWR. The robust disturbance observer to estimate the drift term

$$\begin{aligned}
\dot{\hat{x}}_1 &= \hat{x_2} \\
\dot{\hat{x}}_2 &= \hat{f} + bu \\
\hat{f} &= -\lambda_2 L^{1/2}|\hat{x}_2 - x_2|^{1/2} sign(\hat{x}_2 - x_2) + \hat{x}_3 \\
\dot{\hat{x}}_3 &= -\lambda_1 L sign(\hat{x}_3 - \hat{f})
\end{aligned} \tag{5.27}$$

The control law is given as

$$u = \frac{1}{b}(-\hat{f} - k_1|x_1|^{1/3} sign(x_1) - k_2|x_2|^{1/2} sign(\hat{x}_2)) \tag{5.28}$$

5.5 Results and discussion

The results obtained by smooth super twisting based controller are presented and discussed in Sections 5.3.1 and 5.3.3. The block diagram of control scheme using real twisting algorithm is given in Fig. 5.8. For the design of real twisting controller, the error between the reference temperature and average coolant temperature is taken as sliding surface. Then the derivative of sliding surface is obtained by uniform robust

exact differentiator [7]. The drift term consists of the unknown plant dynamics. It can effect the control effort. Therefore an observer is used to estimate the drift term. We have posed tracking problem to the real twisting controller. It tracks the reference temperature and power satisfactorily. The comparison of reference and output power is shown in Fig. 5.9. The actual power tracks the reference within finite time. The comparison of T_{ref} and T_{avg} is shown in Fig. 5.10. The control effort which is reactivity is shown in Fig. 5.11

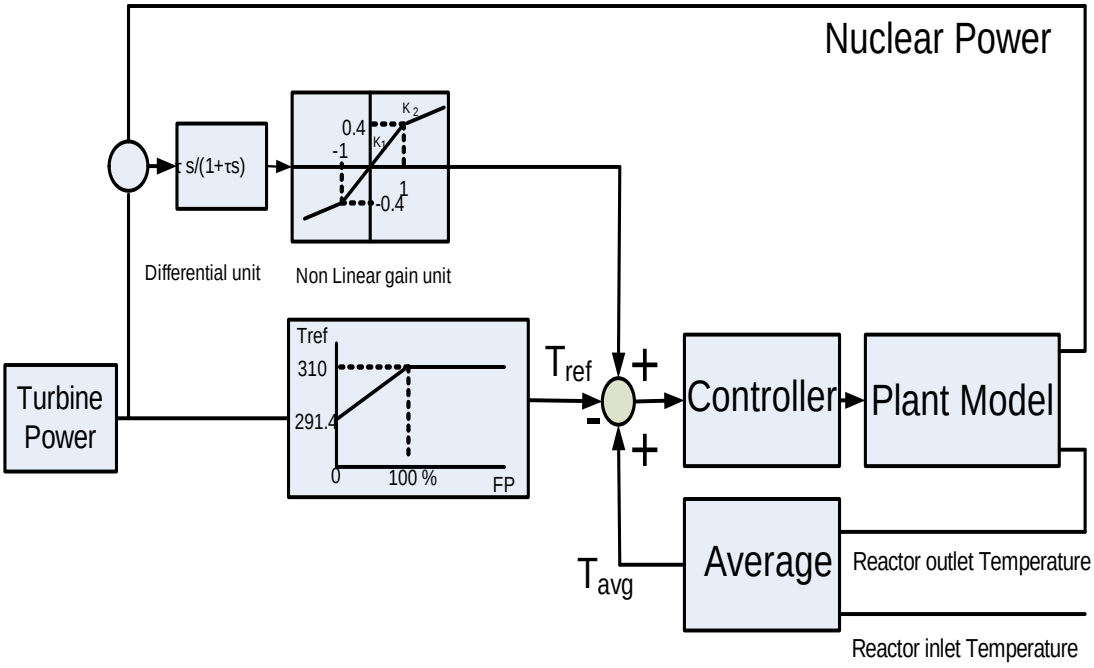

FIGURE 5.8: Reactor average coolant temperature controller

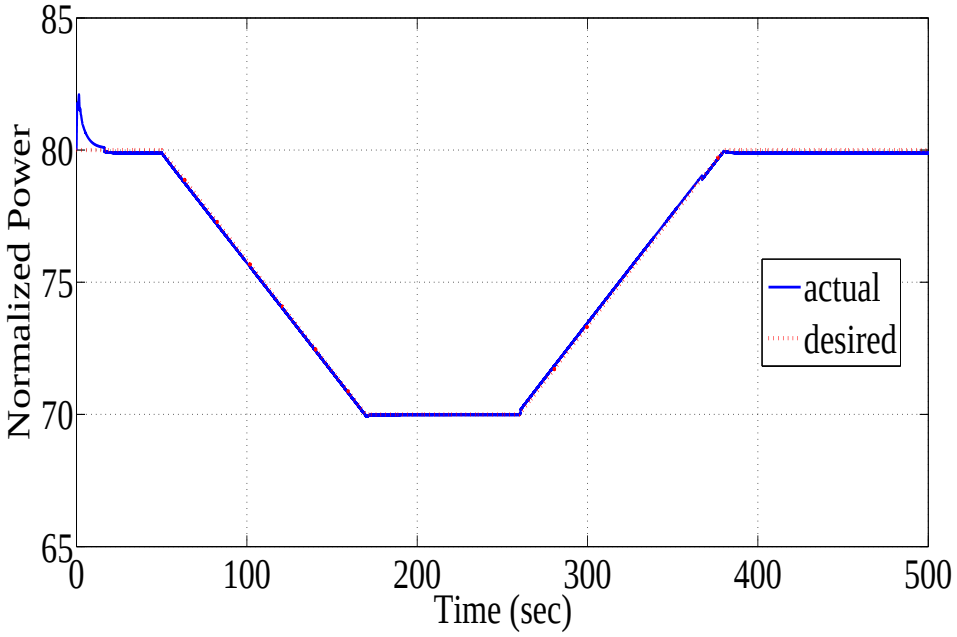

FIGURE 5.9: Comparison of reference and output power

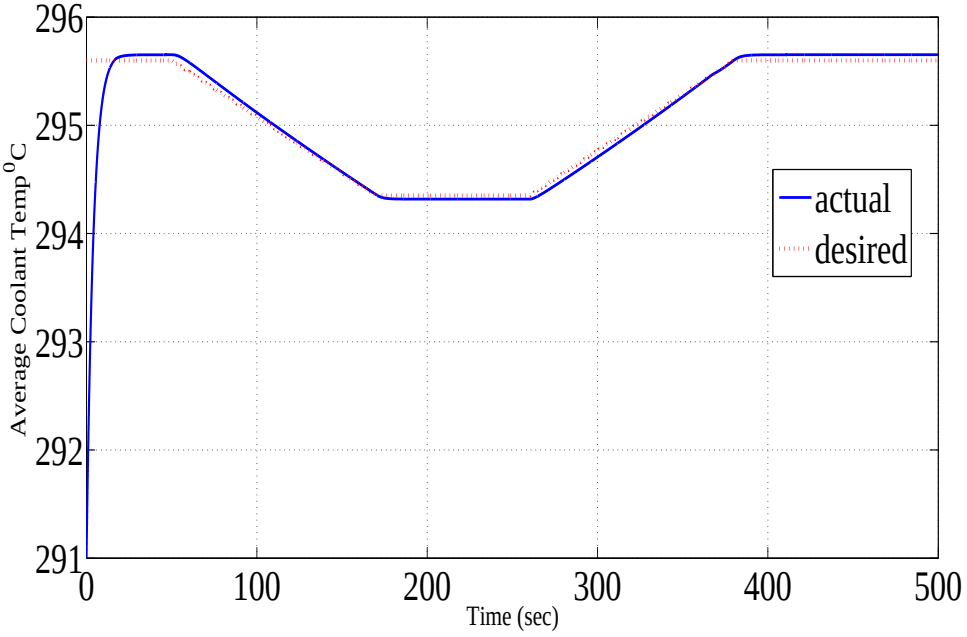

FIGURE 5.10: Comparison of reference and output coolant temperature

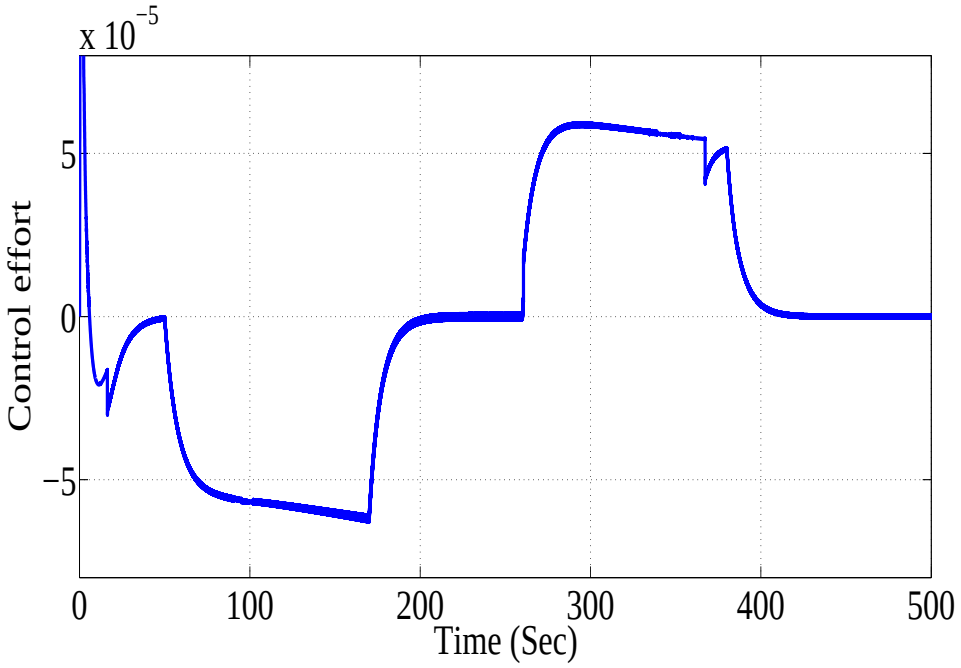

FIGURE 5.11: Control effort, (Change in reactivity)

5.6 Summary

Smooth second order sliding mode control was used for tracking and disturbance rejection in output power of a pressurized water reactor. Two different schemes were used. In first method smooth super twisting algorithm was used to regulate output power of reactor. In second method real twisting algorithm was used to regulate the reactor average coolant temperature and power. Simulation results of both the controllers were satisfactory in the presence of disturbance proved by the simulation results. In the next chapter conclusion of research work will be given.

Chapter 6

CONCLUSION AND FUTURE WORK

6.1 Conclusion

In present work model validation, parameter estimation and controller design of a nuclear power reactor is done under steady state and transient conditions. First, the model validation has been performed with experimental data. The reactor has two measurable outputs and one input. The two outputs are neutron density and coolant temperature. The input is change in reactivity which is control rods. The input of the plant which is change in reactivity was given to nonlinear reactor model. The neutron density and the coolant temperature obtained by model were compared with corresponding measurements. The modeled and measured parameter were close to each other. There is minor difference in steady state and transients condition. This difference is due to unmodeled plant dynamics. After validating model following important parameters of reactor were estimated and controller was designed.

- A second order sliding mode observer is designed for estimation of precursor density. Precursor has very important role in control of nuclear reactor. Precursor produce delayed neutron due to which reactor period increases and reactor power can be controlled easily.
- Furthermore uniform second order sliding mode based robust exact differentiator observer is designed for pressurized water reactor. With the help of this observer two unmeasurable parameters, change in reactivity and average fuel temperature of a pressurized water reactor are estimated. These parameters are estimated from the measurement data of control rod position, reactor coolant temperature and neutron density of a PWR. The estimated parameters are compared with the theoretically calculated value and closely agree in steady state while there is small deviation in transient states.

- A second order smooth sliding controller is also designed for a pressurized water reactor in the presence of disturbance. The controller is designed using two different approaches and simulations show the satisfactory results.

6.2 Future Work

The following problems have been identified for future work.

1. In present work three important parameters of pressurized water reactor have been estimated. These parameters are precursor density, reactivity and average fuel temperature. These parameters can be used for fault diagnosis and fault tolerant control of a PWR.

2. We have used lumped parameter model of reactor, this can be extended to two dimensional and three dimensional problem. By considering the model of conductive heat transfer from fuel to the clad and convective heat transfer from clad to coolant the fuel rod internal temperature distribution and rod surface heat fluxes can be computed. By knowing the internal temperature distribution the peak centre line temperature of the rod can be calculated.

3. The parameters of reactor has been estimated. Similarly the parameters of steam generator and pressurizer can also be estimated.

4. The behavior of Xenon has not been considered as its effect arises after nine hours of transient. The concentration of Xenon can also be estimated by increasing the duration of experiment.

5. In this work three important parameters of the reactor has been estimated. Similarly other parameters like reactivity coefficients of fuel and coolant temperatures of the reactor can also be estimated.

APPENDICES

Appendix-A

Table 1: Parameters of Chashma Nuclear Power Plant

β	0.0065	
Λ	0.0000243	sec
Pao	998	MW
μ_f	14.8	$MWs/^\circ C$
Ω	-25.8nr+40.	$MW/^\circ C$
M	-58.8nr+106.	$MW/^\circ C$
α_f	-0.000025	$\Delta K/K/^\circ C$
λ	0.125	sec^{-1}
f_f	0.98	
Te	290	^0C
μ_c	250	$MWs/^\circ C$
α_c	-0.0001	$\Delta K/K/^\circ C$
T_{fo}	360	$^\circ C$
T_{co}	302	$^\circ C$

APPENDICES

Appendix-B

Disturbance observer for smooth super twisting algorithm [2]

$$
\begin{aligned}
\chi_0 &= \omega_0 + u \\
\omega_0 &= -a_0 L^{\frac{r}{r+1}} |\chi_0 - f|^{\frac{r}{r+1}} sign(\chi_0 - f) + \chi_1 \\
\dot{\chi_1} &= \omega_1 \\
\omega_1 &= -a_1 L^{\frac{1}{r}} |\chi_1 - \omega_0|^{\frac{r-1}{r}} sign(\chi_1 - \omega_0) + \chi_2 \\
&\vdots \\
\dot{\chi}_{r-1} &= \omega_{r-1} \\
\omega_{r-1} &= -a_{r-1} L^{\frac{1}{2}} |\chi_{r-1} - \omega_{r-2}|^{\frac{r-1}{r}} sign(\chi_{r-1} - \omega_{r-2} + \chi_r) \\
\chi_r &= -a_r L sign(\chi_r - \omega_{r-1})
\end{aligned}
\tag{1}
$$

The observer gives the following

$$
\begin{aligned}
\chi_0 &= s(t) \\
\chi_1 &= f(t) \\
&\vdots \\
\chi_i &= f^{(i-1)}, i = 1, 2, ...n
\end{aligned}
\tag{2}
$$

APPENDICES

Appendix-C

Disturbance observer for smooth real twisting algorithm [4]

$$
\begin{aligned}
\dot{\hat{\omega}}_0 &= \hat{\omega}_1 \\
\dot{\hat{\omega}}_1 &= \hat{f}_1 + u \\
\hat{f}_1 &= -\lambda_r L^{1/r} |\hat{\omega}_1 - \omega_1|^{(r-1)/r} sign(\hat{\omega}_1 - \omega_1) + \hat{\omega}_2 \\
\dot{\hat{\omega}}_2 &= \hat{f}_2 \\
\hat{f}_2 &= -\lambda_{r-1} L^{1/r-1} |\hat{\omega}_2 - \hat{f}_1|^{r/r-1} sign(\hat{\omega}_2 - \hat{f}_1) + \hat{\omega}_3 \\
&\vdots \\
\dot{\hat{\omega}}_{r-1} &= \hat{f}_{r-1} \\
\hat{f}_{r-1} &= -\lambda_2 L^{1/2} |\hat{\omega}_{r-1} - \hat{f}_{r-2}|^{1/2} \\
&\quad sign(\hat{\omega}_{r-1} - \hat{f}_{r-2}) + \hat{\omega}_r \\
\dot{\hat{\omega}}_r &= \lambda_1 L sign(\hat{\omega}_r - \hat{f}_{r-1})
\end{aligned}
\tag{3}
\tag{4}
$$

The observer gives the following

$$
\begin{aligned}
\hat{\omega}_0 &= \omega_0 \\
\hat{\omega}_1 &= \omega_1 \\
&\vdots \\
\hat{\omega}_{i-2} &= f^{(i-2)}, i = 2, 3, 4, ...n
\end{aligned}
\tag{5}
$$

REFERENCES

[1] A. Levant, "Sliding order and sliding accuracy in sliding mode control," *International Journal of Control*, vol. 58, no. 6, pp. 1247 – 1263, 2003.

[2] Y. B. Shtessel, I. A. Shkolnikov, and A. Levant, "Smooth second-order sliding modes: Missile guidance application," *Automatica*, vol. 43, no. 8, pp. 1470 – 1476, 2007.

[3] A. Levant, "Sliding order and sliding accuracy in sliding mode control," *Intnation Journal of Control*, vol. 58, no. 6, pp. 1247–1263, 1993.

[4] S. Iqbal, C. Edwards, and A. Bhatti, "A smooth second-order sliding mode controller for relative degree two systems," in *IECON 2010 - 36th Annual Conference on IEEE Industrial Electronics Society*, pp. 2379–2384, 2010.

[5] J. Davila, L. Fridman, and A. Levant, "Second-order sliding-mode observer for mechanical systems," *Automatic Control, IEEE Transactions on*, vol. 50, no. 11, pp. 1785–1789, 2005.

[6] E. Cruz-Zavala, J. Moreno, and L. Fridman, "Uniform second-order sliding mode observer for mechanical systems," in *Variable Structure Systems (VSS), 2010 11th International Workshop on*, pp. 14–19, 2010.

[7] E. Cruz-Zavala, J. Moreno, and L. Fridman, "Uniform robust exact differentiator," *Automatic Control, IEEE Transactions on*, vol. 56, no. 11, pp. 2727–2733, 2011.

[8] S. Hussain, A. Bhatti, A. Samee, and S. Hameed Qaiser, "Estimation of reactivity and average fuel temperature of a pressurized water reactor using sliding mode differentiator observer," *Nuclear Science, IEEE Transactions on*, vol. 60, no. 4, pp. 3025–3032, 2013.

[9] A. Levant, "Robust exact differentiation via sliding mode technique," *Automatica*, vol. 34, no. 3, pp. 379 – 384, 1998.

[10] B. Bose, "Global energy scenario and impact of power electronics in 21st century," *Industrial Electronics, IEEE Transactions on*, vol. 60, no. 7, pp. 2638–2651, 2013.

[11] P. Wang, T. Aldemir, and V. Utkin, "Estimation of xenon concentration and reactivity in nuclear reactors using sliding mode observers," in *Decision and Control, 2001. Proceedings of the 40th IEEE Conference on*, vol. 2, pp. 1801–1806 vol.2, 2001.

[12] S. H. Qaiser, A. I. Bhatti, M. Iqbal, R. Samar, and J. Qadir, "Estimation of precursor concentration in a research reactor by using second order sliding mode observer," *Nuclear Engineering and Design*, vol. 239, no. 10, pp. 2134 – 2140, 2009.

[13] S. H. Qaiser, M. Iqbal, A. I. Bhatti, R. Samar, and J. Qadir, "Estimation of reactivity in a research reactor by using a second-order sliding mode observer," *Nuclear Science and Engineering*, vol. 172, no. 3, pp. 327 – 336, 2012.

[14] Q. Li and J. Bernard, "Design and evaluation of an observer for nuclear reactor fault detection," in *Nuclear Science Symposium Conference Record, 2001 IEEE*, vol. 4, pp. 2493–2497, 2001.

[15] F. Cadini and E. Zio, "Application of particle filtering for estimating the dynamics of nuclear systems," *Nuclear Science, IEEE Transactions on*, vol. 55, no. 2, pp. 748–757, 2008.

[16] C. Fazekas, G. Szederkenyi, and K. Hangos, "Parameter estimation of a simple primary circuit model of a vver plant," *Nuclear Science, IEEE Transactions on*, vol. 55, no. 5, pp. 2643–2653, 2008.

[17] R. M. Edwards., Y. L. Kwang, and M. A. Shultz, "State feedback assisted classical control: an incremental approach to control modernization of existing and future nuclear reactors and power plants," *Nuclear Technology*, pp. 167 – 186, 1990.

[18] A. Gabor, C. Fazekas, G. Szederkenyi, and K. Hangos, "Modeling and identification of a nuclear reactor with temperature effects and xenon poisoning," in *Industrial Electronics, 2009. IECON '09. 35th Annual Conference of IEEE*, pp. 1639–1644, Nov 2009.

[19] S. Qaiser, A. Bhatti, M. Iqbal, R. Samar, and J. Qadir, "Model validation and higher order sliding mode controller design for a research reactor," *Annals of Nuclear Energy*, vol. 36, no. 1, pp. 37 – 45, 2009.

[20] D. Lathouwers, A. Agung, T. van der Hagen, H. van Dam, C. Pain, C. de Oliveira, and A. Goddard, "Dynamics modeling and stability analysis of a fluidized bed nuclear reactor," *Progress in Nuclear Energy*, vol. 43, pp. 437 – 443, 2003.

[21] J. Hung, W. Gao, and J. Hung, "Variable structure control: a survey," *Industrial Electronics, IEEE Transactions on*, vol. 40, no. 1, pp. 2–22, 1993.

[22] W. Gao and J. Hung, "Variable structure control of nonlinear systems: a new approach," *Industrial Electronics, IEEE Transactions on*, vol. 40, no. 1, pp. 45–55, 1993.

[23] V. I. Utkin, *Sliding Modes in Control and Optimization*. Springer-Verlag, 1992.

[24] G. Bartolini, A. Ferrara, and E. Usani, "Chattering avoidance by second-order sliding mode control," *Automatic Control, IEEE Transactions on*, vol. 43, no. 2, pp. 241–246, 1998.

[25] Y. Orlov, "Finite time stability and robust control synthesis of uncertain switched systems," *SIAM Journal on Control and Optimization*, vol. 43, no. 4, pp. 1253–1271, 2004.

[26] G. Rizzoni, S. Drakunov, and Y.-Y. Wang, "On-line estimation of indicated torque in ic engines via sliding mode observers," in *American Control Conference, Proceedings of the 1995*, vol. 3, pp. 2123–2127 vol.3, 1995.

[27] S. Emelyanov, "Theory of variable-structure control systems: Inception and initial development," *Computational Mathematics and Modeling*, vol. 18, no. 4, pp. 321–331, 2007.

[28] M. Saif, W. Chen, and Q. Wu, "High order sliding mode observers and differentiatorsapplication to fault diagnosis problem," in *Modern Sliding Mode Control Theory*, vol. 375 of *Lecture Notes in Control and Information Sciences*, pp. 321–344, Springer Berlin Heidelberg, 2008.

[29] S. K. Spurgeon, "Sliding mode observers: a survey," *International Journal of Systems Science*, vol. 39, no. 8, pp. 751–764, 2008.

[30] H. Alwi and C. Edwards, "Fault detection and fault-tolerant control of a civil aircraft using a sliding-mode-based scheme," *Control Systems Technology, IEEE Transactions on*, vol. 16, no. 3, pp. 499–510, 2008.

[31] V. Sankaranarayanan, A. D. Mahindrakar, and P. M. Abhilash, "Output feedback second-order sliding mode control of the cart on a beam system," *International Journal of Robust and Nonlinear Control*, vol. 20, no. 5, pp. 561–570, 2010.

[32] B. Ganji, A. Z. Kouzani, S. Y. Khoo, and M. Shams-Zahraei, "Adaptive cruise control of a `HEV` using sliding mode control," *Expert Systems with Applications*, 2014.

[33] L.-Y. Hao and G.-H. Yang, "Robust fault tolerant control based on sliding mode method for uncertain linear systems with quantization," *`ISA` Transactions*, vol. 52, no. 5, pp. 600 – 610, 2013.

[34] R. Iriarte, L. T. Aguilar, and L. Fridman, "Second order sliding mode tracking controller for inertia wheel pendulum," *Journal of the Franklin Institute*, vol. 350, no. 1, pp. 92 – 106, 2013.

[35] X. Zhang, L. Sun, K. Zhao, and L. Sun, "Nonlinear speed control for `PMSM` system using sliding-mode control and disturbance compensation techniques," *Power Electronics, IEEE Transactions on*, vol. 28, no. 3, pp. 1358–1365, 2013.

[36] R. Pupadubsin, N. Chayopitak, D. Taylor, N. Nulek, S. Kachapornkul, P. Jitkreeyarn, P. Somsiri, and K. Tungpimolrut, "Adaptive integral sliding-mode position control of a coupled-phase linear variable reluctance motor for high-precision applications," *Industry Applications, IEEE Transactions on*, vol. 48, no. 4, pp. 1353–1363, 2012.

[37] K. Jezernik, J. Korelic, and R. Horvat, "Pmsm sliding mode `FPGA-based` control for torque ripple reduction," *Power Electronics, IEEE Transactions on*, vol. 28, no. 7, pp. 3549–3556, 2013.

[38] B. Beltran, M. El Hachemi Benbouzid, and T. Ahmed-Ali, "Second-order sliding mode control of a doubly fed induction generator driven wind turbine," *Energy Conversion, IEEE Transactions on*, vol. 27, no. 2, pp. 261–269, 2012.

[39] T. Ho and K.-K. Ahn, "Speed control of a hydraulic pressure coupling drive using an adaptive fuzzy sliding-mode control," *Mechatronics, IEEE/ASME Transactions on*, vol. 17, no. 5, pp. 976–986, 2012.

[40] Y.-H. Chang, C.-W. Chang, C.-L. Chen, and C.-W. Tao, "Fuzzy sliding-mode formation control for multirobot systems: Design and implementation," *Systems, Man, and Cybernetics, Part B: Cybernetics, IEEE Transactions on*, vol. 42, no. 2, pp. 444–457, 2012.

[41] Z. Song and K. Sun, "Adaptive backstepping sliding mode control with fuzzy monitoring strategy for a kind of mechanical system," *ISA Transactions*, no. 0, pp. –, 2013.

[42] K. Saoudi and M. Harmas, "Enhanced design of an indirect adaptive fuzzy sliding mode power system stabilizer for multi-machine power systems," *International Journal of Electrical Power Energy Systems*, vol. 54, no. 0, pp. 425 – 431, 2014.

[43] R.-J. Lian, "Adaptive self-organizing fuzzy sliding-mode radial basis-function neural-network controller for robotic systems," *Industrial Electronics, IEEE Transactions on*, vol. 61, no. 3, pp. 1493–1503, 2014.

[44] X. Yu and O. Kaynak, "Sliding-mode control with soft computing: A survey," *Industrial Electronics, IEEE Transactions on*, vol. 56, no. 9, pp. 3275–3285, 2009.

[45] M. Chen and W.-H. Chen, "Sliding mode control for a class of uncertain nonlinear system based on disturbance observer," *International Journal of Adaptive Control and Signal Processing*, vol. 24, no. 1, pp. 51–64, 2010.

[46] M. Iqbal, A. Bhatti, S. Ayubi, and Q. Khan, "Robust parameter estimation of non-linear systems using sliding-mode differentiator observer," *Industrial Electronics, IEEE Transactions on*, vol. 58, no. 2, pp. 680–689, 2011.

[47] Q. Ahmed and A. Bhatti, "Estimating SI engine efficiencies and parameters in second-order sliding modes," *Industrial Electronics, IEEE Transactions on*, vol. 58, no. 10, pp. 4837–4846, 2011.

[48] Q. R. Butt, A. I. Bhatti, M. R. Mufti, M. A. Rizvi, and I. Awan, "Modeling and online parameter estimation of intake manifold in gasoline engines using sliding mode observer," *Simulation Modelling Practice and Theory*, vol. 32, no. 0, pp. 138 – 154, 2013.

[49] H. Imine and T. Madani, "Sliding-mode control for automated lane guidance of heavy vehicle," *International Journal of Robust and Nonlinear Control*, vol. 23, no. 1, pp. 67–76, 2013.

[50] X.-G. Yan, S. Spurgeon, and C. Edwards, "State and parameter estimation for nonlinear delay systems using sliding mode techniques," *Automatic Control, IEEE Transactions on*, vol. 58, no. 4, pp. 1023–1029, 2013.

[51] Y.-T. Liu, T.-T. Kung, K.-M. Chang, and S.-Y. Chen, "Observer-based adaptive sliding mode control for pneumatic servo system," *Precision Engineering*, vol. 37, no. 3, pp. 522 – 530, 2013.

[52] K. Veluvolu, M. Defoort, and Y. Soh, "High-gain observer with sliding mode for nonlinear state estimation and fault reconstruction," *Journal of the Franklin Institute*, no. 0, pp. –, 2013.

[53] Y. Chitour, "Time-varying high-gain observers for numerical differentiation," *Automatic Control, IEEE Transactions on*, vol. 47, no. 9, pp. 1565–1569, 2002.

[54] A. Ball and H. Khalil, "High-gain observers in the presence of measurement noise: A nonlinear gain approach," in *Decision and Control, 2008. CDC 2008. 47th IEEE Conference on*, pp. 2288–2293, 2008.

[55] D. Efimov and L. Fridman, "A hybrid robust non-homogeneous finite-time differentiator," *Automatic Control, IEEE Transactions on*, vol. 56, no. 5, pp. 1213–1219, 2011.

[56] X. Wang and H. Lin, "Design and analysis of a continuous hybrid differentiator," *Control Theory Applications, IET*, vol. 5, no. 11, pp. 1321–1334, 2011.

[57] H. Feng and S. Li, "A tracking differentiator based on taylor expansion," *Applied Mathematics Letters*, vol. 26, no. 7, pp. 735 – 740, 2013.

[58] D. Tian, H. Shen, and M. Dai, "Improving the rapidity of nonlinear tracking differentiator via feedforward," 2013.

[59] B.-Z. Guo and Z.-L. Zhao, "Weak convergence of nonlinear high-gain tracking differentiator," *Automatic Control, IEEE Transactions on*, vol. 58, no. 4, pp. 1074–1080, 2013.

[60] A. Levant, "Exact differentiation of signals with unbounded higher derivatives," in *Decision and Control, 2006 45th IEEE Conference on*, pp. 5585–5590, 2006.

[61] A. Levant and M. Livne, "Exact differentiation of signals with unbounded higher derivatives," *Automatic Control, IEEE Transactions on*, vol. 57, no. 4, pp. 1076–1080, 2012.

[62] S. Kobayashi and K. Furuta, "Frequency characteristics of levant's differentiator and adaptive sliding mode differentiator," *International Journal of Systems Science*, vol. 38, no. 10, pp. 825–832, 2007.

[63] M. T. Angulo, J. A. Moreno, and L. Fridman, "Robust exact uniformly convergent arbitrary order differentiator," *Automatica*, vol. 49, no. 8, pp. 2489 – 2495, 2013.

[64] V. Utkin, "Variable structure systems with sliding modes," *Automatic Control, IEEE Transactions on*, vol. 22, no. 2, pp. 212–222, 1977.

[65] V. Utkin, "sliding modes in optimization and control problems," *Springer Verlag, New York*, 1992.

[66] A. F. Filippov, *Differential equations with discontinuous right-hand sides*, vol. 64. Kluwer Academic Publishers, 1981.

[67] A. Levant, "Robust exact differentiation via sliding mode technique," *Automatica*, vol. 34, no. 3, pp. 379–384, 1998.

[68] Y. Nagaya, G. Chiba, T. Mori, D. Irwanto, and K. Nakajima, "Comparison of monte carlo calculation methods for effective delayed neutron fraction," *Annals of Nuclear Energy*, vol. 37, no. 10, pp. 1308 – 1315, 2010.

[69] S. Kiss, S. Lipcsei, and J. Vgh, "{MTC} estimation based on neutron noise and propagating temperature perturbation in vver-440 reactors," *Annals of Nuclear Energy*, vol. 37, no. 2, pp. 166 – 174, 2010.

[70] N. Sadeghi, "Estimation of reactor power using `N16` production rate and its radiation risk assessment in tehran research reactor (`TRR`)," *Nuclear Engineering and Design*, vol. 240, no. 10, pp. 3607 – 3610, 2010. ¡ce:title¿4th International Topical Meeting on High Temperature Reactor Technology (HTR 2008), with Regular Papers¡/ce:title¿.

[71] G. Hegyi, "Inter-comparison of the recriticality temperature calculated by the karate-440 code system with real plant data," *Annals of Nuclear Energy*, vol. 38, no. 23, pp. 203 – 211, 2011.

[72] G. Monteyne, P. Baeten, and J. Schoukens, "Study of the bias of the `MTC e`stimate by noise analysis due to the presence of feedback," *Annals of Nuclear Energy*, vol. 38, no. 9, pp. 1964 – 1967, 2011.

[73] Y. Nagaya and T. Mori, "Calculation of effective delayed neutron fraction with monte carlo perturbation techniques," *Annals of Nuclear Energy*, vol. 38, no. 23, pp. 254 – 260, 2011.

[74] M. Rahgoshay and O. Noori-Kalkhoran, "Calculation of control rod worth and temperature reactivity coefficient of fuel and coolant with burn-up changes for vvrs-2xa0;mwth nuclear reactor," *Nuclear Engineering and Design*, vol. 256, no. 0, pp. 322 – 331, 2013.

[75] B. Vrban, J. Lley, G. Farkas, J. Hack, R. Hinca, M. Petriska, V. Slugen, and J. imko, "Temperature coefficients calculation for the first fuel loading of {NPP} mochovce 34," *Annals of Nuclear Energy*, vol. 63, no. 0, pp. 646 – 652, 2014.

[76] H. Kazeminejad, "Thermalhydraulic modeling of reactivity insertion in a research reactor," *Annals of Nuclear Energy*, vol. 45, no. 0, pp. 59 – 67, 2012.

[77] J. Perez-Cruz and A. Poznyak, "Estimation of the precursor power and internal reactivity in a nuclear reactor by a neural observer," in *Electrical and Electronics Engineering, 2007. ICEEE 2007. 4th International Conference on*, pp. 310–313, 2007.

[78] D. S. Daz, J. F. F. Ospina, and J. A. R. Sarasty, "Hamming method for solving the delayed neutron precursor concentration for reactivity calculation," *Annals of Nuclear Energy*, vol. 42, no. 0, pp. 47 – 49, 2012.

[79] D. Suescn-Daz, J. A. Rodrguez-Sarasty, and J. H. Figueroa-Jimnez, "Reactivity calculation using the eulermaclaurin formula," *Annals of Nuclear Energy*, vol. 53, no. 0, pp. 104 – 108, 2013.

[80] T. Bhatt, S. Shimjith, and A. Tiwari. in *Estimation of Shutdown Reactivity in Power Reactor: Comparative Study of Inverse Point Kinetics and Kalman Filtering*, 2012.

[81] A. D. Santos, S. M. Lee, R. Diniz, and R. Jerez, "A new experimental approach for subcritical reactivity determination of multiplying systems," *Annals of Nuclear Energy*, vol. 59, no. 0, pp. 243 – 254, 2013.

[82] H. Malmir and N. Vosoughi, "On-line reactivity calculation using lagrange method," *Annals of Nuclear Energy*, vol. 62, no. 0, pp. 463 – 467, 2013.

[83] M. Antolin, A. Martinez, F. S. Fernando, and D. Palma, "Calculation of reactivity in subcritical reactors using the method of partial derivatives," *Annals of Nuclear Energy*, vol. 60, no. 0, pp. 34 – 38, 2013.

[84] L. Tayebi and D. Vashaee, "On the estimation of the unknown reactivity coefficients in a {CANDU} reactor," *Annals of Nuclear Energy*, vol. 53, no. 0, pp. 447 – 457, 2013.

[85] H. Terada, N. Wakayama, H. Ohkawa, H. Ohtsu, and H. Yoshida, "Performance of fuel failure detection system for coated particle fuels," *Nuclear Science, IEEE Transactions on*, vol. 32, no. 2, pp. 1209–1213–a, 1985.

[86] H. Terada, N. Wakayama, M. Obata, T. Tobita, N. Tsuyuzaki, I. Gotoh, N. Oyama, K. Sakuraba, I. Yokouchi, H. Yoshida, and Y. Tomiyama, "Development of fuel failure detection system for a high temperature gas cooled reactor," *Nuclear Science, IEEE Transactions on*, vol. 34, no. 1, pp. 567–570, 1987.

[87] H. Terada, N. Wakayama, M. Obata, T. Ogawa, F. Kobayashi, K. Fukuda, N. Oyama, K. Sakuraba, I. Yokouchi, H. Yoshida, K. Suzuki, and S. Asami, "Development of fuel failure detection system for a high temperature gas cooled reactor. ii," *Nuclear Science, IEEE Transactions on*, vol. 35, no. 3, pp. 1041–1045, 1988.

[88] M. Katagiri, M. Kishimoto, H. Terada, N. Wakayama, S. Kawame, M. Obata, H. Ito, H. Yoshida, and F. Kobayashi

[89] A. M. Vaidya, N. K. Maheshwari, and P. K. Vijayan, "Estimation of fuel and clad temperature of a research reactor during dry period of de-fuelling operation," *Nuclear Engineering and Design*, vol. 240, no. 4, pp. 842 – 849, 2010.

[90] Z. Dong, J. Feng, X. Huang, and L. Zhang, "Power-level control of nuclear reactors based on feedback dissipation and backstepping," *Nuclear Science, IEEE Transactions on*, vol. 57, no. 3, pp. 1577–1588, 2010.

[91] D. Zhe, "Nonlinear state-feedback dissipation power level control for nuclear reactors," *Nuclear Science, IEEE Transactions on*, vol. 58, no. 1, pp. 241–257, 2011.

[92] K. Torabi, O. Safarzadeh, and A. Rahimi-Moghaddam, "Robust control of the pwr core power using quantitative feedback theory," *Nuclear Science, IEEE Transactions on*, vol. 58, no. 1, pp. 258–266, 2011.

[93] H. Hashemian, "Applying online monitoring for nuclear power plant instrumentation and control," *Nuclear Science, IEEE Transactions on*, vol. 57, no. 5, pp. 2872–2878, 2010.

[94] S. Dasgupta, A. Routh, S. Banerjee, K. Agilageswari, R. Balasubramanian, S. Bhandarkar, S. Chattopadhyay, M. Kumar, and A. Gupta, "Networked control of a large pressurized heavy water reactor PHWR with discrete proportional-integral-derivative (pid) controllers," *Nuclear Science, IEEE Transactions on*, vol. 60, no. 5, pp. 3879–3888, 2013.

[95] E. Rojas-Ramrez, J. S. Bentez-Read, and A. S.-D.-L. Ros, "A stable adaptive fuzzy control scheme for tracking an optimal power profile in a research nuclear reactor," *Annals of Nuclear Energy*, vol. 58, no. 0, pp. 238 – 245, 2013.

[96] G. Li and F. Zhao, "Multimodel-based power-level control with state-feedback and observer for load-follow PWR core," *Annals of Nuclear Energy*, vol. 63, no. 0, pp. 696 – 710, 2014.

[97] R. Munje, B. Patre, and A. Tiwari, "Non-linear simulation and control of xenon induced oscillations in advanced heavy water reactor," *Annals of Nuclear Energy*, vol. 64, no. 0, pp. 191 – 200, 2014.

[98] H. Eliasi, M. Menhaj, and H. Davilu, "Robust nonlinear model predictive control for a PWR nuclear power plant," *Progress in Nuclear Energy*, vol. 54, no. 1, pp. 177 – 185, 2012.

[99] J. Ye and H. Ji, "The research of simulation technology in nuclear power plant and the application of fuzzy control in temperature control system," in *Web Information Systems and Mining (WISM), 2010 International Conference on*, vol. 2, pp. 205–208, 2010.

[100] Z. Huang, R. Edwards, and K. Lee, "Fuzzy-adapted recursive sliding-mode controller design for a nuclear power plant control," *Nuclear Science, IEEE Transactions on*, vol. 51, no. 1, pp. 256–266, 2004.

[101] R. Munje, B. Patre, S. Shimjith, and A. Tiwari, "Sliding mode control for spatial stabilization of advanced heavy water reactor," *Nuclear Science, IEEE Transactions on*, vol. 60, no. 4, pp. 3040–3050, 2013.

[102] S. Hussain, A. I. Bhatti, A. Samee, and S. H. Qaiser, "Estimation of precursor density of a power reactor using uniform second order sliding mode observer," *Annals of Nuclear Energy*, vol. 54, no. 0, pp. 233 – 239, 2013.

[103] J.-J. E. Slotine and W. Li, *Applied Nonlinear Control*, vol. 62. Prentice Hall, 1991.